THE MECHANICAL DESIGN AND OPTIMIZATION OF A WEARABLE MULTIMODAL HEALTH SENSING SYSTEM

A Dissertation
Presented to
The Academic Faculty

by

Brandi Nevius

In Partial Fulfillment
of the Requirements for the Degree
Master of Science in the
School of Mechanical Engineering

Georgia Institute of Technology
December, 2020

THE MECHANICAL DESIGN AND OPTIMIZATION OF A WEARABLE MULTIMODAL HEALTH SENSING SYSTEM

Approved by:

Dr. Omer Inan, Advisor
School of Electrical and Computer Engineering
Georgia Institute of Technology

Dr. Frank Hammond, Co-advisor
School of Mechanical Engineering
Georgia Institute of Technology

Dr. Aaron Young
School of Mechanical Engineering
Georgia Institute of Technology

Date Approved: November 19, 2020

PREFACE

The greatest thing I have learned in the medical research and development industry, both in my time in this lab and before, is to occasionally remind myself what all of this hard work is really for. While these devices and algorithms and findings are indeed exceptional at securing publications in leading biomedical engineering journals, or guaranteeing graduate school diplomas with remarkable accolades, these achievements are hardly all that the effort is good for. It becomes so easy to tune out the world while sitting endlessly behind a computer on CAD or processing signals on MATLAB, working vigorously in the space between deadlines. You forget that the device you are designing will one day adorn the body of another human being, one that may be suffering from a painful, unpredictable or frightening illness; and perhaps this device can offer some reprieve or at least some insight into that suffering. You forget that the disembodied ECG you are reviewing and cursing because the R-peak detection algorithm is failing to interpret the irregular rhythm for the third time this week, is far more than a line on a figure to be labeled – it is the footprint of a beating heart from a real living breathing human being, who can just maybe benefit from the work we are doing, so long as we do it well.

ACKNOWLEDGEMENTS

First and foremost, I would like to thank my research advisor, Dr. Omer Inan, who embodies all the most amazing attributes of a leader. Thank you for your inexhaustible confidence in and support of each of us. I will truly miss having you as my boss. To my reading committee, co-advisor Dr. Frank Hammond and Dr. Aaron Young, I am grateful for your willingness to facilitate the conclusion of my time in the Inan Lab.

I would like to thank several of my fellow IRL members. To Caitlin Teague, Nick Bolus, and Andrew Carek – I feel honored to have worked alongside such hardworking, intelligent, determined individuals. Caitlin, thank you for all of your genius and hard work that paved the way for the entire first aim of my research, and thank you also for the friendship in the meantime. To Venu Ganti and Göktuğ Özmen, thank you for your comradery, for the laughs, for your support and counsel, and for your immeasurable patience while helping me. I will truly miss working with you two by my side. To Mohsen Safaei, I could not have completed the entire second aim of my research without your assistance. Thank you for your selfless willingness to help, your remarkable degree of personal investment into the success of others' work, and your patience through it all.

Lastly, thank you to my wonderful family who have supported me with love and encouragement since day one of this adventure. To my husband Jordan in particular, I quite literally wouldn't be here without your confidence in me having manifested into an email to your favorite former research advisor. Thank you for your unending support and belief in me.

TABLE OF CONTENTS

LIST OF TABLES

LIST OF FIGURES

LIST OF SYMBOLS AND ABBREVIATIONS

ACL	Anterior Cruciate Ligament
ARDS	Acute Respiratory Distress Syndrome
COTS	Commercial Off the Shelf
COVID-19	Corona Virus Disease 2019
DAQ	Data Acquisition Unit
DARPA	Defense Advanced Research Projects Agency
EBI	Electrical Bioimpedance
FDM	Fused Deposition Modeling
FEA	Finite Element Analysis
HCW	Health Care Worker
IDC	Insulation Displacement Connector
IMU	Inertial Measurement Unit
IRL	Inan Research Lab
LED	Light Emitting Diode
MCL	Medial Collateral Ligament
Mic	Microphone
microSD	Miniaturized Secure Digital Card
MODS	Multiple Organ Dysfunction Syndrome
NIH	National Institutes of Health
PCB	Printed Circuit Board
PLA	Polylactic Acid

PUI	Patient Under Investigation
RA	Rheumatoid Arthritis
ROM	Range of Motion
SIRS	Systemic Inflammatory Response Syndrome
UMinn	University of Minnesota
USB	Universal Serial Bus
V1	Knee Brace Version 1
V2	Knee Brace Version 2
V3	Knee Brace Version 3
YM	Young's Modulus

SUMMARY

The objective of the following research was to create and optimize the wearable packaging of the first ever apparatus for both physiological (i.e., fluid presence and kinematics) and structural (i.e., acoustics) health monitoring, for the knee joint and later for the lungs. The internal sensing modalities which have been formerly validated by prior members of the Inan Research Lab include contact accelerometers, electrical bioimpedance sensors, temperature sensors and inertial measurement units. In response to internal lab review as well as feedback from clinical affiliates, the wearable knee device underwent innumerable minor reforms and ultimately three global revisions. Later, in response to the COVID-19 pandemic, the device was adapted from knee monitoring to lung monitoring. All updates were made in various design categories, including robustness (e.g., water-tightness, component strength), ergonomics (e.g., comfort, adaptable sizing), and usability (e.g., labeling, designing for unfamiliar users), all while naturally prioritizing the base function and protection of the enclosed electronics. As a complementary aim, the accelerometer packaging was specifically optimized for clinical-usability and microphone performance. The following dissertation chronicles the entire aforementioned design process, including sample recordings and user feedback where applicable to support the usability of the various form factors.

CHAPTER 1. INTRODUCTION

Wearable health sensing devices have satisfied a critical need for inexpensive, unobtrusive, and convenient technology to longitudinally monitor physiological signals beyond the snapshots obtainable in the clinic. In 2013, the Inan Research Lab (IRL) identified such a need in joint rehabilitation, where millions of people annually navigate through knee injury recovery using primarily subjective metrics or a generalized timeline of anticipated full rehabilitation. While commercialized wearables commonly surveil signals like heart rate, activity level, or blood oxygen status, the Inan Lab sought to explore more creative modalities for the joint like multilocation digital auscultation via contact accelerometers and fluid presence assessment using electrical bioimpedance (EBI), all while synchronously tracking temperature and motion for contextualizing the audio/EBI signals. In the years following, IRL members have demonstrated the potential of these sensing modalities in isolation with custom built hardware, firmware and data analysis methods, successfully employing acoustic and EBI signals to distinguish between knees in various conditions - healthy versus arthritic [1-3], loaded versus unloaded [4, 5], and heathy versus injured [6-10]. With the sensing capabilities now highly supported, the time arrived to physically coalesce all modalities into a single, fully-untethered wearable apparatus, with the ultimate goal of translating the device from the lab to the clinic for further validation and eventually for at-home use. The following dissertation chronicles the mechanical design, testing and optimization of this all-encompassing wearable joint monitoring device through three

iterations, as well as the later adaptation for clinical lung health monitoring in response to the recent novel coronavirus disease (COVID-19) pandemic. Further, considering the sensitive nature of contact microphones, the accelerometer packaging itself was also iteratively optimized with regards to frequency response and clinical-readiness (i.e., water-tightness, robustness, ergonomics, etc.). To the best of the available knowledge, this apparatus as a whole is the first ever wearable device to combine physiological (i.e., fluid presence and kinematics) and structural (i.e., acoustics) measurements for both the knee and the lungs, specifically designed for use by naïve-users. Ideally, this device can one day complement the existing clinical approaches for diagnosis and monitoring, whether in the clinic or at home, ultimately enabling more objective and timely decision-making regarding knee and lung health.

CHAPTER 2. BACKGROUND

2.1 Overview

The body readily emits a variety of information with every passing second, whether electrical impressions from activating muscles or the animated brain, or mechanical signals from the beating heart or the breathing lungs, to name a few. Many of these signals can be perceived extracorporeally with the application of wearable sensing devices. In particular, wearable devices of late have employed kinematic, acoustic and/or bioimpedance sensors to noninvasively infer structural and physiological information about the body within. Two such anatomical locations that have been subjects of these specific sensing explorations are knee joints and lungs.

2.2 Knee Joint Pathophysiology and Assessment

The knee is the largest joint in the body, and being that it is among the three most weight-bearing joints (besides ankles and hips), and that its structural stability overwhelmingly depends on a system soft tissue in the form of cartilage and ligaments, the knee is particularly vulnerable to injury. On average, 18 million knee-related clinical visits occur each year in the United States alone [11]. Knee maladies commonly include acute injuries like anterior cruciate ligament (ACL) tears, medial collateral ligament (MCL) tears, or meniscus tears, or chronic knee conditions like rheumatoid arthritis (RA), osteoarthritis (OA), or tendonitis. Osteoarthritis alone impacts 25-30% of the entire adult population [11, 12]. Meanwhile, even after recovery from an acute injury, the knee is prone

to reinjury: for instance, 30% of knees with previously torn ACLs experience reinjury [13]. The symptomatic impact of such ailments ranges from swelling (edema), crepitus, reduced range of motion (ROM), pain and even loss of knee function [14, 15]. Unfortunately, the existing means of assessing these symptoms and their underlying causes include either expensive and/or invasive examinations like imaging or blood tests, or are more qualitative or observational (as opposed to objective) in nature (subjective pain reporting, ROM assessment, stability/capability assessment, or even simply time-passed since injury or surgery as compared to a typical recovery schedule) [16-18]. Furthermore, these examinations are generally inconvenient as they tend to occur within a clinical setting, and a single test rarely captures the whole picture of the ailing joint. In sum, acute injuries and chronic conditions of the knee impact millions worldwide, yet an inexpensive, comprehensive, convenient, real-time, non-invasive and quantitative means of knee assessment has yet to enter the market, leaving many in a state of limbo throughout recovery or through the course of their chronic experience.

2.3 Lung Pathophysiology and Assessment

Respiratory diseases are among the top ten causes of death worldwide, ranging from chronic conditions like emphysema, bronchitis, and chronic obstructive pulmonary disease (COPD), to environmental diseases like asthma, lung cancer, or mesothelioma, or those brought on by bacterial, viral, or fungal infections [19, 20]. Symptoms naturally vary per illness, but may include shortness of breath, fluid accumulation, coughing, chest tightness, discomfort, pain, and death [20]. A particularly harmful lung disease known as COVID-19 debuted onto the world stage at the end of 2019, reaching pandemic status by March of

2020 [21]. Symptoms of COVID-19 range from none at all (asymptomatic), to those previously mentioned, as well as fever, headache, digestive upset, fluid in or around the lungs (pneumonia and pleural effusions, respectively), as well as an uncontrolled production of immune cells known as cytokines, resulting in a harmful and even deadly "cytokine storm" [22, 23]. Such severe immune responses can progress further into syndromes such as acute respiratory distress syndrome (ARDS), systemic inflammatory response syndrome (SIRS), multiple organ dysfunction syndrome (MODS), and/or sepsis syndrome [22]. In a single study (N=201), more than 40% of all assessed patients developed ARDS, which is characterized by fluid filling the lung's alveoli, ultimately depriving the body of oxygen [24, 25]. Despite artificial ventilation for each of these patients, sadly half of them died. Likewise, the mortality rates for SIRS, MODS and sepsis syndrome alone are 7%, 50%, and >40% respectively, and only compound further when combined with each other and/or existing comorbidities [26, 27]. Initial COVID-19 studies thus far suggest that early identification of and subsequent intervention for cytokine storm and associated syndromes is critical for patient survival [23].

Lung conditions are clinically diagnosed and monitored in a variety of means, including auscultation with a stethoscope, imaging like X-rays, computed tomography (CT) scans, or magnetic resonance imaging (MRI) scans, blood tests, or impedance pneumography [28]. However, akin to the joint health monitoring and diagnostic tools, each of these sensing modalities either come at sizeable costs, are invasive or obtrusive, monitor in only discrete time intervals, or at the very least require a trained medical professional to make sense of the signal (in the case of the relatively simple and portable

stethoscope). Moreover, in the era of a highly contagious disease like COVID-19, health care workers (HCWs) have been forced to minimize their physical contact with COVID-positive patients for their own and others' safety. As such, there is a need for an inexpensive lung sensing system capable of longitudinal monitoring both in the clinic and at home, that could additionally simultaneously monitor the multiple symptoms indicative of the early onset of conditions like SIRS, ultimately for better patient outcomes.

2.4 Wearable Health Monitoring Devices

2.4.1 Overview

Wearable health sensing devices have assumed countless forms and functions since the rise of portable technology. These devices fill innumerable gaps created by obtrusive and expensive clinical testing like imaging or laboratory tests, measuring signals such as movement [29, 30], heart rate [30, 31], and oxygen saturation [32]. Form factors range from utilizing the sensors already equipped on a standard smart phone, to wrist watches, even to electronics embedded within flexible bandages or clothing [33]. Considering the ever-changing condition of the human body, from morning to evening, during rest or wakefulness, while under the weather or in wellness, the data obtained from wearable devices can paint a more comprehensive picture of the individuals wearing them as compared to isolated glimpses into one's health provided by a yearly physical or post-op appointment. In some instances, wearable health devices have granted freedom to those managing chronic illnesses, exchanging inconvenient and costly doctor's visits for autonomy and self-awareness.

2.4.2 Existing Non-Invasive Knee and Lung Sensing Modalities

Several non-invasive devices already exist, whether in literature or commercially, specifically for knee or lung monitoring, but few of them are fully wearable and even fewer integrate multiple sensing modalities at once. Concerning the knee, myriad devices exist for tracking gait, range of motion or joint angle [34, 35], often employing inertial measurement units (IMUs) as the primary sensor. Some devices use EBI to assess the presence of fluid (edema) and/or the general condition of the underlying soft tissues and joint spacings, and have been able to successfully sort healthy from unhealthy knees based on EBI signals alone [7, 36]. Acoustic emissions from the joint have also been of interest, being measured by various contact accelerometers [2, 8-10, 37], air microphones [38, 39], and even including one monitoring approach that is more commonly applicable to the lungs – stethoscopes [40, 41]. These acoustic emissions have been used to distinguish between loaded and unloaded joint conditions [8], between healthy knees and those recovering from a musculoskeletal injury [9], between healthy and arthritic joints [2], and between surfaces with normal and abnormal cartilage [40].

Existing devices for lung monitoring include respiration belts for monitoring respiration rate and tidal volume [42, 43], and wearable bioimpedance tomography apparatuses for assessing the respiration rate as well as lung ventilation and aeration [44, 45]. Lung health has additionally be characterized by acoustics, including the aforementioned ubiquitous stethoscope since its invention in 1830 [46], as well as more recent methods using contact accelerometers [47, 48]. As of yet, no COVID-19-specific devices have debuted in the academic or commercial arenas, although many have

recognized the need for such devices and have proposed the recombination of existing devices to fill this need [49, 50].

2.4.3 Proposed Sensing Modalities

While the previous sensing modalities are all promising in isolation, it was hypothesized by the IRL that a device encompassing not only acoustic sensors, but also the capability for EBI, as well as IMUs and temperature sensors for further contextualizing the acoustic and EBI data, could provide a comprehensive assessment of both structural and physiological health. In time, the data obtained from such a device could be fed into feature extraction and machine learning algorithms, which would ultimately generate a universal "joint health score" with which a clinician or an individual could make more objective decisions about their recovery status. The device was initially intended for the knee, and has since been reconsidered for lung health monitoring in response to the COVID-19 pandemic. While the COVID-19 effort is currently within the prototyping and initial testing phase, and therefore conclusions may not yet be drawn about the efficacy of the device, it may still be conceived that the four sensing modalities will serve slightly different purposes for the lungs versus joints. The microphones on the joint detect the aforementioned sounds which correlate to healthy vs. unhealthy knees, while theoretically the accelerometers on the lungs will perceive differences in lung sounds indicative of lung disease state. The joint EBI data reveals the swelling status of the knee, while the lung EBI will ideally confer whether or not fluid is in the lungs, and where, as well as patient tidal volume. The joint IMUs communicate the leg's position in space and time during flexion and extension, providing context for the joint sounds; meanwhile, the IMUs in the lung application will

largely provide context for the EBI recordings, considering fluid of a pleural effusion is gravity-dependent, so patient posture and position will be vital to deriving meaning from the EBI data. Lastly, the temperature sensor in the joint setting reveals information regarding inflammation of the joint, largely to be used in conjunction with the EBI data, while the lung temperature sensor will monitor fever status.

Many electronic challenges were faced and overcome by former students amidst the founding and progression of this system, including data storage, establishing a mobile power supply, or creating a system that could record such high-throughput signals on an untethered device. The following dissertation chronicles the evolution of the mechanical design of this system, including the eventual adaptation of the device for use on the torso for lung health monitoring, and the optimization of the microphone sensor housings.

CHAPTER 3. WEARABLE MULTIMODAL HEALTH SENSING DEVICE EVOLUTION

3.1 Prior IRL Versions

The joint sensing hardware existed in a few form factors before the conglomeration of all four sensing modalities into a single wearable device. The EBI system began as most projects do as a tethered benchtop setup, which was designed and validated by Hersek et al. for its ability to distinguish between injured and contralaterally healthy knees within a small (N=9) feasibility study [51]. The system consisted simply of the four necessary female electrode snaps and accompanying cables (positive current, negative current, positive voltage, negative voltage), the corresponding Ag/AgCl gel electrodes, and the benchtop electronics. By the following year, Hersek et al. had successfully adapted the device into an untethered, wearable form factor and also introduced accelerometers and temperature sensors for monitoring subject movement and tissue temperature respectively [7]. Now with a larger subject pool (N=49), Hersek et al. were once again able to discriminate between healthy and injured knees, as well as able to quantify the system's sensitivity using various tissue temperatures. Later, Mabrouk et al. improved upon the sensing hardware even further (new techniques for calibration and accounting for postural variations), and validated the updated hardware on the healthy versus injured ankles of eleven subjects [52].

The joint sounds sensing hardware likewise began as a benchtop system, first implemented by Töreyin et al. using a MEMS MP33AB01 miniature airborne microphone (STMicroelectronics, Geneva, Switzerland), and accelerometers for angle sensing [53]. This proof-of-concept system suggested that joint sounds, specifically the "clicks" that routinely characterize them, could be reliably measured even despite background noise. Soon after, Teague et al. further validated the findings of Töreyin et al., that joint acoustic events occur at repeatable joint positions within the flexion/extension cycle, as well as evaluated and compared the performance of two airborne microphones (the previously used MEMS MP33AB01, and a new electret microphone (COS11D, Sanken Microphone Co., Ltd., Japan)) and one contact microphone (piezoelectric film, SDT, Measurement Specialties, Hampton, VA, USA) [37]. The Teague et al. setup is shown in **Figure 1a**.

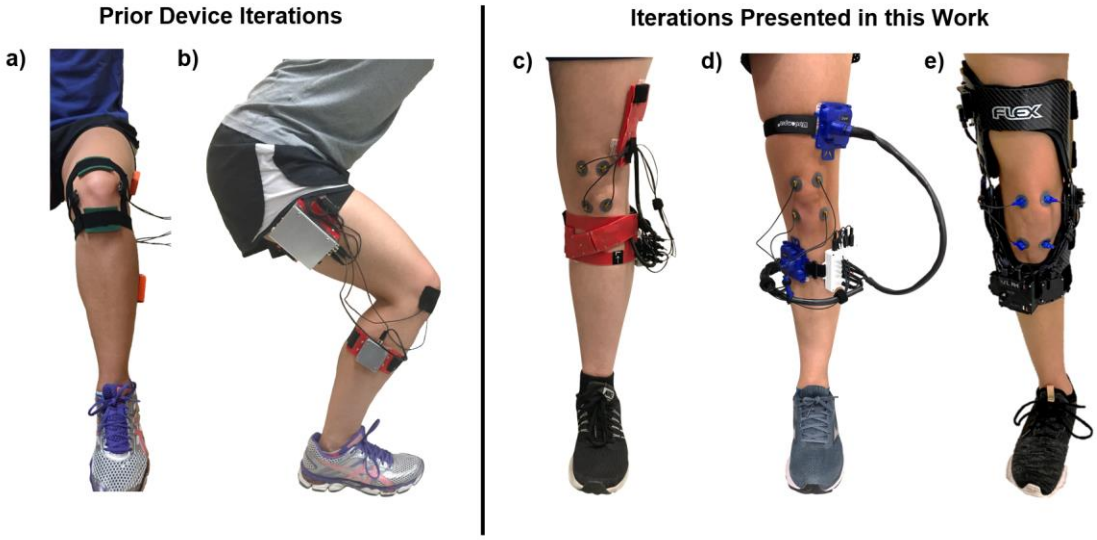

Figure 1. The evolution of the wearable joint sounds hardware. (a) System developed by Teague et al. for testing 3 microphone types (MEMS MP33AB01, piezoelectric film, COS11D electret microphone) and IMUs [37]. (b) The subsequent iteration that more closely approximated a wearable form factor, but was still tethered and bulky [54, 55]. (c)

The first fully untethered, wearable joint health system ("V1") to also include sensors for acoustic emissions, EBI recording, motion tracking, and temperature tracking. (d) The following iteration ("V2") with improved packaging and internal components for clinical robustness. (e) The latest iteration ("V3") where all components have been integrated into a COTS rigid knee brace.

At the conclusion of this study, the MEMS microphone was suggested as the least expensive and least-susceptible-to-noise microphone of the three tested, and was again tested in a new form factor which more closely approximated a long-term wearable solution (**Figure 1b**) [54, 55]; however, ensuing packaging concerns ultimately ruled this solution out. In a wearable knee health review later published by Inan et al., a new a piezoelectric contact accelerometer (BU-23173, Knowles, Itasca, IL) was introduced [56], and employed in a study performed by Jeong et al. which suggested a connection between joint loading and the subsequently generated joint sounds [8]. While the quality of this microphone did not quite compare to that of the Dytran contact accelerometer (series 3225, Dytran Instruments, Inc., Chatsworth, CA, USA) used in contemporary studies [1-4], the Knowles accelerometer was ultimately chosen for its still relatively high fidelity signal at a fraction of the cost. All joint sounds systems until this point were still tethered to benchtop data acquisition units and controllers.

3.2 Wearable Joint Monitoring Device Version I

3.2.1 V1 System Overview

With years of testing having validated the EBI and joint sounds capabilities in conjunction with the contextualizing IMU and temperature data, it was desired to finally A) incorporate all four sensing modalities into a single system and B) migrate the system

from the desktop to a fully untethered wearable form factor, with the ultimate goal of clinical implementation. As such, development for the first truly wearable and untethered version of a joint sound and motion sensing device that also included measurement capabilities for temperature and electrical bioimpedance was initiated, and is aptly referred to as the "V1" brace.

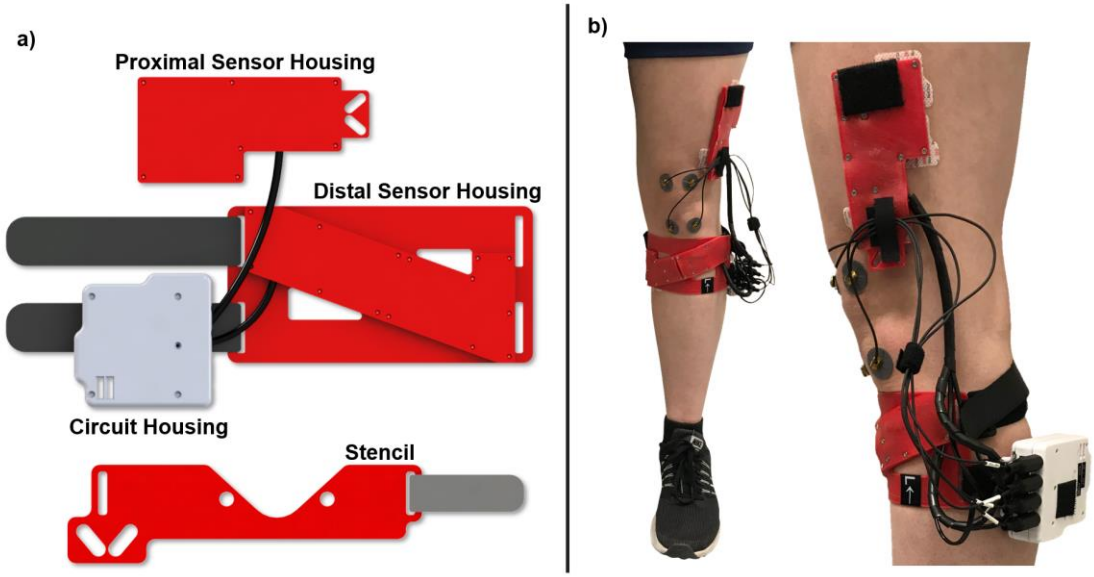

Figure 2. V1 brace overview. (a) Renders of the various 3D printed housings and the placement stencil. (b) The intended placement of the brace on the right leg, front view and zoomed side view.

A primary goal was to create a device that could appear readily familiar to new users despite being novel technology. Therefore, the design took inspiration from generic off-the-shelf flexible knee braces. There was also a concerted effort to make the donning process both intuitive and repeatable, and of course at a bare minimum an effort to protect the internal components.

The enumerated bill of materials for this V1 iteration can be seen in the Appendix, **Table 7**, with an overview of the design depicted in **Figure 2**. All electronic components were designed by Caitlin Teague, Alex Heller, and Samer Mabrouk. Broadly speaking, the packaging is composed of two distinct flexible sensor housings (one proximal, one distal) and one rigid case for circuitry storage. For ease of donning, a custom, flexible, anatomically-referencing stencil was also designed. The stencil and all housings were 3D printed on fused deposition modeling (FDM) printers (LulzBot and Ultimaker 3+) using either flexible thermoplastic polyurethane (TPU) or rigid polylactic acid (PLA). All housings attach to the body using either adjustable Velcro straps, adhesive-backed cloth electrodes, or a combination thereof.

Designed by Alex Heller, the rigid circuit case houses the custom audio printed circuit board (PCB), the custom "main" PCB (responsible for controlling the EBI, IMU and temperature sensors), two batteries, and the cable which connects the boards.

Personally designed, each of the flexible sensor housings contain one IMU PCB, one temperature PCB, two EBI electrodes, and all accompanying cables. The microphones remain independent from the housings besides the audio plugs which interface with the audio board, and are instead individually placed in an array around the patella using the stencil as a guide and double-sided foam Rycote "stickies" (Lavalier Adhesive Stickies, Rycote, Rycote Microphone Windshields Ltd, Gloucestershire, United Kingdom) as the adhesive.

3.2.2 V1 Design Review

While the system was functional, its performance was not sufficient for supporting translation to clinical settings. Each sensor type was capable of recording its respective physiological signal, but the connectors and cables which coordinated these recordings were unreliable. The housing attempted to mitigate this unreliability and, in some scenarios, did so successfully, but ultimately suffered from a few of its own inherent flaws as well.

In hindsight, this initial prototype fulfilled a tried and true tale – even a fully functioning bench top setup scarcely translates to a well-functioning packaged (and wearable at that) form factor on the first try. Nonetheless, many lessons were learned to be applied to the next iteration. An in-depth review of said "lessons" can be viewed below in **Table 1**.

Table 1. V1 design review. All electronic features may be credited to Caitlin Teague and Alex Heller, and features related to the circuit housing may be credited to Alex Heller.

	Line	Design Pros	Design Cons
Packaging-Related Features	1	First legitimate wearable and multimodal joint sensing approach to date	Switches are difficult to access manually (recessed deep within the case; requires tool like tweezers for use)
	2	3D-printed housing for rapid prototyping	LEDs obstructed by stacking the boards
	3	Compact (distal housing: 20cm x 10cm x 0.5cm, proximal housing: 15cm x 5cm x 0.5cm, circuit case: 2.5cm x 7cm x 7cm) and light-weight (<4lbs) packaging	Box assembly is difficult due to A) internal components that are positioned only in respect to other internal components as opposed to rigid external case references B) a double sided stacking process as opposed to a bottom up assembly C) lack of uniformity in hardware
	4	Flexible sensor housings for body contouring and mechanical compliance during motion	Multiple stencil sizes required for varying patient bodies
	5	Rigid circuit board housing for board protection	Use of hex nuts instead of preferred heat-set inserts due to too-soft filament choice (NinjaFlex, TPU 85A)
	6	Lower housing designed to imitate a COTS knee brace for both familiarity and comfort	Without intervention, the microphones freely dangle on the skin and potentially perturb one another. The Velcro routing strap on the proximal sensor housing helps but still results in some cable-sensor interference
	7	Readily-available low profile COTS hardware to secure all housings	Uncleanable spiral cable wrap for cable management, made even more difficult by inconsistent cable lengths and branching
	8	Adjustable/exchangable Velcro straps for attaching housings to body, further supported by adhesive gel electrodes yielding both secure attachment as well as adaptable sizing	Asymmetrical housings (i.e. distinct "left" and "right" braces would be required for feasible clinical deployment)
	9	All components conveniently stored in 3 housings	Relative large surface areas of housings which could potentially introduce more vibrations dermally
	10	Commercially available sensor cables (IMU and temp)	
	11	Custom flexible stencil that uses anatomical features for component placement, enabling accurate, consistent and therefore comparable sensor recordings. Usable by even inexperienced researchers/clinicians	
Electronic-Related Features	12	Two switches on audio board for switching recording mode (audio vs BIS) and to initiate/end recording	Full device disassembly required for electronic hard-reset (only achievable by unplugging/replugging batteries)
	13	>7 hours of battery life for continuous recording on audio board (realistically, even longer since a typical recording lasts fewer than 2 minutes)	IDC cables for the IMU and temp boards effortlessly break and/or disconnect amidst standard use
	14	>33 hours of battery life for continuous recording on main board (realistically, even longer since a typical recording lasts fewer than 2 minutes)	Fragile/unreliable custom BIS electrode snaps + cables (at both the electrode snap end and the coaxial connector)
	15	32GB storage on either board (typical audio file size: 12MB, and typical main board file size: 0.25MB)	
	16	Fully untethered system with battery power and local storage combined	
	17	LEDs to readily indicate device status (recording, charging, error state, etc.)	
	18	Micro USB ports on either board for easy computer interfacing	
	19	Custom computer application (Heart Pulse) for seamless data uploading	

3.2.2.1 Accomplishments

Despite some drawbacks which are discussed below, many noteworthy successes occurred in the mechanical design department of this first brace generation. For instance,

the flexible sensor housing material was specifically chosen for both convenient rapid prototyping on a 3D printer and for its ability to contour to the user's body, unlike the former metal housings of the latest wearable attempt. Furthermore, the components are lightweight and low profile, especially when compared to the large metal cube housings of their predecessor. Subtle features within the sensor housings like PCB "pockets" and wire "tunnels" aided in simple and organized assembly. Some of these successful features are demonstrated in **Figure 3**.

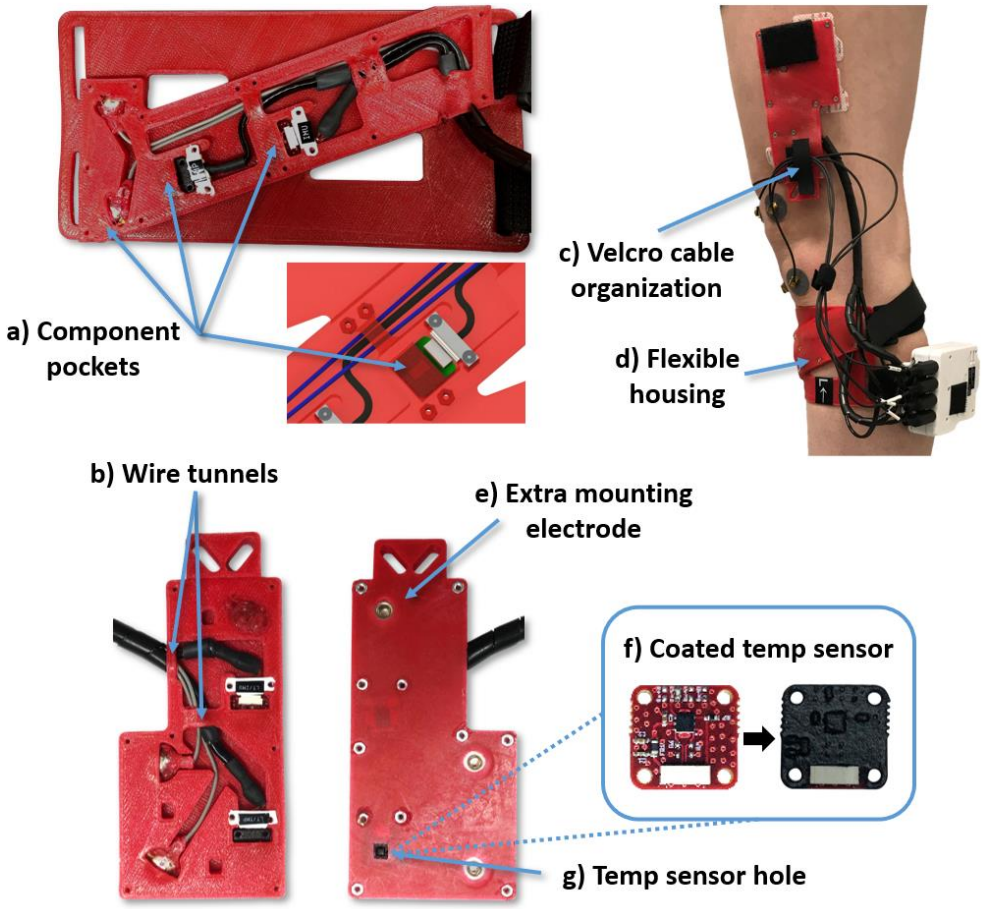

Figure 3. Noteworthy design features of the V1 sensor housings. (a) Built-in "pockets" for simple installation of the PCBs and electrode snaps. (b) Built-in "tunnels" for cable

management and protection. (c) Velcro mounting locations for cable routing. (d) Flexible sensor housings for body contouring. (e) Extra non-electrically connected electrode snap for increased mounting strength. (f) Temperature PCB coated in aerosolized rubber, PlastiDip, for electric insulation. (g) Hole in housing to maximize thermal transfer from skin to temperature sensor.

From an organizational perspective, the entire system is contained within three housings, two of which (the distal sensor housing and the circuit case) combine into a single assembly, ultimately yielding only two components and four microphones for the user to place. However, the user still needed a manner in which to do so, repeatably.

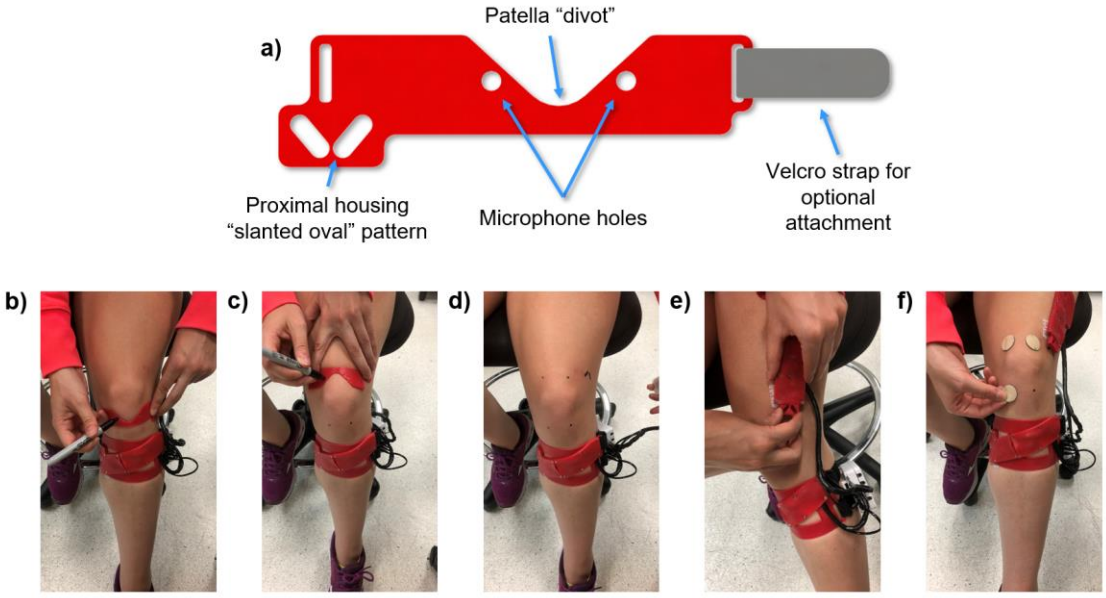

Figure 4. Process of device donning using the custom stencil. (a) Render of the 3D-printed flexible stencil with all features labeled. (b) Marking the distal microphone locations using the stencil and a marker. (c) Marking the proximal microphone locations using the stencil. Unpictured, the slanted oval pattern is also traced when the stencil is aligned for proximally, for later placement of the proximal sensor housing. (d) Picture of appropriate markings from the stencil. (e) Placing the proximal sensor housing using the slanted oval pattern as a guide. (f) Placing the Rycote stickies per the microphone stencil pattern.

As such, the stencil was born, in which a "divot" aligns with anatomical features (namely the distal and proximal edges of the patella) after which the user marks (with a

marker) the patterns in the stencil (**Figure 4**). For distal stencil use, just the two holes are needed for microphone placement; proximally, the user marks the two microphone holes as well as the slanted oval pattern which can be later matched to the identical pattern on the proximal sensor housing **(Figure 4e**). The microphone locations were previously validated in the aforementioned studies [2-4, 8, 9, 39, 54]. Theses angled lines (as opposed to straight lines, a box, or many other patterns) ensure that the proximal housing is accurately placed both horizontally and vertically. The stencil guarantees that the IMU is located as medially as possible to the leg of choice for optimal sensing, as well as promotes the proper vertical and lateral distances of the EBI electrodes relative to the joint [7]. Furthermore, considering that for joint acoustics, the positioning of the microphones with respect to the joint may influence the type of sounds measured, and that for EBI measurements, the electrode spacing must be maintained to capture the same segment of the limb and thus the same gross tissue volume measured, consistent placement is paramount. In sum, this simple stencil not only enables ease of use for device-naïve users as confirmed by early internal UMinn clinical partners, but also fosters the consistent placement of sensors in their intended locations, and furthermore that longitudinal recordings may actually be reliably compared to one another.

Notable successful electronic features contributed by Caitlin Teague and Alex Heller include those that promote ease of use for unfamiliar users, such as light emitting diodes which indicate device status; switches to control recording mode and initiation/termination; microSD cards for local storage; batteries for local power; microUSB ports for simple computer interaction; and a custom computer application called

Heart Pulse for seamless uploading of the deidentified patient data. With the local storage and battery power combined, the system is fully untethered from any benchtop setup.

3.2.2.2 Challenges

Despite the systems' few broad successes, many individual challenges prevented it from ever being deployed clinically. The issues were varied, from hardware challenges, to basic ergonomic issues, and a few ultimately fatal complications pertaining to sensors and cables. Some of these challenges are demonstrated in **Figure 5**.

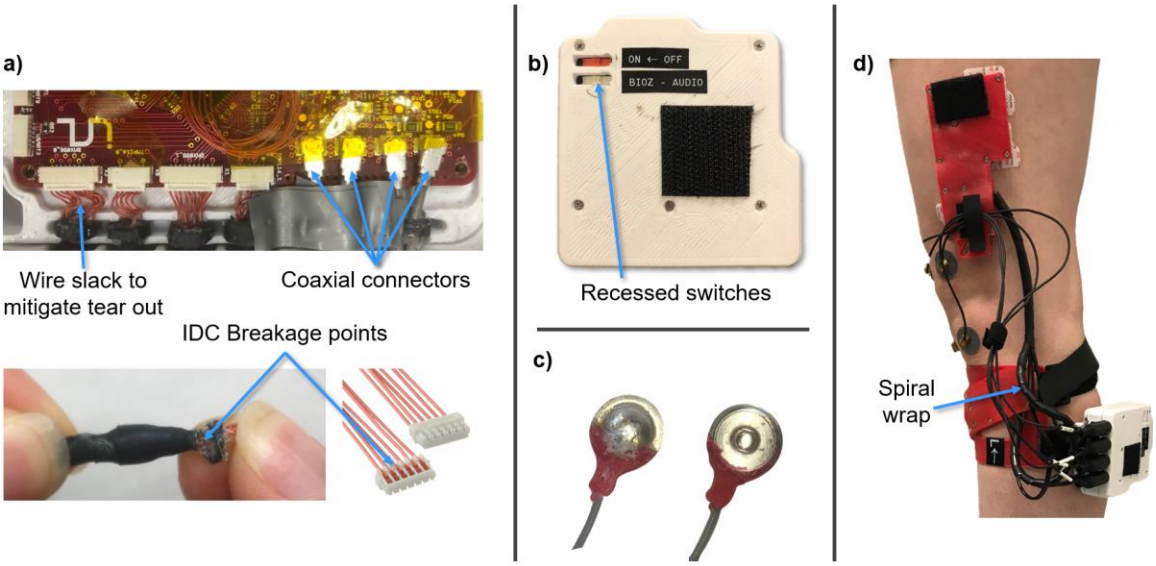

Figure 5. Various challenges with the V1 brace. (a) Finicky and fragile IDC cables and coaxial connectors. Using heat shrink as pull relief mitigated damage, but the cables were ultimately still too fragile. Tape reinforced the coaxial connectors, but they too continued to disconnect despite efforts. (b) Power and mode switches too recessed for reasonable/convenient use. (c) Fragile manually built electrode snap cables. Melted plastic

attempted to reinforce the junction, but they continued to break. (d) Convoluted wire routing, and spiral wrap not suitable for clinical sanitization.

The circuit case restricts easy access to the switches within by virtue of too-deep switch wells (**Figure 5b**), obstructs LED visibility simply by the manner in which the boards are stacked, and was difficult to assemble. Meanwhile, the sensor housings suffered from hardware tear-out due to the too-soft filament.

The most critical issue for the V2 brace however entails the fragile insulation displacement connector (IDC) cables required for communication between the main board and the four sensor boards (two IMU and two temperature). While the cables are commercially available and off-the-shelf (COTS) which circumvents the hassle of having to manually constructing them, the cables lack any form of strain / flex relief. As such, the individual wires frequently broke away from the plastic terminal, “breaking” the device as a whole since the main board will not initiate unless all sensors are detected. Heat shrink was introduced in a variety of approaches in an attempt to ameliorate the tension on the cables (**Figure 5**), but these were merely stop gap solutions. The housing was modified to encase the cables for as great of a length as possible to prevent environmental exposure, but this solution had the unfortunate trade off of increased skin surface area contact, which naturally has the potential to introduce more unwanted rubbing vibrations into the skin to be detected by the accelerometers.

The accelerometers and the EBI electrode cable assemblies presented some issues as well. It was soon realized that the mic wires required some manner of routing them off and away from each other and the skin otherwise rubbing/bumping would ensue. As shown

in **Figure 3**, a simple pair of Velcro strips served just that purpose, yet the process of securing the mic wires was tedious and imprecise and occasionally still failed to prevent the wires from rubbing. More critical however was the EBI electrode cable. Following a previously established work instruction, the EBI electrode snap cables were made in-house by soldering an insulated lead directly to the back of a bare electrode snap. These solder joints were then protected with a melted plastic coating (**Figure 5**). Despite being reinforced, however, these joints were finicky and brittle, in part due to an existing layer of inert material on the electrode which made soldering difficult as many materials refused to bind, and what did bind was often effortlessly snapped off. Therefore, not only were the electrode cables time consuming and tedious to produce, but also fragile. Meanwhile, the other end of the EBI cable was a coaxial connector which would effortlessly disconnect if torqued even slightly. A strip of tape attempted to mitigate disconnects, but sooner or later the cables would again detach.

Broader challenges include the device being asymmetrical, or in other words, incapable of being used on the contralateral leg as is. As such, a clinic would require two complete working devices for data collection, one for the left leg and one for the right. Moreover, too many steps were needed for setup (marking mic and sensor housing locations proximally and distally, placing the distal housing and case, placing the proximal housing, then the four mics). Due to inconsistent cable lengths extending from the case, the cables were also difficult to neatly organize. A simple spiral cable wrap was employed in an attempt at cable consolidation, but this wrap was by no means up to clinical standards

considering the consistent spiral opening down the length of the wrap rendered the cable bundle nearly impossible to realistically sanitize (**Figure 5**).

Overall, while many of these design flaws could be better summarized as inconveniences, the IDC cable and EBI electrode issues were simply insurmountable. The system was fragile and thereby unreliable, hence development of the second version of both the circuitry and the housing began almost immediately.

3.3 Wearable Joint Monitoring Device Version II

3.3.1 V2 System Overview

After the many aforementioned challenges of the V1 device, the scope of this particular stage of prototyping was re-evaluated. It was decided that the overriding goal at present was to assess the effectiveness and usefulness of such a device, more specifically the new *internal* technology, in a clinical setting.

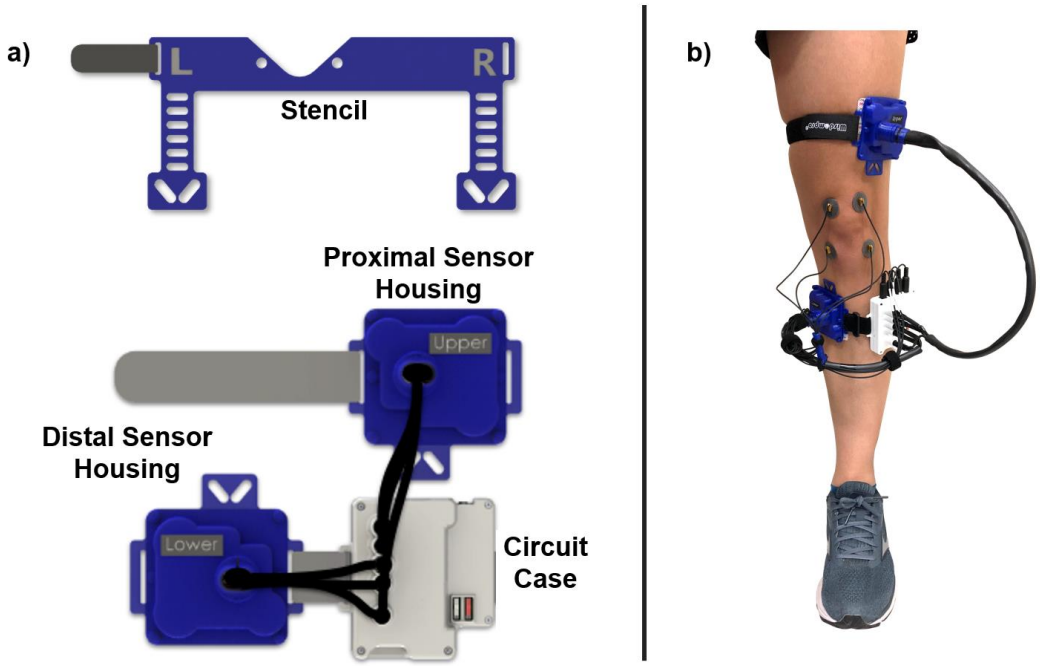

Figure 6: V2 brace overview. (a) Renders of the various 3D printed housing and the placement stencil. (b) The intended placement of the brace on the left leg.

With this in mind, aesthetic concerns were not heavily weighed, and the housings were optimized for efficiency and function, from both a manufacturing and a user experience perspective. In theory, once the technology itself was validated, *then* form factor could be prioritized, by per se incorporating all components into a pre-existing COTS knee brace (i.e., the later V3 brace). The bill of materials for this second iteration can be seen in **Table 8**, with the changes since the last version highlighted in green, revealing that nearly every component experienced a change in some form or fashion. An overview of the V2 brace can be seen in **Figure 6**, with a detailed exploded view of the housings in **Figure 7**.

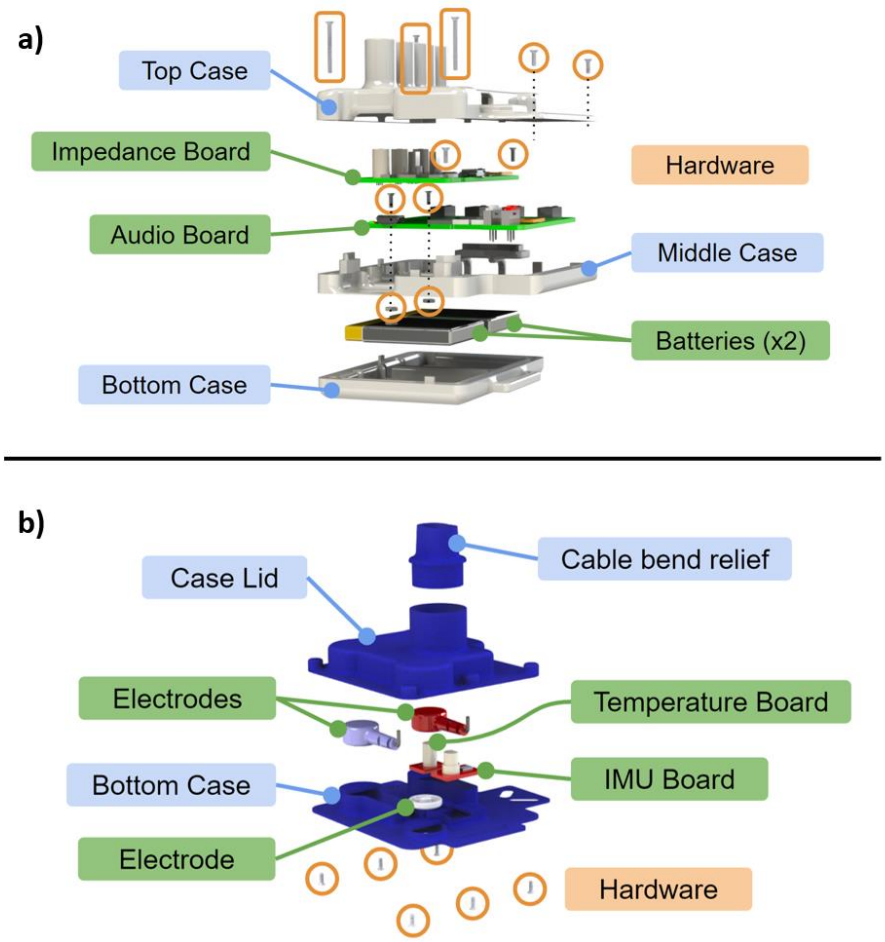

Figure 7. V2 exploded views. (a) Exploded view of the circuit board housing. (b) Exploded view of the sensor housing which is used both proximally and distally, reducing manufacturing complexity. The sensor "pocket" technique was continued from V1, as well as a hole through the base for the temperature sensor.

Akin to the first version, the V2 design consists of a rigid circuit case that houses an audio board, a main board, the cable which enables them to communicate, and the two batteries which power them; two flexible sensor housings (one proximal and one distal) which each contain two EBI electrode snaps, one temperature board, and one IMU board; one flexible stencil for device donning; and four individually placed microphones (**Figure**

6 - Figure 7). The battery life, memory space, LED indicators, simple switch control, USB data transfer capabilities and convenient Heart Pulse application were all preserved.

While the housing functions remained the same (to house and protect the components within), their form factors changed dramatically. Both minor changes like material choices as well as substantial changes like connector replacements yielded repeatable and reliable results, as discussed below.

3.3.2 V2 Design Review

Overwhelmingly, this new version has been a success, so much so that Caitlin Teague et al. published a paper on the early promise of the V2 brace (pertaining to both the electronic embedded systems and the ergonomic design), before even being deployed clinically [57]. The device has since been readily integrated into its intended purpose: a clinical study funded by the Defense Advanced Research Projects Agency (DARPA) conducted in collaboration with affiliates at the University of Minnesota (UMinn) assessing the ability of a multimodal joint health sensing device to monitor the joint health of patients with rheumatoid arthritis. So far, both the subjects themselves as well as the researchers/clinicians coordinating the study largely approve of the device. From both internal and clinical testing, it has been deduced that, unlike V1, the drawbacks of V2 largely pertain to aesthetics or unintended consequences faced in the manufacturing process, but not overall functionality. A summary of the V2 design review can be seen in **Table 2**.

Table 2. V2 design review. All electronic contributions were performed by Caitlin Teague, although the decision-making process was often collaborative.

	Line	Design Pros	Design Cons
Packaging-Related Features	1	More user-friendly assembly process (fewer and more modular case components, all externally-referencing placements, batteries localized in base of case, bottom up build procedure, uniform hardware)	Despite having the stencil, placement is still not always intuitive as A) patella is not always palpable, B) the housings are dissimilar from any recognizable knee brace
	2	Smaller package surface area on skin (__ vs __), which in turn reduces potential for added dermal rubbing vibrations	No improvement in number of donning time/steps since previous iteration
	3	Achiral design (i.e. a single device can be used for both left and right legs by simply reversing the distal sensor housing Velcro strap and the accompanying circuit case)	Housings are not waterproof/debris-proof
	4	Adjustable/changeable Velcro straps for attaching both sensor housings to the body, further supported by adhesive gel electrodes yielding both secure attachment as well as adaptable sizing	Connectors/cables all exit the circuit case and sensor housings in obtrusive paths (mics and main board connectors perpendicular to each other at the circuit case; sensor housing bundles perpendicular to the skin's surface) in part due to the new straight Omnetics connectors as opposed to say a right angle connector
	5	Custom flexible stencil that uses anatomical features for component placement, enabling accurate, consistent and therefore comparable sensor recordings. Usable by even inexperienced researchers/clinicians	The adhesive in the Kapton tape which secures the accelerometer solder joints eventually wears out over time, lessening the solder joint protection and introducing noise from loose tape rubbing the skin
	6	Abundant labeling for ease of donning/recording	
	7	All LEDs now visible due to A) improved board stacking and B) custom dual-extruded circuit case, featuring LED "windows" made of semi-transparent PLA filament	
	8	Improved accessibility to typical-use switches, while maintaining deep recesses for the new hard-reset switches to avoid accidental switching/resetting	
	9	Built-in bend relief solutions for both cases (sensor housing "plug" solution and circuit housing Omnetics connector "channels" and later zipties)	
	10	Now more durable Cheetah flexible filament (TPU 95A) for the sensor housings, enabling the use of more convenient heat set inserts for hardware attachment	
	11	Custom heat shrink solution for graduated bend relief on new Omnetics connectors	
	12	Loosened constraints on housing as a cable protection source since the cables themselves are now stronger, yielding smaller sensor housings and a reduction in skin surface contact	
	13	Flexible silicone heat shrink sleeving over entirely of sensor cable bundles (save microphones) for added protecting and to enable sanitization	
	14	Custom mic standoff for securing/routing the mic wires off and away from the skin	
	15	External Omnetics connectors to enable modularity (sensor bundles can easily be swapped between units)	
Electronic-Related Features	16	New stronger Omnetics brand connectors to replace the IDC connectors of the temp and IMU boards, and the coaxial cable of the BIS electrodes. Also new ability for custom cable lengths as well as latching option for more secure attachment	New hard-reset battery switches difficult to implement as the battery cable and case must both be retrofitted/adapted to accommodate a new switch
	17	Additional battery hard-reset switches for both boards, enabling easier system resetting without having to disassemble the device	Tedious and longer manufacturing time for A) soldering leads to the new Omnetics connectors (to build the custom IMU, temp, and BIS cables) and B) soldering the board-mounted Omnetics connectors to the boards
	18	Smaller (from 3.5mm to 2.5mm) audio jacks on audio board, allowing both space savings and protection from accidental foreign plug-ins considering the less common commercial use of 2.5mm audio plugs	Complicated and tedious cable splitting/organization into respective sensor bundles using heat shrink
	19	New more robust COTS overmolded electrode snaps to replace the former brittle custom made BIS snap + cable assembly	Mic wires excessively long which causes cable management issues and bump risks (which could introduce audio signal artifacts)

3.3.2.1 Accomplishments

Temporarily prioritizing function and efficiency over aesthetics enabled the V2 packaging to overcome many of V1's challenges. For instance, the sensor housings were reduced in size to a footprint just large enough to contain all necessary components, which reduced the surface area of contact with the skin, thereby lessening the theoretical vibrations introduced dermally. This size reduction was made possible in part due to the now stronger sensor cables which no longer required excessive housing for additional protection (more on this later).

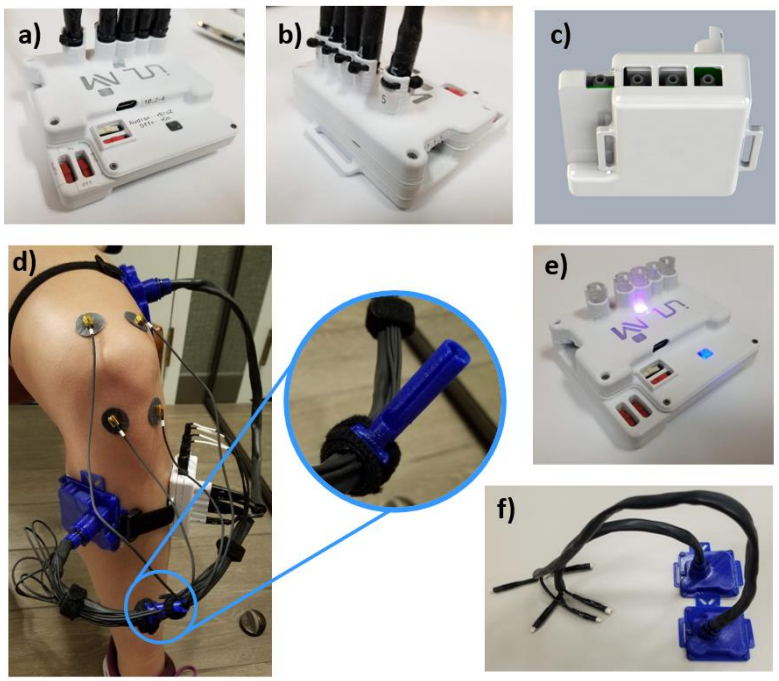

Figure 8. Noteworthy design features of the V2 design. (a) Labels for ease of use, new battery hard-reset switches for simpler troubleshooting and power cycling, and easier access to the typical use switches. (b) Built-in bend relief conduits, with added zip ties to prevent cable disconnection. (c) Built-in loops for Velcro strap attachment. (d) Microphone "standoff" designed by Caitlin Teague to route the mic wires off the skin and mitigate

bumping. (e) Built-in clear plastic “windows” for seamless LED viewing. (f) Silicone heat shrink for flexible cable consolidation that also permits cleaning.

Additionally, the new housings have no “sidedness”, i.e. are applicable for use on either leg with a simple reconfiguration of the Velcro straps. The circuit case meanwhile was optimized for modularity (largely to aid in component swapping in the case of troubleshooting or repair), as well as with assembly/disassembly in mind (consolidated hardware types, single-sided bottom-up assembly direction, fewer pieces overall). In the electronic design, two new switches were also added by Caitlin Teague to serve as hard-reset battery switches to be used in the event of device error and/or troubleshooting; these were intentionally recessed as compared to the typical use switches to prevent accidental resetting. Simple yet impactful changes also include improving the normal switch accessibility (**Figure 8a**), adding LED “transoms” in the circuit case for better LED visibility (**Figure 8e**), equipping both sensor housings with built-in bend relief features (**Figure 8b**), organizing the sensor cables into two sanitizable heat-shrunken bundles (**Figure 8f**), and abundantly labelling the housings (**Figure 8a**). These added features along with the carried over stencil method for placing the housings and mics overall elicited positive feedback from device-naïve and non-engineer users.

Perhaps the most impactful update however entailed transitioning from the fragile IDC connectors (for connecting the temperature and IMU boards to the main board) and the finicky coaxial connectors (of the EBI electrode cables) to the more robust COTS Omnetics brand connectors (**Figure 9**). These individual connectors are small (largest connector used is 7mm in diameter and 8mm tall) yet strong due to their plastic overmold.

Custom cables were manufactured in house, which allowed for cables to be made in the exact desired lengths. To protect the integrity of the solder joints, a system of layered heat shrink was devised to behave as a graduated bend relief and to also redistribute pull forces onto the plastic connector rather than the solder joints (**Figure 9**).

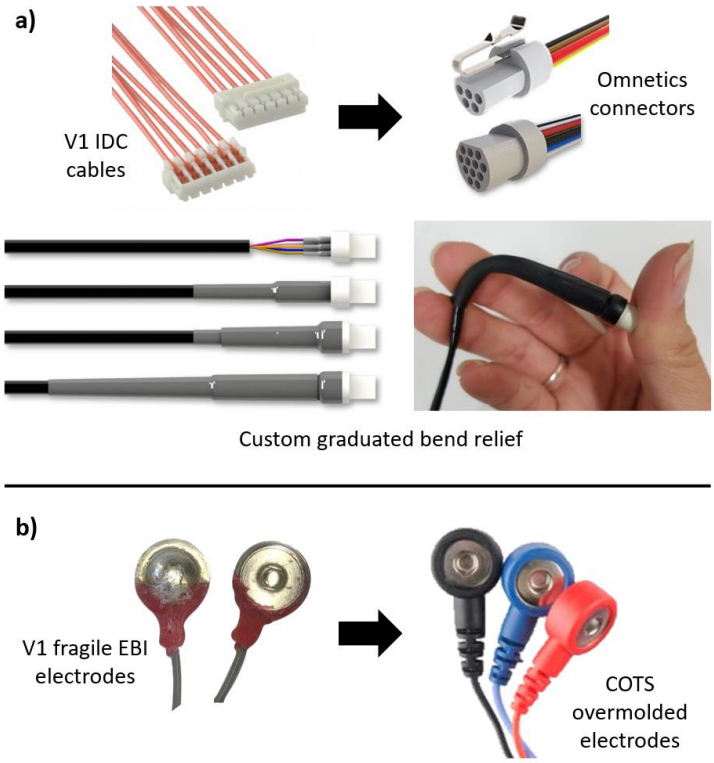

Figure 9. V2 cable improvements. (a) The former fragile IDC cables were exchanged for more robust Omnetics connectors to be used in custom-built cables. A system of graduated bend relief using layers of heat shrink of varying durometers was devised to protect the solder joints. (b) The fragile V1 EBI electrodes were replaced by COTS overmolded snaps.

Likewise, the previously fragile EBI cables/snaps were also overhauled by a new COTS overmolded electrode snap and cable (**Figure 9**). Not only does the new electrode snap overmold ensure the integrity of the electrode and corresponding conductor

connection, but also the open lead can be soldered directly to an Omnetics connector, replacing the unreliable coaxial connector as well.

While the microphone assemblies received no such modifications, the method of routing the cables away from the skin was improved. Caitlin Teague devised a simple yet effective flexible hollow tube, deemed the "mic standoff" which directs the wires away from their dermal contact points nearly tangentially, as opposed to the less optimum lateral routing of V2, reducing the potential for wire-related signal artifacts (**Figure 8**).

A proof-of-concept recording from the V2 brace is reported in **Figure 10**-**Figure 12** where all four biosignals were measured from a single healthy subject (female, age: 27 years, height: 165 cm, weight: 52 kg). The data were recorded under a protocol approved by the Georgia Institute of Technology Institutional Review Board per the following previously established joint sounds and EBI protocols: for the joint sound measurement, the subject completed 10 cycles of unloaded, seated flexion/extension exercises with the microphones attached in an array surrounding the patella using Rycote stickies; EBI measurement was recorded with the subject in a relaxed, seated position with legs fully extended and supported for 10 frequency sweeps from 5kHz-99.605kHz [56]. Similarly, the data were processed akin to previous methods. The accelerometer data were bandpass filtered (1 kHz – 10 kHz) and plotted with respect to the synchronously recorded IMU data, which was converted into flexion/extension angle per the algorithm presented by McGrath et al. [58]. Per the Mabrouk et al. calibration method, the raw EBI data was converted into actual impedance values, which were then ensemble averaged and plotted [52].

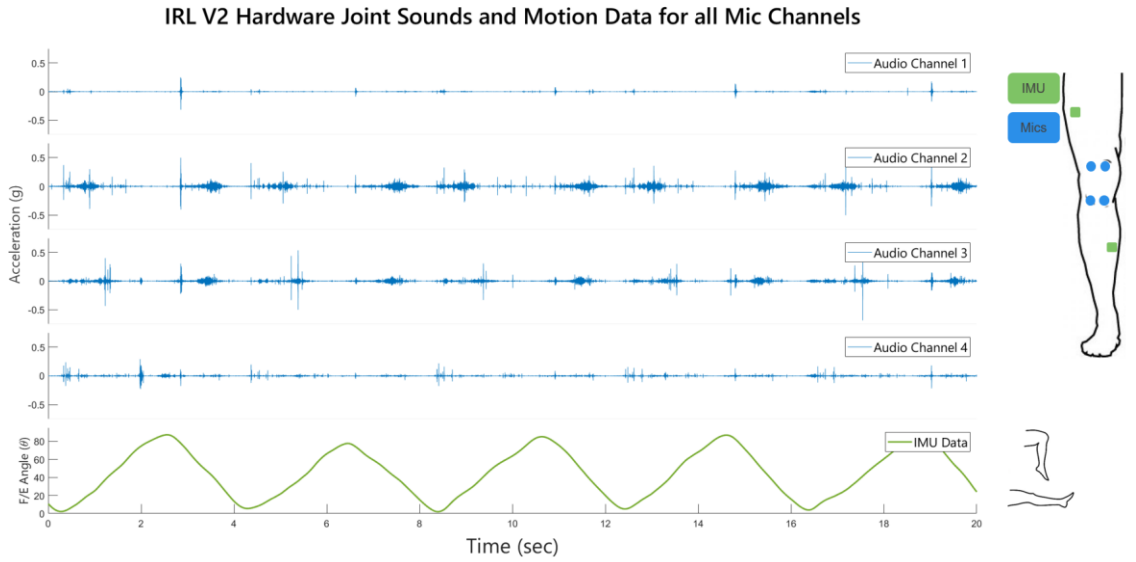

Figure 10. Proof-of-concept audio and IMU data from the V2 joint sensing brace. The signals are consistent with previous joint data in that cyclical "clicks" occur in the joint sounds as the leg moves through the flexion/extension cycle.

The figures depict results consistent with previous findings – joint sound "clicks" (i.e., high-amplitude, short-duration, broad bandwidth events) appear cyclically and consistently across the flexion/extension exercises [37], and the EBI data demonstrates remarkable repeatability, with all sweeps remaining within 1 ohm of the ensemble average. The spectrogram in **Figure 12** also mimics that depicted by Hersek et al. [6] with an elevated frequency/power content near the 10kHz microphone natural resonance, with another concentration of information below 5kHz, all generally organized in vertical "bands" of high-content joint sound events, to relatively quiet gaps in between.

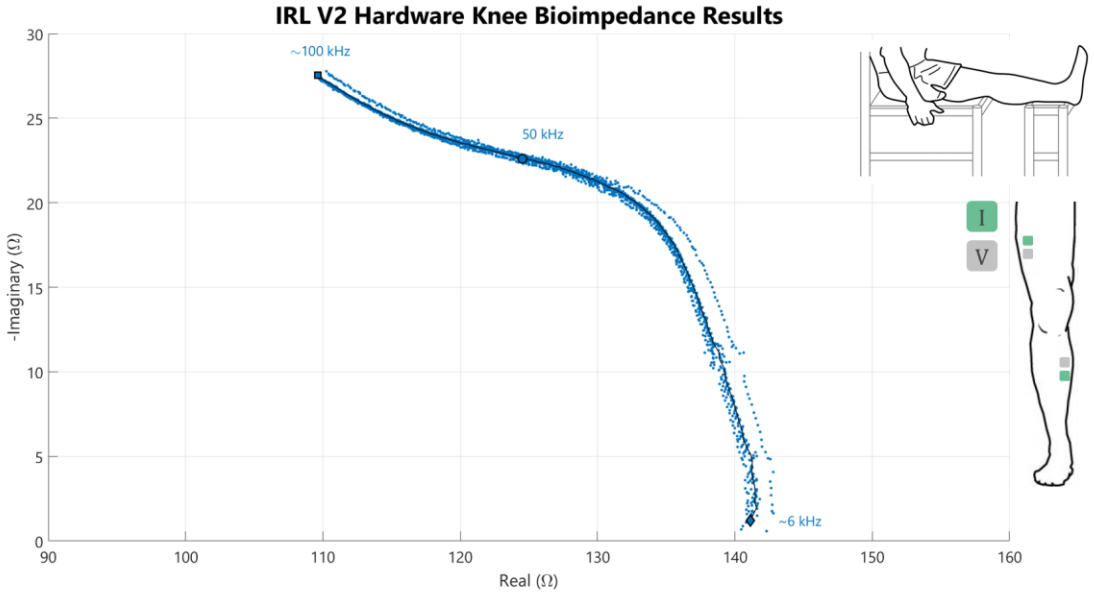

Figure 11. Proof-of-concept EBI data from the V2 joint sensing brace. The data mimics that of prior studies, with repeatability across sweeps within one ohm of the ensemble average.

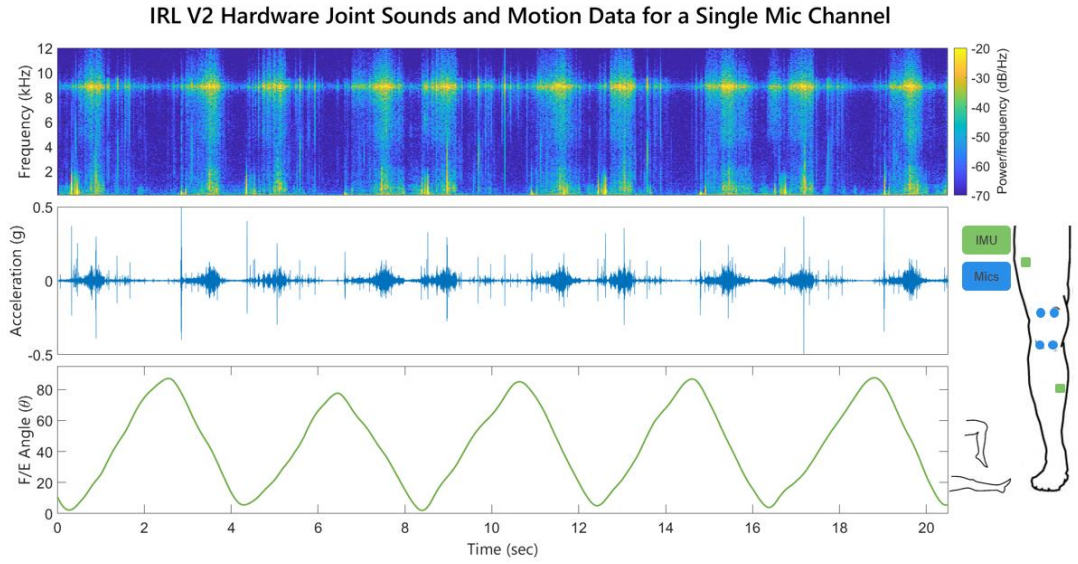

Figure 12. Proof-of-concept audio and IMU data from a single mic channel. The spectrogram reveals the expected 10kHz resonance of the Knowles microphone, as well as bands of activity followed by relative "quiet" as the joint cycles through click events.

Since the use of these signals as physiological markers of joint health has already been supported in previous studies [56], this brief initial testing was intended to simply demonstrate the feasibility of the technology in this new wearable form factor during a typical use case. Overall, this test confirmed the early technical and ergonomic functionality of the device. The ability of the device to discern between healthy and unhealthy knee joints is yet to be revealed by the final results of the UMinn study.

Lastly, as part of the UMinn RA study protocol, the participants have provided feedback about the brace which has so far been compiled below in **Table 3**. The responses have been color-coded in accordance to the tone of their feedback in regards to the brace itself (green for positive feedback, orange for negative, or gray for neutral or unrelated to the brace).

Upon first glance, one can observe that the reception of the device was largely positive. Most notably, participants overwhelmingly indicate that the brace is unobtrusive and easy enough to don that they themselves would be willing to attempt use even on their own, and daily at that. The questionnaire also reveals that many people do indeed experience confusion about their RA, whether in regards to severity or unpredictability, and could appreciate a monitor that would ultimately enable them to regain some amount of control over their chronic illness. One participant even described that even though existing RA lab tests may be informative, they poorly correlate to the real-world experience of pain, and was hopeful that such a device could fill that gap. A discussion of the critical feedback received from study participants can be found in the below section, 3.3.2.2 Challenges.

Table 3. V2 brace user feedback collected from University of Minnesota rheumatoid arthritis study by the UMinn study coordinators. Colors correlate to the tone of feedback as it pertains to the brace (green = positive, orange = negative, gray = neutral or unrelated). N/A indicates that the question either wasn't asked, or was asked but not answered.

Question		Subject						
		1	2	3	4	5	6	7
1	Were you comfortable with length of recording?	Yes	Yes	Yes	Yes	Yes	Yes	Yes
2	Any discomfort with the brace?	N/A	No	Yes*	Yes*	No	No	No
3	Would you be willing to do recordings at home?	Yes	Yes	Yes	Yes	Yes	Yes	Yes
4	If so, how often?	Daily	Daily	Daily	Daily	Daily	Daily	Whatever is needed
5	Would you be able to don the brace by yourself?	N/A	N/A	Yes	Yes	Yes	Yes	Yes
6	Do you ever experience confusion about the severity of your rheumatoid arthritis?	No	No	Yes	Yes	Yes	Yes	No
7	Would knowing when your arthritis is flaring up help you better meter your activities?	No	Yes	Yes	Yes	Yes	Yes	Yes
8	Would it be valuable if this device was able to give you an early warning to worsening condition?	No	Yes	Yes	Yes	Yes	Yes	Yes
9	Was the concept of using the sounds your joints make to understand your arthritis interesting to you?	Yes	No	Yes	Yes	Yes	Yes	Yes
10	Would you recommend other patients volunteer for this research study?	Yes	Yes	Yes	Yes	Yes	Yes	Yes
11	Can you think of any changes you would make to the brace?	N/A	No	No	Yes**	No	Yes***	No
12	Do you wear, or have you worn in the past, any braces or knee sleeves regularly?	Yes	Yes	Yes	No	Yes	No	No
13	If so, can you describe the type of brace, sleeve, or other support materials worn?	N/A	Cloth wrap with velcro straps	Soft sleeve and brace	N/A	Neoprene sleeve	N/A	N/A
14	Any other comments about the biosensors part of the study?	N/A	Interested in study outcome	No	No	Kind remarks to Georgia Tech	No	No

* "Heavy after flexing/extending so many times"
** "Make it more like a knee brace; encase the cables internally"
*** "Electrode snaps are difficult to attach, and switches are hard to access"

3.3.2.2 Challenges

The prevailing negative feedback from participants revolved around ergonomic factors, perhaps to be expected as functionality was prioritized for this iteration. Two participants highlighted the need to make the device as lightweight as possible, as after many flexion/extension cycles their legs became tired. One subject suggested a housing in which all cables were encased, as opposed to the current solution with two large cable bundles protruding from the circuit housing; another cited that the cloth electrodes were difficult to attach to the corresponding electrode snaps as the flexible case would deform in the process. Two participants reported having a general lack of interest in or perceived usefulness of another means of quantitatively assessing their RA, although both of these subjects still stated they would be willing to use the device at home as well as recommend the study to others.

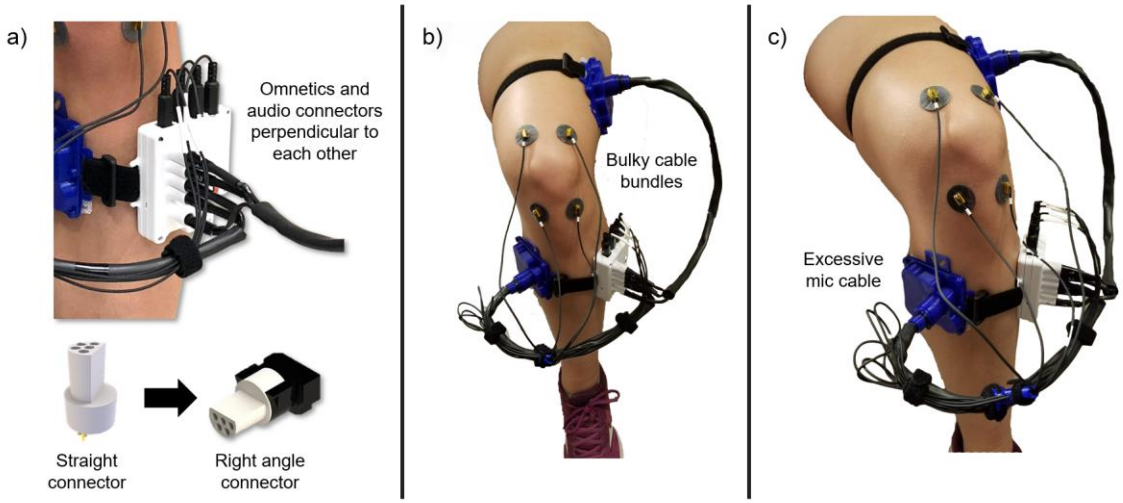

Figure 13. Various challenges with the V2 brace. (a) The Omnetics and audio cables exit the case perpendicularly which is aesthetically unappealing as well as bulky and perhaps

confusing to an unfamiliar user. Future versions will explore the use of right-angle connectors instead. (b) The cable bundles protrude noticeably from the brace. (c) The mic cables are excessively long and as such require additional cable routing; the excess cables run the risk of introducing artifacts into the audio signals by bumping.

Other challenges with this device include the fact that it is not waterproofed/debris-proofed, i.e. is susceptible to damage from bodily fluids like perspiration or general dirt. As both an ergonomic and aesthetic concern, the audio jacks and Omnetics connectors exit the case perpendicularly to one another, increasing both damage risk and unsightliness (**Figure 13**). Additional dual ergonomic-aesthetic concerns are the bulky cable bundles that extend to each sensor housing. While the EBI cables within are quite flexible and compliant, as well as the outermost soft silicone heat shrink, the IMU and temperature cables do not follow suit, resulting in a semi-rigid obtrusive bundle that bows out from the body on both the proximal and distal sensor housings. One factor in both of these design flaws (cables exiting the case perpendicularly and the protruding cable bundles) was the choice of the straight board-mounted Omnetics connector, as opposed to right-angle connectors which simply had not been known of at the time of board design (**Figure 13**).

Despite the integrity of the sensor assemblies improving dramatically with the exchange of IDC for Omnetics connectors, as well as abandoning the manually-built electrode snaps for the COTS overmolded snaps, many new issues arose, specifically in the manufacturing realm. For instance, in the process of replacing the EBI coaxial connectors on the main board, all four electrode positions (I+, I-, V+, V-) were loaded onto a single Omnetics connector, rendering the cable routing quite tedious and convoluted. Meanwhile, the Omnetics connectors required timely and careful manual soldering, both

for the cable manufacturing as well as for board attachment. Eventually, a custom cable manufacturer (Cable Quest, Ball Ground, Georgia) was contracted to reduce error and regain internal manufacturing time, but regardless it became abundantly evident that the ideal long-term solution must entail a connector and accompanying cable that are both durable and available in custom lengths (unlike the V1 IDC connectors) and COTS (unlike the final cable assemblies using the Omnetics connectors).

The microphones presented some issues as well. First, the cables were unnecessarily long (with the original intention of always ensuring having enough cable), which yielded the unintended consequence of convoluted cable management to mitigate noise artifacts from loose wire being bumped/tugged (**Figure 13**). While the mic standoff certainly assisted in this process, the portion of cables routed along the sensor housing bundles were still vastly exposed and thereby prone to bumping. Moreover, in repeated practice, the Kapton tape solution for protecting the mic solder joints proved mechanically insufficient over time due to loss of adhesion. Ultimately, the need for better cable management and a more robust solution for protecting the microphone solder joints, all while preserving the mic's frequency response in the desired joint sounds bandwidth became apparent. Meanwhile, on the other end of the microphone cable, the board mounted audio jacks with which the microphone plugs interface were frequently accidentally ripped from the audio PCBs during standard plugging/unplugging of the audio cables, stripping the solder pads in the process, and ultimately rendering an entire unit broken.

Lastly, while the custom stencil and conspicuous labelling certainly aid in device donning, the housing form factors are still quite foreign to the unfamiliar eye. An all-in-

one housing could not only help with cable management as suggested by a UMinn study participant, but also with more intuitive placement, would likely reduce the time/steps required, and as one study suggests, perhaps even encourage user adherence [59].

3.4 Wearable Joint Monitoring Device Version III

3.4.1 V3 System Overview

After validating the internal sensing hardware in a wearable form factor, it was finally time to pursue a fully functional *and* ergonomic design. User feedback and original intent converged on this iteration which prioritized user experience and device robustness.

As delineated in **Table 9** and displayed in **Figure 14 - Figure 15**, many components were roughly retained albeit updated, such as the audio board, main board, batteries, SD cards, temperature sensor boards, and microphones to name several. However, perhaps most noticeably, the V3 brace took quite a visual departure from the previous two iterations as all technology was integrated into an off-the-shelf orthopedic rigid knee brace. The Össur Flex brace was chosen in collaboration with Göktuğ Özmen, Daniel Hochman and Mohsen Safaei, after comparing three top-rated orthopedic knee braces across various parameters, including brace stability and strength, surface area for hardware mounting, ease of movement, inherent brace vibration and/or noise during movement, and slippage during movement.

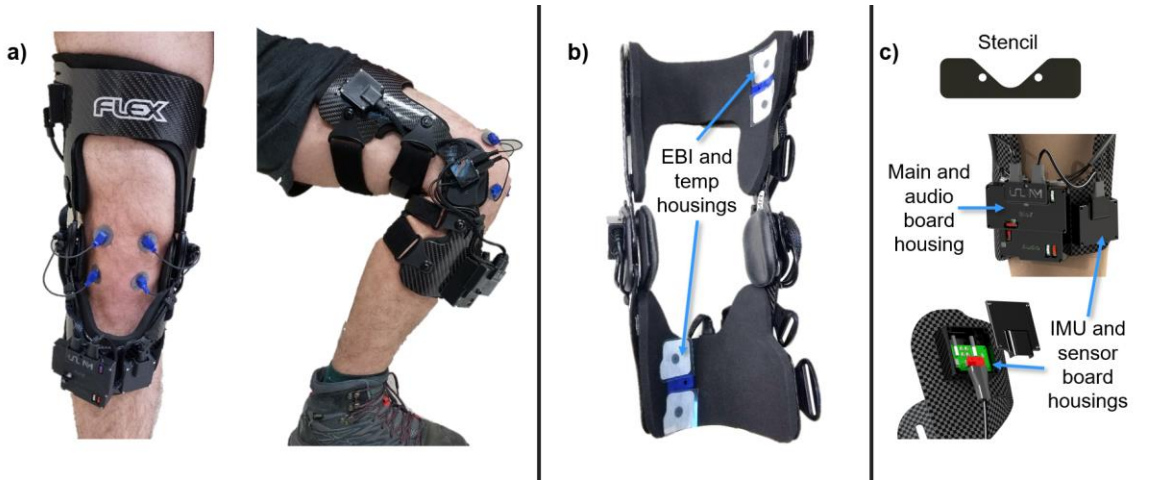

Figure 14. V3 brace overview. (a) Front and side views of the fully donned retro-fitted Össur Flex brace. (b) The inside of the brace, demonstrating the EBI and temperature sensor housings within the custom cut foam. (c) The placement stencil which has been reduced for solely mic placement considering the new straight-forward brace form factor. Pictures demonstrating the main and audio circuit housings as well as one of the two sensor housings.

Additionally, three other overarching changes impacted the form factor of several components: namely, 1) the two former bulky cable bundles consisting of EBI, temperature and IMU cables were all condensed into two 20-pin Samtec brand cables which 2) interfaced with two respective new sensor boards, and 3) intermediary microphone wires were introduced. The electronic updates were established in collaboration with Göktuğ Özmen. The impacts of these updates are discussed below in Section 3.4.2 V3 Design Review. The battery life, memory space, LED indicators and accompanying housing windows, placement stencil, simple switch control, USB data transfer capabilities and convenient Heart Pulse application were all preserved from the prior iteration.

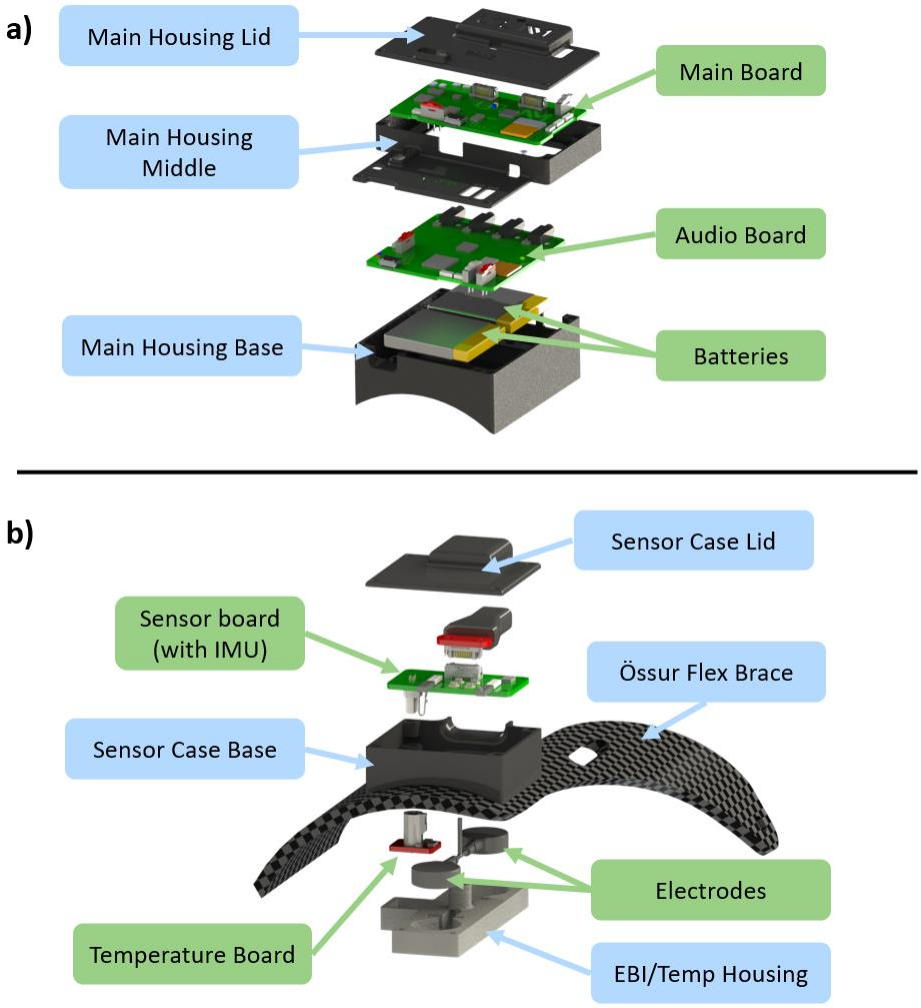

Figure 15. V3 exploded views (a) Exploded view of main housing. (b) Exploded view of new sensor board housing and EBI/temp housing.

3.4.2 V3 Design Review

Thus far, the V3 brace prototype appears to be promising, considering successful mechanical integration of the electronics and early feasibility recordings. This being said, the system has yet to be fully validated on its intended subjects, specifically for its efficacy as a diagnostic tool between healthy and unhealthy knee joints, as the project was

temporarily paused in response to the COVID-19 outbreak. Regardless, several pros and cons have already been noted for this early prototype, as outlined in **Table 4.**

Table 4. V3 design review. All electronic contributions were performed by Göktuğ Özmen, although the decision-making process was often collaborative.

	Line	Design Pros	Design Cons
Packaging-Related Features	1	New COTS knee brace form factor which A) aids in more intuitive device donning, B) serves as a scaffold for an all-in-one design, C) reduces user input	Despite having the stencil, placement is still not always intuitive as A) patella is not always palpable, B) the housings are dissimilar from any recognizable knee brace
	2	All components except microphones are rigidly attached to the brace, which encourages more secure electrical connections and reduces damage/pull risks, specifically for the cables which are no longer in large exposed bundles	Discrete brace sizing (i.e. not perfectly adaptable for every single leg shape/size like the Velcro strap form factor of V1 and V2)
	3	3M-expert-recommended double-sided foam adhesive for attaching the sensor cases to the carbon fiber brace; specifically chosen for both material types for maximum hold, and also dampens vibrations	Noise/vibration could be introduced into the signals by the rubbing of the brace itself (to be determined empirically)
	4	Custom drill template for creating holes through the carbon fiber brace to pass through the BIS cables and the Omnetics connector of the temperature board; reduces manufacturing time and improves consistency	Heavier than V2/V1 (5lbs)
	5	Custom Samtec cable protection (cable wrap with rigid + adhesive heat shrink at ends for bend relief)	Audio/main board sensor housing not ideal - awkward/somewhat large footprint forced by the need for access/visibility to LEDs, switches, connectors
	6	Features in circuit case lid to reinforce audio jack connections on the audio PCB in conjunction with new holes in the audio PCB for zip tying the 2.5mm audio jacks to the board itself, mitigating conector breakage	As observed during fit testing, maintaining secure electrode attachment to skin with current design may be difficult, especially if the brace is too large for a user (to be further explored empirically)
	7	Custom electrode/temp housing secured to the brace via Zip Ties which provides rigid/strong attachment and is reversible in the case of replacement or troubleshooting	As observed during fit testing, the brace has a tendency to slip down the leg, causing the hinge to be misaligned with the knee joint, and further to disrupt the prefered sensor placement locations
	8	COTS soft rubber foam for the underside of the brace with custom cuts to seamlessly accommodate the electrode/temp housings. Chosen to be ~2mm shorter than the electrode housing to ensure BIS and temperature sensor contact	More components and longer manufacturing time (but in exchange for less required user input)
	9	Multiple Flex brace sizes (S, M, L, XL) to accommodate multiple participant sizes; all custom technology packaging is also adaptable for every brace size	
	10	Many improvements to audio sensors - new intermediary wires that A) have right angle audio plugs for a low profile connection at the audio board, B) are then rigidly mounted along the brace until either hinge at which point C) four shorter loose mic cables extend from the hinges to the four circa-patella locations	
Electronic-Related Features	11	Broadly speaking, V3 electronic updates were made with packaging in mind (namely, Samtec cables and new sensor PCBs)	The setup has yet to be fully vetted in its intended wearable application (to be completed internally and eventually clinically once project is resumed)
	12	Battery hard-reset switches now rigidly incorporated into the boards themselves	Audio and main boards not optimized for packaging (must finagle packaging to accommodate LED visibility, switch access, port/connector access, etc.)
	13	New ability for dynamic BIS recording, controlled by a new rigidly incorporated switch	
	14	New intermediary sensor PCBs to enable better cable management	
	15	BIS, temperature, and IMU all incorporated into a single cable (Samtec) now	
	16	All circuit board updates tested and succeeded in a benchtop setup thus far (full system to be tested once project is resumed)	
	17	New entirely COTS overmolded BIS electrodes + cable assembly with COTS mating board-mounted connector (i.e. fully protected/durable electrode snap that already arrives connectorized)	

3.4.2.1 Accomplishments

For starters, this iteration finally fulfils the original description of the DARPA project – a fully wearable *brace* capable of audio, EBI, temperature and IMU sensing. While V1 was a valiant but unsuccessful first try, and V2 functioned as desired but fell short of qualifying as a "brace" per se, V3 achieves both of these goals. Moreover, the rigid brace form factor serves many additional purposes – users can more readily understand the intended physical application; all components may incorporate directly into the single brace scaffold, approximating an all-in-one design save the separately added cloth EBI electrodes and mic placement; and as such user input is drastically reduced while device robustness is improved.

As a result of all the components being rigidly attached to the single brace, the system is overall more damage-proof as there are fewer moving parts. The cables themselves are fixed along the stiff carbon fiber portions of the brace, held in place by a combination of 3M double sided tape which was specifically recommended by a 3M expert for the materials in use (3M, 5952) and Zip Ties, both of which are reversible if needed, by design (**Figure 16**). The 3M tape is also employed in adhering the circuit housings (for both the main/audio board stack as well as the new sensor boards) to the brace, and doubles as a vibration damper.

Figure 16. Noteworthy design features of the V3 design. (a) New, permanently affixed, low-profile, right-angle intermediary mic wires interface with the audio board. (b) The intermediary mic wires are adhered along the brace until reaching a custom terminal housing at the hinge. (c) The mics plug into the jacks at the hinges and can be placed more intuitively. (d) The EBI and temperature sensors directly contact the skin from the inside of the brace, communicating through a wire conduit drilled through the brace. (e) New

Samtec connectors to replace the former Omnetics connectors. (f) LED windows maintained for V3. (g) Mic placement stencil maintained for V3.

The transition from the multiple Omnetics connectors to the single Samtec cables (in conjunction with the supporting sensor boards) perhaps was the greatest facilitator to the mechanical success of the new brace form factor. No longer burdened by the bulky and relatively stiff cable bundles of V2, the flexible and low profile Samtec cables could be easily and discretely routed along the brace to either of the two sensing locations (**Figure 16b, e**). A close second was the introduction of the intermediary audio cables, which reduced the connector profile directly exiting the circuit case (**Figure 16a, b**), reduced the user interaction with the fragile board-mounted audio jacks, and enabled the shortest possible length of loose microphone cable to mitigate wire bumping artifacts. With the loose portion of the microphone cables now extending from the hinges, the mic placement also becomes somewhat more intuitive as the cables are already roughly organized in an array around the knee.

With a solid brace now in between the circuit boards and the signal source (the skin), a solution was needed to allow the EBI and temperature sensors to contact the skin while communicating with the sensor boards above. As such, a custom flexible housing was devised that would pass directly through holes drilled into the carbon fiber brace, which doubles as a sturdy scaffolding with which to attach and detach the electrodes with ease (as opposed to the V2 electrode snaps and housing which were comparatively compliant and difficult to use per UMinn participant feedback) (**Figure 16d**). To reduce manufacturing time and to improve consistency across braces, a 3D printed flexible guide

was designed for drilling said holes. Meanwhile, custom foam inserts (cut from COTS foam rubber material) were designed to envelop the new sensor housings. From a manufacturing stand point, this iteration is decidedly more involved than either V1 or V2, but requires less final input from users and appears to be the most robust version yet, which ultimately makes the additional front-end effort worthwhile.

The same proof-of-concept trial recording performed on the V2 brace was again performed using the V3 hardware, with all else held the same (subject, procedure, data analysis methods). The results from said recording are depicted in **Figure 17** - **Figure 19**. These early results are promising for the intended clinical use, considering despite the complete overhaul in form factor and many electronic updates, the signal quality is nearly indistinguishable from the V2 setup which was specifically optimized for electronic function/signal quality. Akin to published results as well as the V2 device performance, the V3 EBI data depicts high repeatability across all sweeps (within 1 ohm of ensemble average), and the joint sounds data again presents consistent “clicks” throughout the flexion/extension exercise, with a spectrogram to match.

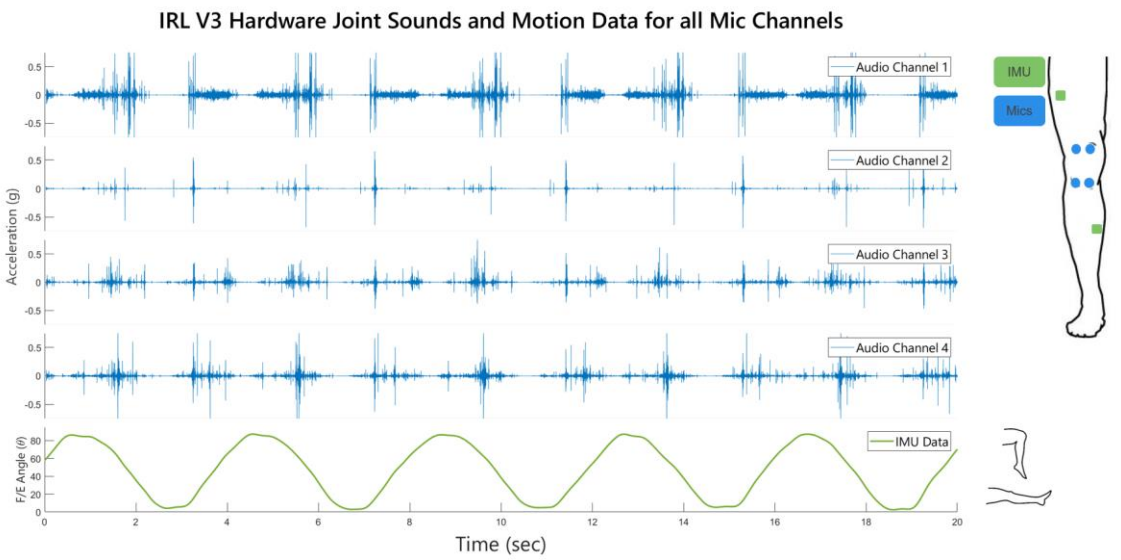

Figure 17. Proof-of-concept audio and IMU data from the V3 joint sensing brace. The signals appear consistent with expected joint sounds and IMU data.

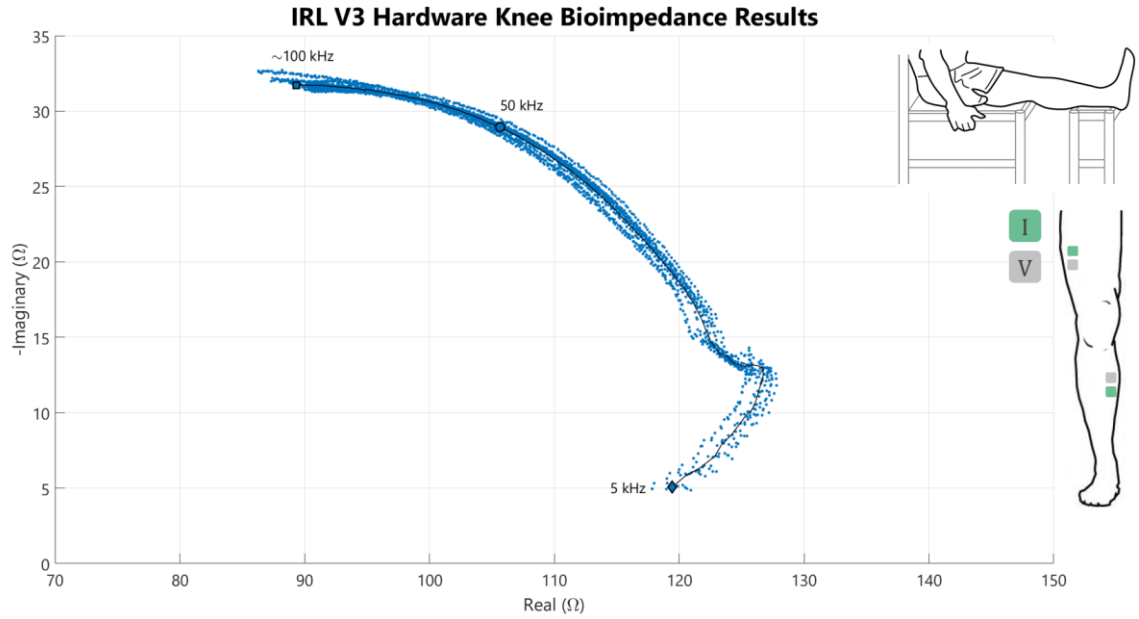

Figure 18. Proof-of-concept EBI data from the V3 joint sensing brace. The data mimics that of prior studies, with repeatability across sweeps within one ohm of the ensemble

average, suggesting that the brace form factor does not disrupt the ability to record this signal.

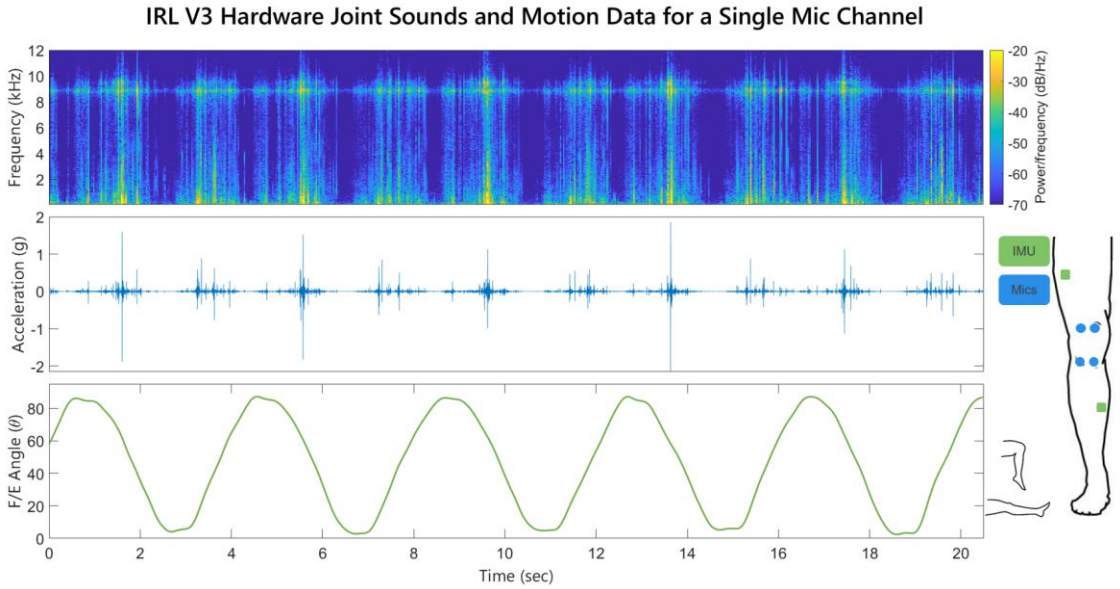

Figure 19. Proof-of-concept audio and IMU data from a single mic channel. Once again, the spectrogram reveals a signal similar to previous joint sounds studies, thus promoting the usefulness of this new brace form factor to measure these tried and true signals.

3.4.2.2 Challenges

As previously mentioned, this device has yet to be used across a varied patient population (injured vs. healthy, different leg sizes/shapes, etc.), but a few avenues for potential challenges have already been identified. For instance, this brace is heavier than the previous design which had itself already been deemed too heavy by the end users. This concern may be offset by the supportive brace form factor, but only time and experimentation may tell. Furthermore, during initial internal fit testing, if the user's leg was slightly too small for a given brace size (but not small enough to justify moving to the next size down), the electrode snaps would occasionally detach from the user's skin after

repeated flexion and extension. Likewise, the braces have a tendency to slip down the leg even in a more aptly fitting situation, perhaps because of the weight or the lack of anti-slip material. Either scenario could naturally disrupt reliability within even a single recording session due to changing sensor positions or sensor-skin disconnects.

The main/audio circuit boards and their respective housing presents a couple issues as well. The interactive board components (switches, connector ports, LEDs) were simply not organized with packaging in mind, most likely because they began as a means for a functional prototype and have only received minor updates along the way (i.e. have never been fully overhauled to better coordinate with ergonomic packaging). As such, while the V3 circuit housing is functional, it is awkward. To ensure access to the switches, connectors and LEDs, while also attempting to minimize contact area to the brace (considering the carbon fiber real estate is limited, especially on the size small brace), the boards were stacked with a substantial (and unsightly) offset. While the outcome is aesthetically acceptable, it still highlights the need for collaborative design between internal electronics and final mechanical implementation.

As discussed, the manufacturing process for this brace is more elaborate than the previous versions – drilling the brace, installing sensors/boards into respective housings, rigidly attaching housings to the brace (whether via double-sided adhesives or Zip Ties), securing all cables neatly and stably along the carbon fiber, just to name a few steps. However, this all-encompassing assembly process enables the device to be more or less readymade for the user, besides attaching cloth electrodes before donning, and using the stencil to place the microphones on the skin.

3.5 Hardware Adaptation for COVID-19 Monitoring

In April of 2020, in response to the need for improved monitoring technologies for patients with COVID-19, Dr. Inan proposed adapting the aforementioned brace hardware into a new form factor for monitoring lung health instead of joint health. Broadly speaking, the project entails two primary aims – adapting the technology and packaging for use on a torso to be initially tested on healthy volunteers, and by December of 2020, deploying this hardware to COVID-19 patients under investigation (PUIs, i.e., those awaiting results of a COVID test) and confirmed cases.

3.5.1 COVID System Overview

For the most part, all functional components were more or less retained from the knee sounds configuration, but adapted to address a new application (see bill of materials in **Table 10**). Considering both the urgency of the deployment timeline as well as the desire for discretized sensor placement, the V2 electronic architecture was chosen for its existing more or less 1-1 connector-to-sensor configuration (as opposed to the bundled sensor setup of the V3 electronics). Only minor updates were made such as integrating the battery hard-reset switch into the audio board and switching from straight to right-angle Omnetics connectors to improve cable management.

The main and audio boards are still stored in a single central case, alongside the accompanying batteries and cables. Meanwhile, since freedom of individual placement is desired for each of the sensors, the all-encompassing sensor housings of prior designs were retired. Considering these now bare sensors need protection, a new overmolded design was

explored and is presently being implemented by a contract manufacturer. More on these designs in the following section, 3.5.2.1 Accomplishments.

For sensor placement, clinical feedback was sought from the study affiliates at Emory and Grady Hospitals; the proposed placements can be seen in **Figure 20**. Based on the typical location of fluid during a pleural effusion, three of the four microphones will be placed on the right middle lobe, the right inferior lobe, and the left inferior lobes, respectively, with the fourth microphone placed sternally for heart sounds. The EBI electrodes will be placed laterally in line with the xiphoid process for measuring lung fluid status. It was desired to leave one IMU and one temperature sensor locally to the sensor housing for reference measurements, while the free IMU will be placed sternally to gather postural data, and the free temperature sensor will be placed within the armpit for axillary temperature measurement.

In the data processing phase, three of the four biosignals will be compared to clinical gold standards – the microphones to digital stethoscopes; the EBI data to typical pleural effusion imaging (x-rays, CT, ultrasounds); and the temperature sensors to standard oral probe thermometers (postural data is not clinically tracked, therefore there will be no referential gold standard for the IMU signal).

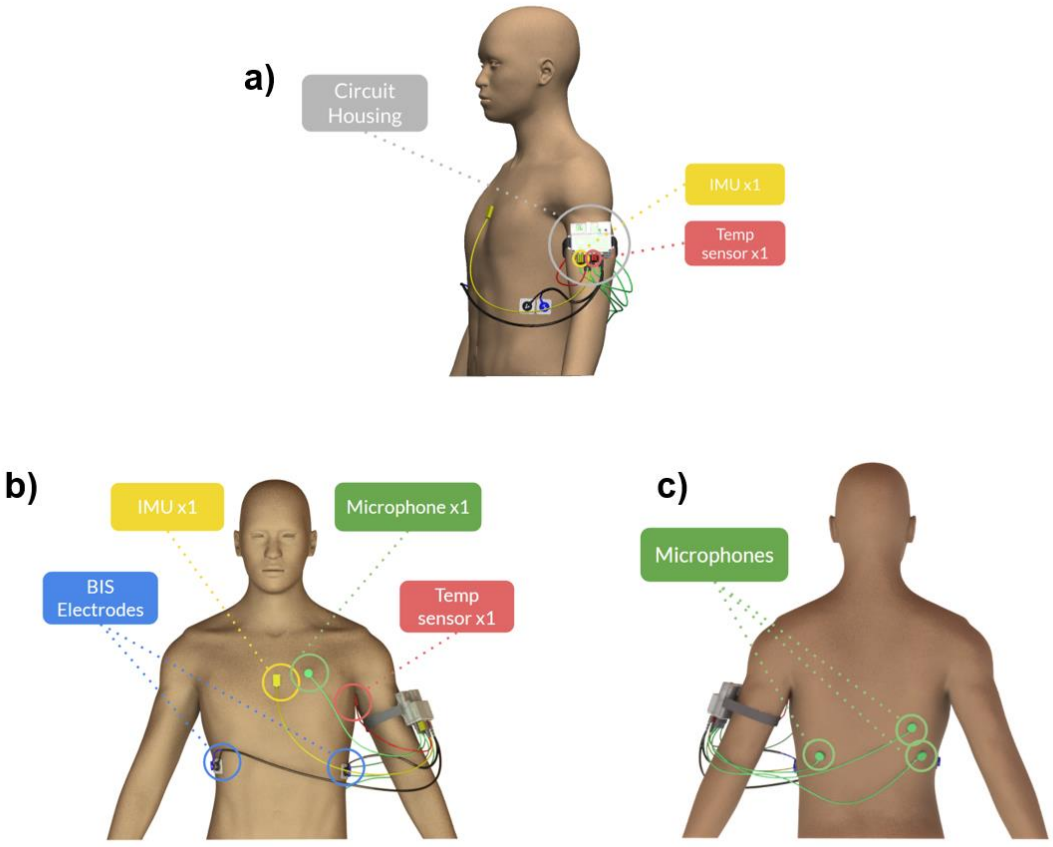

Figure 20. Proposed sensor placement for the COVID application. (a) The case which also has one IMU and one temperature sensor for reference recordings will attach to the patient's arm. (b) The bioimpedance electrodes will be placed laterally in line with the xyphoid process; the free IMU will be placed sternally for postural measurements; one microphone will be placed on the chest for heart sounds; and the free temperature sensor will measure axillary temperature. (c) The remaining three mics will record lung sound data in either inferior lobe and the right middle lobe.

3.5.2 COVID Design Review

Considering the device has thus far yet to be fully assembled and tested as some of the components are still being manufactured (specifically at the time of dissertation submission, the IMU and temperature cable assemblies and the injection molded circuit case), the following design review is largely hypothetical and will naturally have many gaps to be filled once physical testing begins. A synopsis of the review thus far can be seen in **Table 5**.

Table 5. COVID design review. All electronic contributions were performed by Göktuğ Özmen and Venu Ganti, although the decision-making process was often collaborative.

	Line	Design Pros	Design Cons
Packaging-Related Features	1	Clinical-grade overmolding for all four sensor types for sanitation and electrical insulation (new custom overmolding for three of those, one pre-existing)	Custom sensors/cables more expensive and time consuming to construct; however no COTS alternatives currently available
	2	Color-coded and labeled sensors for intelligible donning even by unfamiliar users	Each sensor must be individually placed/adhered. Could be cumbersome/irritating for both patients and health care workers
	3	Flexible (75A) and low profile (<8mm) sensor overmolds for comfortable skin/body interfacing and to avoid pressure injuries	Ideal sensor locations to be determined (as this work initially exploratory)
	4	Each sensor completely individualized for adaptable placement to maintain patient comfort and/or as the study generally progresses and more is learned	
	5	New high-fidelity sensors could be used for joint monitoring as well	
	6	Placement guides to be in multiple form factors for convenient use (miniaturized badge versions, signs in patient rooms, digital versions)	
	7	Semi-transparent case for convenient LED viewing	
	8	Soft Velcro strap and foam backing for comfortable and portable case attachment	
	9	Clip for alternative attachment	
	10	Generous cable lengths (up to 36") to accommodate various patient demographics	
	11	All cables exit the case in the same direction	
	12	New custom microphone overmold which A) protects solder joints and B) behaves like a trampoline allowing the microphone to more freely vibrate on the skin surface also without adhesive between the microphone and the skin	
Electronic-Related Features	13	New audio and main boards verified on bench top setup thus far (using previously existing sensors)	Expensive Omnetics connectors which also often have long lead times
	14	Temperature sensor for longitudinal temperature measurement, as opposed to the only intermittent clinical readings	Main board battery hard-reset switch not integrated into the PCB
	15	IMU sensors for longitudinal motion tracking, as opposed to only being tracked if/when a patient is at risk for falling	
	16	Website (or otherwise a single central digitally available platform) for all experiment and device information for HCWs	

3.5.2.1 Accomplishments

Many seemingly subtle yet impactful design features have been incorporated into this COVID hardware adaptation. For instance, the audio and main boards have been reoriented 90° relative to one another compared to the previous knee braces, and right-angle Omnetics connectors were introduced to the main board, which once combined, will enable all connectors to exit the case in the same direction (**Figure 21d**), thus improving visual organization, usability, and robustness.

For the free IMU and temperature sensors, a design was conceived in which the cable conductors would be soldered directly to the raw IMU and temp PCBs, and then overmolded for integrity, thereby eliminating the bulky Omnetics connectors, while modularizing and waterproofing the sensors. Importantly, the accelerometer lacked proper protection, and as such a custom housing was designed and modelled using finite element analysis (FEA), as well as physical prototyping to ensure the packaging would not disrupt the frequency response in the desired lung sounds bandwidth. This process is thoroughly described in section 4.4 Accelerometer Form Factor Version III. The soft plastic overmold material (Technomelt, PA 658, Henkel, USA) which will be used for all three adaptations will be dyed and labelled according to sensor type to facilitate more intuitive placement (**Figure 21b**). The overmolds will be relatively compliant and low profile (>8mm) to enable comfortable skin interfacing as well as to avoid pressure injuries during prolonged use (**Figure 21b**). Each cable has been designed with generous cable lengths to accommodate varying patient sizes and the general exploratory nature of this early endeavour. For the two reference sensors (IMU/temp boards to remain at main housing),

protection and waterproofing will be ensured through the use of custom-built 3D-printed "sleeves" that easily slip over the PCBs and are secured with epoxy (**Figure 21**d).

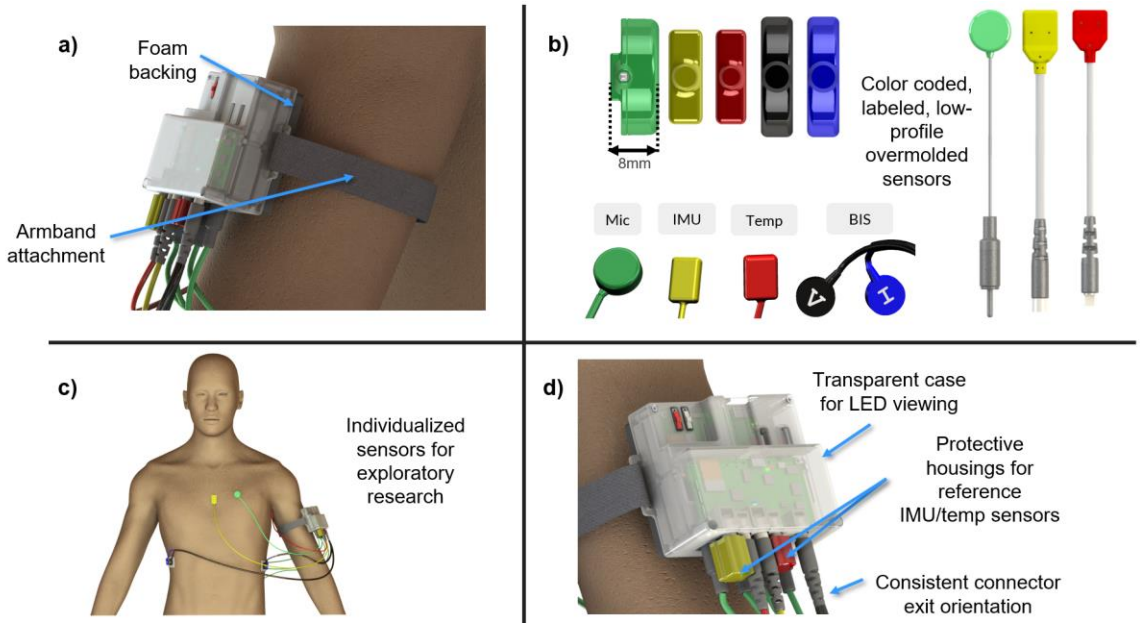

Figure 21. Noteworthy design features of the COVID hardware. (a) The final case will be professionally injection molded and attached to the body via a Velcro strap with a soft foam backing for comfort. (b) To ensure clinical usability, all sensors will be contract manufactured, and three of them will receive custom overmolding for water-tightness. All sensors are low profile for unobtrusiveness and comfort, and color-coded and labeled for ease of placement. (c) Each sensor is intentionally independent for this early exploratory work. (d) The case will be a transparent plastic for LED viewing; custom 3D-printed cases will protect the reference IMU and temperature sensors. With the use of Omnetics right-angle connectors and a reorientation of the boards, all connectors exit in the same direction.

Pertaining to usability features, placement guides will be made available to HCWs in a variety of form factors (small, laminated versions to be attached to the HCW's badges, printed versions to be displayed in the patients' rooms, and digital versions). The circuit case as a whole will be semi-transparent to enable LED light transmission, and will sport two built-in attachment methods – a Velcro strap intended to be placed on the arm (but that could theoretically also be placed elsewhere), and a clip for placement on clothing or bed

sheets for instance (**Figure 21a, d**). An additional bag-type solution (e.g., fanny pack or shoulder sling bag) is being explored by students in the IRL per clinical feedback.

Thus far, the revised audio and main circuit boards as well as the first articles of the new microphone and EBI assemblies have already arrived at the IRL. Considering these two sensing modalities (audio and EBI) are the primary sensors for this technology anyway, preliminary data was taken as a proof-of-concept, using existing IMU and temperature sensors in place of the pending professional cables.

While the device is ultimately intended for lung monitoring, in an effort to enable direct comparison of the COVID hardware quality to some known baseline, the new COVID hardware was first used in the same fashion as the V2 and V3 demo recordings (i.e. on the knee). Again, the same subject, protocol and analysis was performed, resulting in the signals depicted in **Figure 22 - Figure 24**. The signal quality and characteristics closely mimicked the previous two versions, suggesting that the hardware received thus far functions as desired.

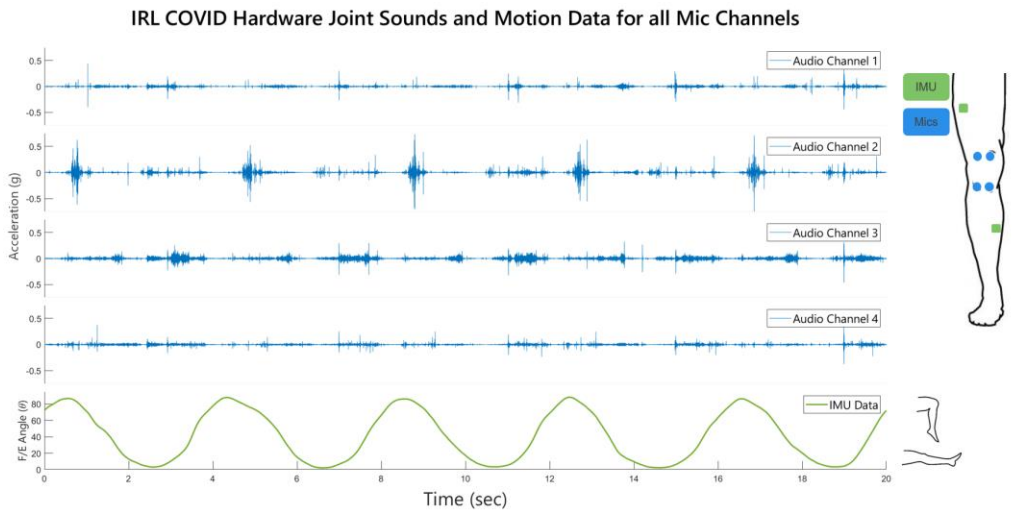

Figure 22. Proof-of-concept audio and IMU data from the COVID lung sensing brace used on the knee for comparison to previous gold standards. The signals appear consistent with expected joint sounds and IMU data.

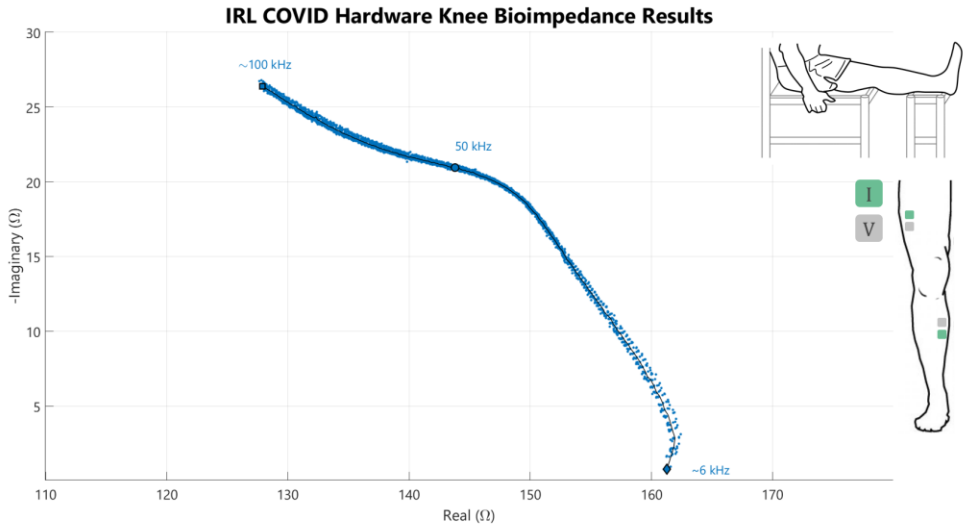

Figure 23. Proof-of-concept EBI data from the COVID lung sensing brace used on the knee. The data mimics that of prior studies, with repeatability across sweeps within one ohm of the ensemble average, suggesting that the bioimpedance hardware is in working fashion.

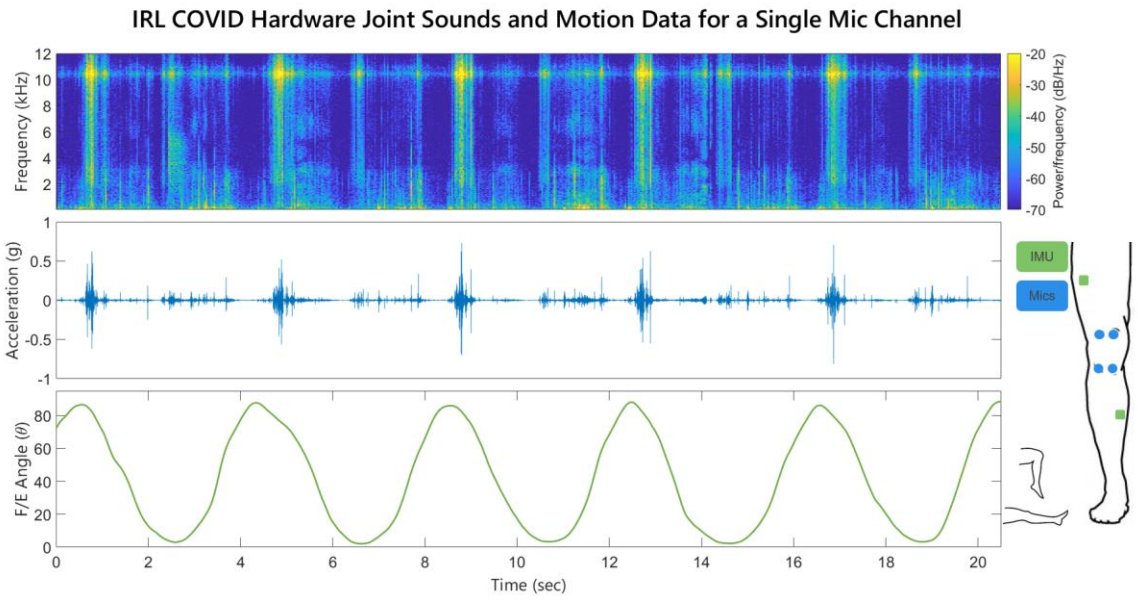

Figure 24. Proof-of-concept audio and IMU data from a single mic channel of the COVID hardware. The spectrogram reveals a signal similar to previous joint sounds studies.

After being validated on the knees, the hardware was then attached in the intended use case, on the torso for lung monitoring. All sensors were placed as previously proposed in **Figure 20**. As described, three microphones were placed on the back for lung sounds recordings, and the fourth was placed on the chest for heart sounds capturing. The free IMU sensor was likewise placed sternally although the data was not used as the subject was healthy and remained in a constant upright posture throughout recording. Likewise, the temperature sensor for now was simply secured out of the way considering the assembly lacked a protective overmold. A digital stethoscope was simultaneously employed as a reference point for the lung sounds data, recorded nearest to the mic on the left inferior lobe. The obtained data is depicted in **Figure 25** - **Figure 28**.

The bioimpedance data demonstrates the ability of the EBI hardware to detect changes in tidal volume as depicted by the relative "narrowness" of error between sweeps on the shallow breath plot, compared to the much wider error on the deep breath plot (**Figure 25**). The general shape across sweeps though is promisingly consistent. Meanwhile, **Figure 26** clearly depicts the ability of the overmolded Knowles microphone to perceive heart sounds sternally. Contrarily, the lung sounds in the time domain do not appear particularly interesting (**Figure 27**); however, when plotted in a spectrogram, respiration bands are evident and synchronous with the stethoscope data, albeit possibly noisier (**Figure 28**). Overall, this preliminary data holds promise for the clinical deployment of this system.

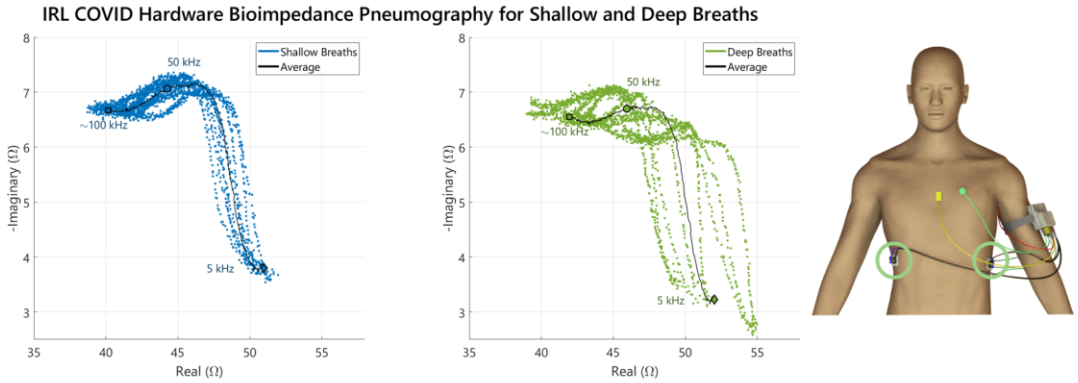

Figure 25. Proof-of-concept lung EBI data obtained from the new COVID hardware. The results suggest that at a minimum the hardware is capable of measuring differences in tidal volume (as evidenced by the data spread within the deep vs shallow plots).

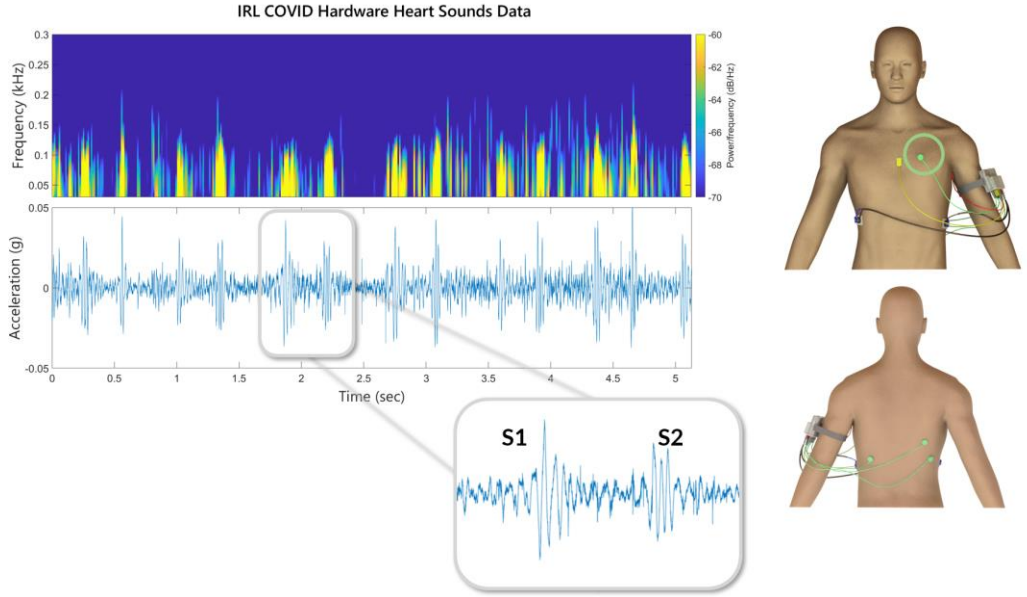

Figure 26. Proof-of-concept heart sounds data using the COVID hardware. A single Knowles accelerometer with the latest Winchester overmold packaging was placed in the highlighted position for a standing, relaxed subject. The heart sounds (S1, marking the start of systole and S2, marking the end of systole) are clearly visible to the naked eye.

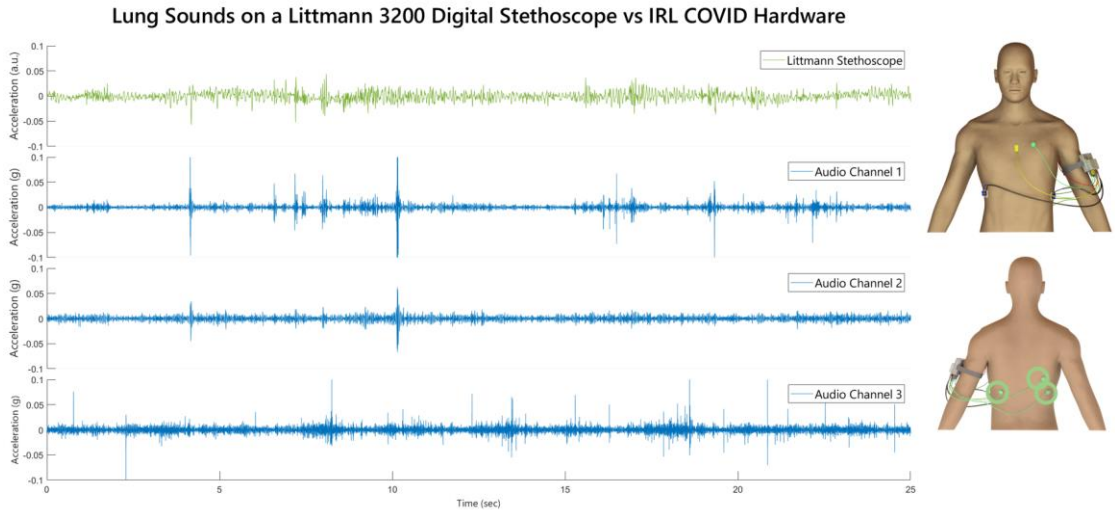

Figure 27. Proof-of-concept lung sounds recordings from the new COVID hardware. The signals do not appear to reveal any meaningful information in the time domain, but granted neither does the digital stethoscope.

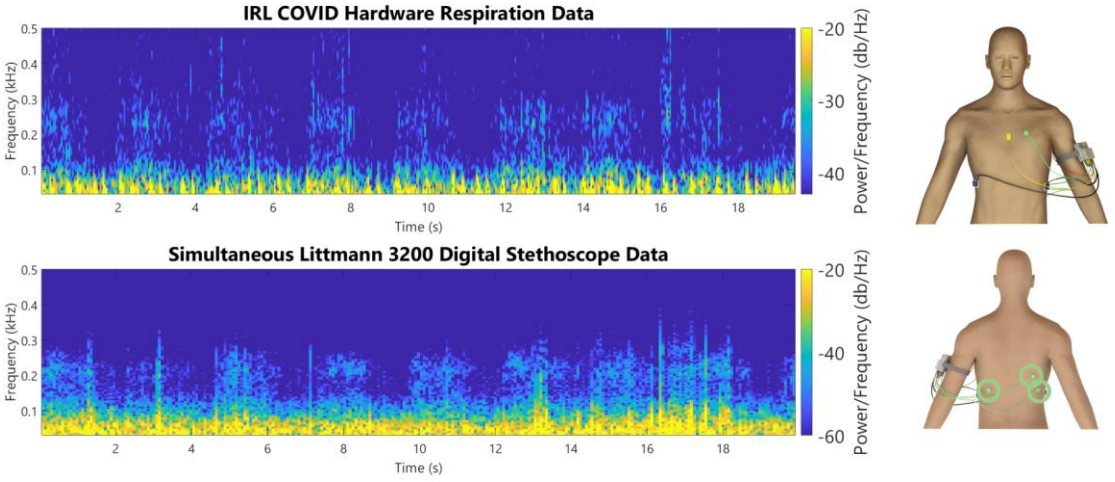

Figure 28. Proof-of-concept respiration data gathered from the COVID hardware. Respiration bands are evident in both the COVID hardware and of course the gold standard stethoscope data. The COVID hardware is decidedly noisier, but the signal is present nonetheless.

3.5.2.2 Challenges

As with any design, especially the first generation, problems are bound to arise. While these will likely reveal themselves during the initial testing to come, a few drawbacks have already been noted. The Omnetics brand connectors are relatively expensive ($8-90 per connector), and if not already in stock, can have several-week lead times. Further, the connectors must be made into custom cables, which naturally also increases cost and manufacturing time. A COTS alternative would ultimately be preferred, but considering the short turnaround time before clinical deployment, there was no time to explore/validate a new connector and cable setup. As previously mentioned, this work is relatively ground breaking in that lung sounds, temperature, postural data, and EBI have never before been longitudinally monitored on lung-compromised patients; consequently, despite having clinically-recommended starting points, the ideal sensor placement is ultimately unknown and as such entails the specific placement of each individual sensor. This process may be cumbersome or irritating for patients and HCWs alike, but will optimistically improve as the study progresses and more is learned.

3.6 Hardware Adaptation Discussion

3.6.1 Lessons Learned

Countless lessons have been learned over the last year-and-a-half-long journey since the V1 knee brace was very first discussed. While many of these lessons consist of esoteric technical realizations, the arguably more important broader meditations on design principles at large are described below.

First, the design of internal technology must always take into account the end application and vice versa, i.e. design cannot occur in a vacuum. For example, while the V1 IDC connectors were sufficient for a benchtop application, they failed to thrive for a wearable one. Second, device robustness is non-negotiable. Whether regarding individual connectors, all-encompassing housings or anything in between, if the device breaks, it simply does not matter how impressive or ergonomic it appears. Third, project scope should always be identified preceding the design process and revisited intermittently throughout. For instance, as previously discussed in section 3.2 Wearable Joint Monitoring Device Version I, the V1 brace was overly ambitious, reaching for a fully functional and ergonomic design in one iteration. When the brace design returned to the drawing board, the scope was reevaluated and ultimately reigned in for the time being. As such, the V2 brace was optimized for sensor functionality with a "side" of user experience, so to speak, sprinkling in features for heightened user interaction like LED transoms only later, and as such, was highly successful overall. Having validated the system functionality, the V3 system was free to prioritize user experience while further optimizing robustness. For the most recent COVID-19 adaptation, clinical readiness (i.e., waterproofing, ease of use, etc.) have been prioritized and the design has once again evolved as a result. In sum, at every new stage of design, scope management has been and will always be crucial for design success. In sum, these lessons will ultimately inform personal design practices for a lifetime.

3.6.2 Future Work

Like the above lessons learned, the paths forward for each respective project entail both specific technical updates as well as wider-ranging general goals.

On a micro-scale, the V2 project is largely finalized – the device is already acquiring data in the UMinn clinical study and will likely be discontinued in exchange for the V3 design once completed, therefore any design changes would be trivial. On a macro-scale however, the data obtained from this study has yet to be comprehensively analyzed, from which conclusions can be drawn about the device's ability to assess joint health longitudinally, which of course is the ultimate goal of the study overall.

Alternatively, the V3 brace has much room for minor improvements before clinical deployment, or even internal use for that matter. To name a few, the brace requires both waterproofing and slip-proofing, which may for example entail altering the case geometry to conceal the connector ports, adding gaskets or seals, or material substitutions. Additionally, while the current Zip Tie solution for wire routing serves its intended purpose, perhaps an adhesive, conduit or bracket solution could more efficiently or in a more visually appealing fashion route the cables along the brace. If the device ever ventures into at-home or long-term territory, a few more modifications should be considered, focusing on device robustness as well as simplifying user interactions. For instance, perhaps the next brace iteration could entail a flexible sleeve as opposed to a rigid brace that the user simply slides onto the leg. Additionally, the circuitry should be refurbished with the packaging in mind (i.e. move connectors, switches, and LEDs to more packaging-

friendly locations) which would both improve the design process and more importantly reduce the housing footprint. A means of ensuring repeatable flexion and extension motion should also be considered to promote repeatable recordings, perhaps by using the IMU data to detect both position and velocity of the limb and subsequently outputting real-time feedback for the user in the form of LEDs or audible indicators. Alternatively, the brace could one day be actuated, thereby eliminating any potential for user-induced motion variation. Either way, a means of repeatable donning of the brace itself should also be considered, such as an adapted stencil approach or an additional anatomically-referencing component (e.g., a rigid heel bar to maintain the hinge position at the knee). Broadly speaking, the V3 device has yet to be thoroughly evaluated on human subjects, and should be rigorously tested internally before likely clinical deployment for the DARPA project.

Lastly, the COVID lung monitoring project will require minor updates as well, such as discerning the most effective means of sensor attachment (Micropore tape, Tegaderm patches, etc.), the ideal manner of case attachment (Velcro strap on arm, clothing clip, hanging accessory bag, etc.), and the most efficient and meaningful protocol (where to place the sensors, how often and for how long to record, etc.), all of which will likely evolve as the study itself progresses. All materials should also be optimized for the reduction of germ transmission, including waterproofing for more stringent sanitization or perhaps using an antibacterial material or coating on the device itself. The algorithms which are fine tuned for making sense of joint signals will need to be updated for instance for respiratory signals as opposed to joint sounds, or pleural effusions rather than joint edema. From a testing standpoint, the system will need to be tested internally on healthy

subjects before deployment to the clinics for PUI and COVID patient testing. The data will be compared to the gold standard measurements (digital stethoscope, pleural effusion imaging, etc.) and the system will be assessed for its feasibility to extract clinically meaningful data from the multimodal sensors. Assuming the system is validated, the packaging could theoretically be formalized into a wearable all-encompassing vest or band. Further use could entail longitudinal monitoring of patients at home, or broadening the application beyond just COVID monitoring to other conditions like pneumonia, cancers, or ARDS to name a few.

An even broader potential avenue for the COVID hardware could be the early diagnosis of the aforementioned SIRS [60]. As discussed, the extreme immune response can lead to end-organ dysfunction and even death, therefore early detection is paramount for patient survival [60]. SIRS status is established if a patient exhibits at least two of the following four conditions: 1) extreme body temperature, 2) tachycardia, 3) tachypnea, or 4) extreme leukocyte imbalance, at which point a patient's treatment is escalated [61]. With relatively straight forward data analysis techniques, heart rate could be derived from a single accelerometer placed sternally, respiratory rate could be extracted from the lung sounds data, and body temperature could be monitored via the axillary sensor. Therefore, with this device alone, three of the four SIRS criteria will be monitored longitudinally, generating the potential of informing HCWs of early SIRS status, which would consequently enable sooner intervention and perhaps even save lives.

CHAPTER 4. CONTACT ACCELEROMETER HOUSING AND ATTACHMENT OPTIMIZATION

4.1 Overview

After years of trial and error, the IRL finally settled upon the Knowles BU-23173-000 piezoceramic contact accelerometer, depicted in **Figure 29**, for performing a significant portion of the ongoing acoustic experiments. However, finding a reliable means of protecting and attaching said microphones while preserving the signal of interest has continued to present challenges. The following chapter first briefly explores the aforementioned challenges of housing and attachment, then proceeds through the evolution of three proposed packaging and attachment solutions for the Knowles BU-23173 microphone and their respective performances.

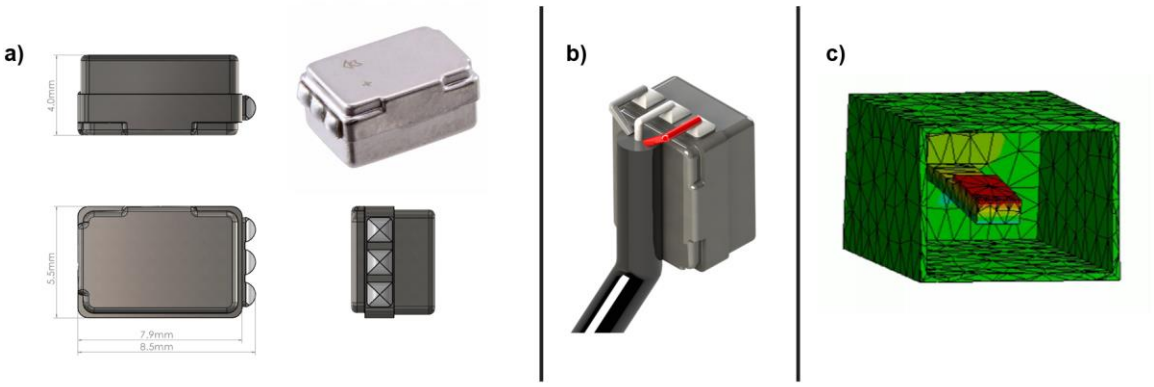

Figure 29. The Knowles BU-23173 contact accelerometer. (a) Dimensions and appearance of the small piezoceramic accelerometer. (b) Example of how the leads are attached to the

microphone. (c) Snapshot of the accelerometer in under excitation as evidenced by the cantilever deformation.

Knees emit vibrations deep within the joint, which unfortunately do not translate well to the surrounding air due to the high acoustical impedance mismatch between the tissue and the air. As such, the Knowles contact microphone was chosen over previously reviewed air microphones to bypass this air gap loss. However, the sounds of interest only occur during knee movement; herein lies the problem - it is preferred for the mic to directly interface with the skin to capture as much of the signal as possible, but the knee deforms considerably during movement, causing the mic to rub against the skin, thus introducing significant noise into the desired signal. To prevent the mic's movement relative to the skin, the leading IRL solution of late has been double-sided adhesive foam dots ("Rycote Stickies"), which have more recently been found to have the unfortunate draw-back of attenuating the valuable high-frequency end of the signal spectrum, as well as introducing more noise as they themselves deform during movement [62].

Meanwhile in the packaging realm, as is the nature of vibrating objects, any additional mass or connection point will inevitably behave as a mechanical filter to the substrate, ultimately altering the microphone’s inherent frequency response. In the case of joint sounds, whose content resides predominantly below 5kHz (i.e., spectral roll-off frequency, or the frequency below which 95% of the spectral energy lies [62]), the need to protect the solder joints in a clinical setting while maintaining linearity within the sensing signal bandwidth presents a genuine challenge.

The frequency response of the bare Knowles BU-23173-00 accelerometer is shown in **Figure 30**. Largely, the response is sufficiently linear until a natural resonance which peaks around 12kHz. In previous studies, joint sounds range from 1kHz to 10kHz [57], while lung sounds exist within 50–2500 Hz.

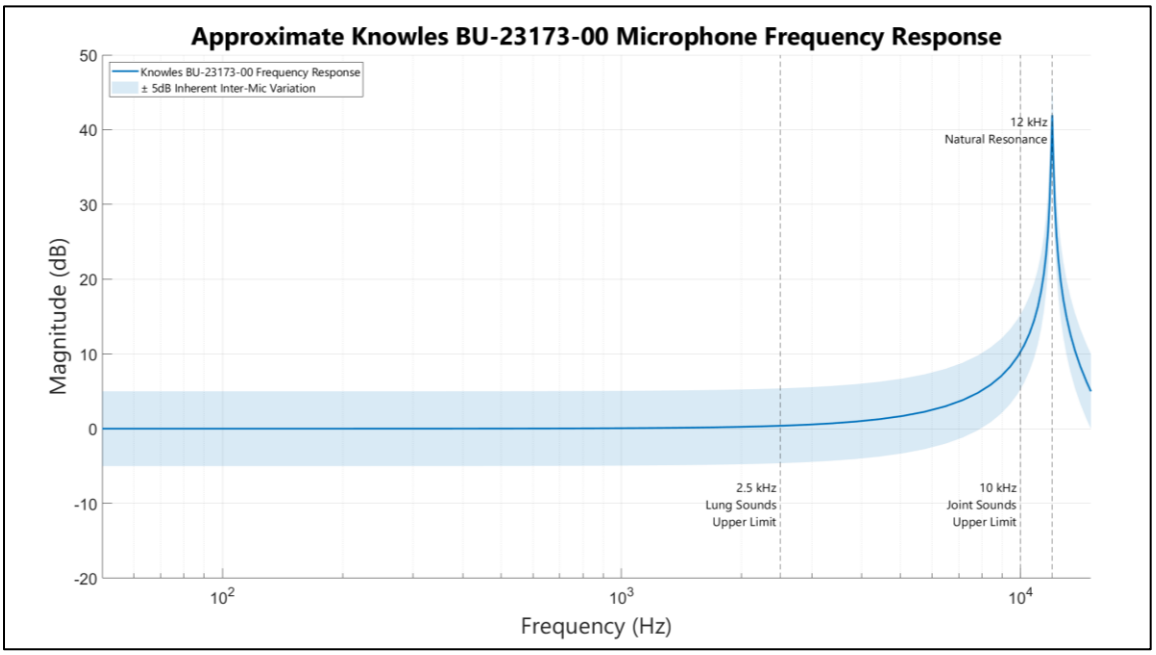

Figure 30: A MATLAB-generated recreation of the factory frequency response of the Knowles BU-23173-00 contact microphone, based on the Knowles data sheet. The response is linear until a resonance at approximately 12 kHz. The upper portion of the joint sounds bandwidth falls within this non-linear region; however, 95% of the spectral energy of a typical joint sounds recording occurs below 5kHz therefore the non-linearity can be overlooked [62]. The lung sounds bandwidth (50-2500 Hz) is sufficiently within the linear potion of the response.

In light of the described challenges, deciding upon packaging design and attachment methods for contact accelerometers is a notoriously challenging endeavor. Suggested means of attachment for industrial use vary from rubber bands, to miscellaneous tapes and epoxies, suction cups, clamps, Zip Ties, and even beeswax [63]. Previous IRL studies on

human subjects have employed Kinesio-tape as a backing tape [1, 4, 8], Rycote stickies [4, 57], thin double-sided craft tape [62], and even super glue and/or sutures for cadaver studies [10]. However, many of the industrial applications have the added advantage of attachment to either an inanimate object, i.e. where subject comfort is not a concern, or more directly to a rigid contact (e.g., jaw bone), or are measuring signals with larger amplitudes (i.e., human voice or an instrument vs. joint sounds). Common industrial packaging varies from having no packaging at all (i.e. just bare piezoelectric sensors), to simple rubberized coatings, to silicone overmolds [63]. Until now, IRL has only explored a couple of packaging methods, such as a built-in glove form factor [4], but otherwise the mics have largely been bare.

As these microphones have evolved from the lab to the clinic, packaging has become a critical need to ensure the structural integrity of the sensor in less-controlled clinical environments, as has a manner for simple and repeatable attachment by unfamiliar users.

4.2 Accelerometer Form Factor Version I

Before the joint sensing hardware ever ventured beyond the four walls of the lab, the accelerometer's solder joints were secured with the electrically passive polyimide tape commercial known as Kapton tape (**Figure 31**).

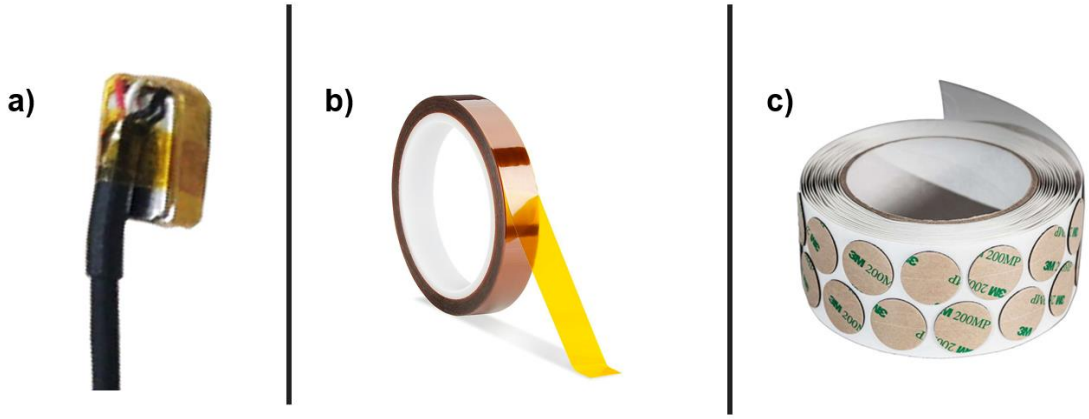

Figure 31: Mic packaging and attachment form factor 1. (a) The soldered Knowles microphone, wrapped with Kapton tape to secure the solder joints. (b) A roll of Kapton tape. (c) A roll of Rycote double sided stickies, the chosen means of attaching the microphones.

The thin tape ensured that minimal mass was added to the sensor (as to not change the frequency response by mass addition), while also being electrically passive. The established attachment method of the day was 3M Rycote stickies, which were previously proven for use in two IRL studies [2, 4]. These foam stickies have been used for years in the audio industry for this very purpose, are inexpensive and commercially available, and feature strong yet comfortable adhesion.

This Kapton tape and Rycote solution proved sufficient for highly-controlled in-lab use cases. However, with the deployment of the V2 knee brace to the UMinn affiliates, it quickly became apparent that the solution, especially the tape, is non-ideal. While removing the paper backings of the Rycotes is tedious, they still perform well enough at maintaining consistent contact between the microphone and skin throughout the relatively short recordings to overlook the tedium. The Kapton tape however loses adhesion over

time, rendering itself useless in bend-relieving the solder joints, and in some occasions even introduces noise if/when the loose portions brush against the skin.

To quantify the impact of the tape and foam pads on the microphone's frequency response, the microphone underwent shaker vibration testing per the setup in **Figure 32**.

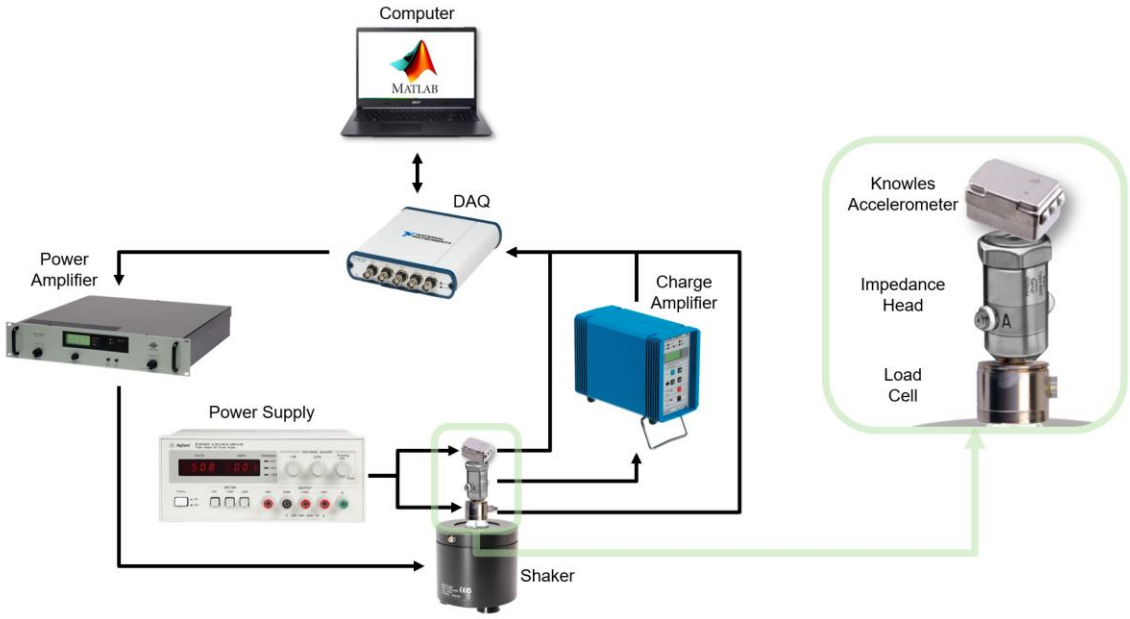

Figure 32. Testing setup for the microphone case testing. The microphones were excited with a 1g swept sine signal from 50 – 10050 Hz to assess the impact of the various microphone packaging and attachment methods on the microphone's frequency response.

A custom MATLAB (The MathWorks, MA) computer script built by Mohsen Safaei which ensures consistent 1g swept-sine shaker excitation is sent to a data acquisition unit (USB-4431 DAQ, National Instruments, TX). The information then passes from the DAQ along its only analog output channel ("AO 0") to a power amplifier (B&K Type 2718 Power Amplifier, Brüel & Kjær, Denmark) and finally arrives at the shaker for excitation (B&K Type 4810 Mini Shaker, Brüel & Kjær, Denmark). Attached to the shaker, an in-line

reference impedance head (B&K Type 8001 Impedance Head, Brüel & Kjær, Denmark) measures the input acceleration to ensure 1g acceleration, and is powered and amplified by a charge amplifier (Type 5011, Kistler, Switzerland) before returning to the DAQ analog input zero ("AI 0") channel, sampled at 50 kHz. Meanwhile, the testing accelerometer (Knowles 23173-000, Knowles, USA) attaches to the top of the impedance head and measures the output acceleration. The accelerometer is powered by an external power supply at 2.15V (E3630A DC Power Supply, Agilent, USA), with two probes directly measuring and communicating the output voltage back to the DAQ "AI 1" channel, likewise sampled at 50 kHz. An in-line force sensor (Model 31 Miniature Load Cell, Honeywell, USA) is also attached to the shaker, powered by the second channel of the aforementioned power supply at 9.9V and communicated through the third DAQ input channel ("AI 2") through direct probing. The load cell signal is only necessary for the later testing described in section 4.4 Accelerometer Form Factor Version III, but was installed throughout all testing nonetheless for consistency.

Figure 33 presents the results of this shaker test. For this figure and all following, the black line and accompanying +/-5dB shaded region correspond to the recreated Knowles factory frequency response and the inherent variability between units, respectively (as shown in **Figure 30**). Each bold line of the microphone response represents the average of a single mic over three separate shaker runs, between which the microphone was subtly repositioned on the impedance head in an attempt to simulate some degree of placement variability that occurs in reality. The shaded region around each bold line represents the standard deviation of the three shaker runs, for each mic respectively. For

example, **Figure 33** depicts three bold orange lines, which represent three different accelerometers that were tested with the Kapton “packaging”. Each of these mics was tested three times, and the standard deviation of each mic across those three runs is plotted in the surrounding shaded regions.

As shown in **Figure 33**, The Kapton tape and Rycote stickies produced a linear response until a resonance that begins at approximately 1kHz and peaks around 2.5kHz, at a magnitude over 10dB. This response unfortunately falls directly within the bandwidths of both joint sounds and lungs sounds, and considering it extends beyond the expected variation of a stock Knowles microphone (± 5dB), it must be concluded that the resonance is indeed due to the tape and/or the Rycote stickie. However, even had the modality performed well, the Kapton tape was ultimately unreliable for longitudinally protecting the solder joints, so a new protection solution was sought anyway.

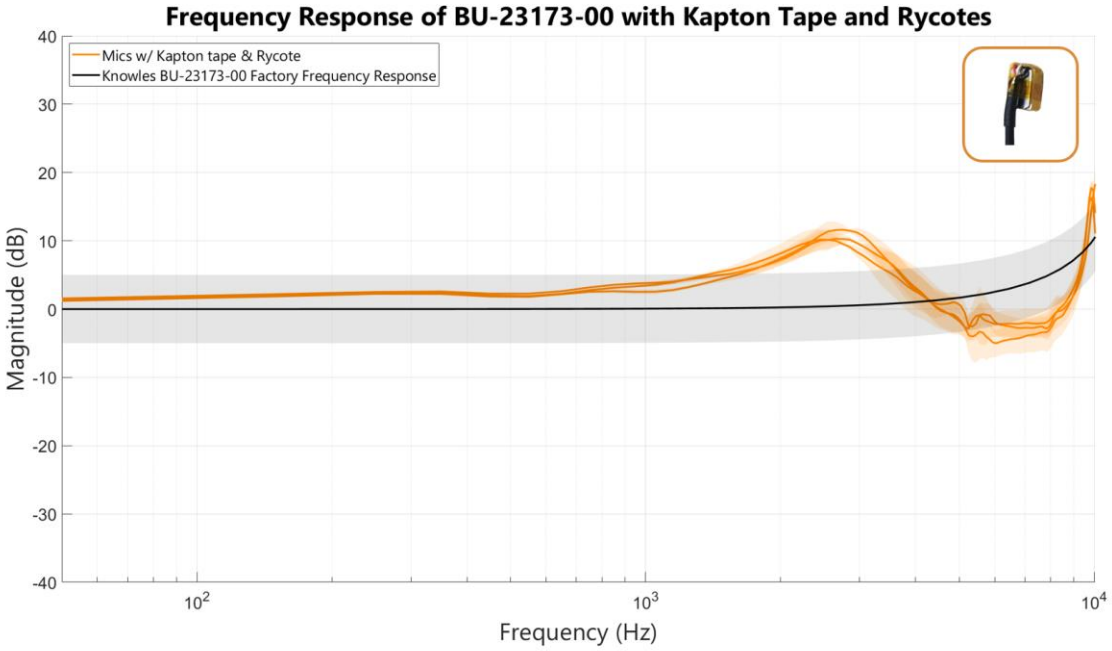

Figure 33. Measured frequency response of the Kapton tape and Rycote mic form factor. The setup produced a resonance around 2.5kHz which is unfortunately within both the joint sounds and lung sounds bandwidths, with another resonance near the microphone natural resonance of 12kHz.

4.3 Accelerometer Form Factor Version II

In response to the suboptimal performance of the Kapton tape, as well as out of consideration for eventual/potential at-home use, a new solution was sought for protecting the solder joints. As such, a 3D-printed flexible case (Cheetah 95A TPU, NinjaTek, USA) was designed that closely conforms to the mic and solder joints, with a wire "conduit" angled at 45° from the contact surface to direct the lose wire away from the skin, thus lessening the potential for wire rubbing noises (**Figure 34**). The angled conduit additionally mitigates accidental wire pulls from introducing artifacts directly along the axis of acceleration (as opposed to a conduit angled perpendicularly to the contact surface for

instance, i.e., directly along the axis of measurement). The cases are coupled to the microphones with a hot-melt adhesive (i.e., “hot glue”) which serves three purposes – to electrically isolate the solder joints from the outside world, to fill any air gaps between the mic and the case for optimal impedance matching, and to minimize the possibility of the case moving respective to the mic which could introduce rubbing noises itself. The attachment method of Rycote stickies were still employed at this stage of development as some of the noted problems thus far were largely a matter of convenience/comfort, and the more vital suspicion of frequency damping had not yet been explored (first suggested by Bolus et al. in 2019 [4] and then empirically evaluated by Özmen et al. in 2020 [62]).

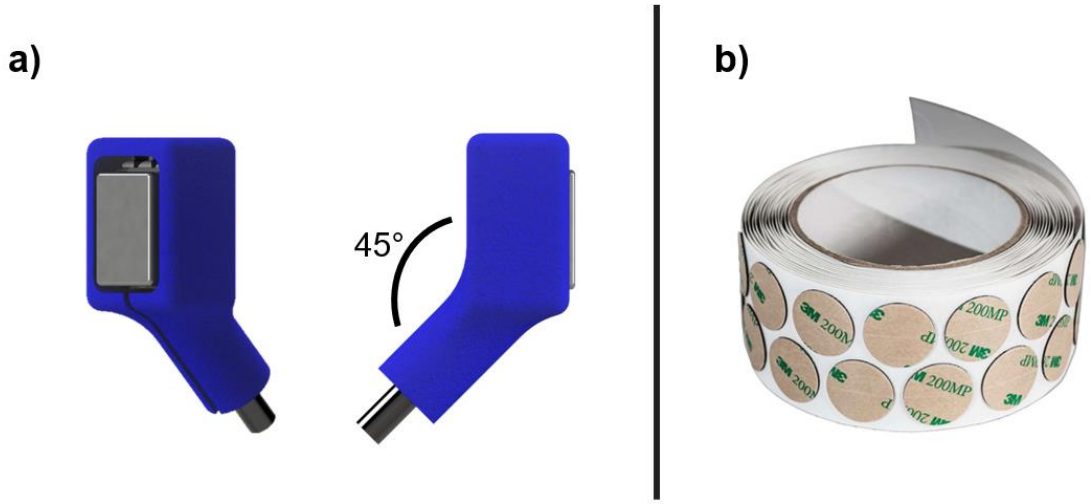

Figure 34. Mic packaging and attachment form factor 2. (a) Isometric and side views of the 3D-printed semi-flexible housing. The housing is secured to the microphone using hot melt adhesive, and serves to protect the solder joints while also directing the microphone wire away from the skin to mitigate rubbing. The microphone intentionally sits slightly proud of the case along the sensing axis to promote mic to adhesive coupling (as opposed

to coupling with the packaging first). (b) Rycote stickies were still the preferred method of placement for this form factor.

The aforementioned 1g acceleration shaker test was repeated for this microphone solution (3D-printed cases and Rycote stickies). As shown in **Figure 35**, the 3D-printed cases and Rycote stickie modality resulted in a resonance even lower than that of the prior form factor (beginning around 800Hz, peaking 1500Hz, just below 10dB).

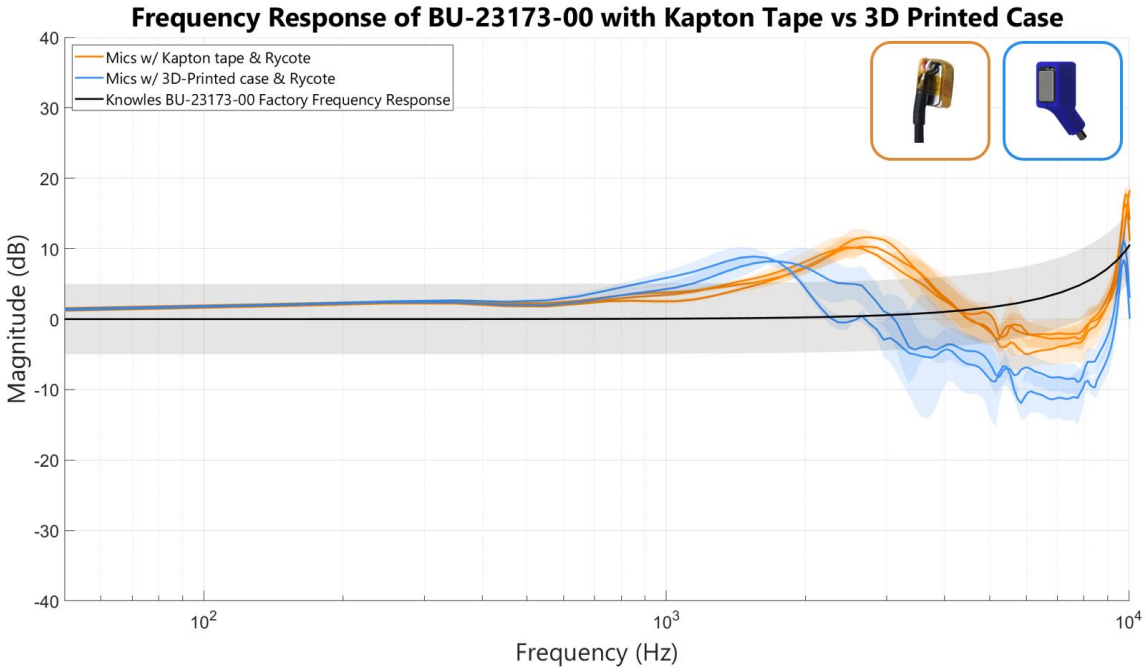

Figure 35. Measured frequency response of the 3D-printed blue housing and Rycote form factor, compared to the original Kapton tape design. The resonance migrated further down to approximately 1.5kHz. This decrease could potentially be explained by the added mass of the casing on the accelerometer.

In hindsight, this response is to be expected considering the construction of the microphone. Dy definition, the piezoceramic accelerometer utilizes an internal cantilevered beam for acceleration sensing. Considering the general relationship between

mass and resonant frequency of a cantilever beam as shown in Equation 1, it should be expected that if mass is increased, the natural resonance will decrease (where ω_n is the natural frequency, *C* is a constant dependent upon vibration mode, *E* is the Young's modulus, *I* is the moment of inertia, *m* is beam mass, and *L* is beam length).

$$\omega_n = C\sqrt{\frac{EI}{mL^4}} \tag{1}$$

While the frequency response was decidedly non-linear, the magnitude of the resonance was still below that of the Kapton tape solution, which has been employed for countless laboratory and even published experiments. Therefore, while the response is non-ideal, the casing could theoretically still work in a bind if solder joints must be protected. Better yet, the design could simply be reprinted using a higher durometer filament (i.e. increase stiffness, *E*), thereby theoretically migrating the resonance into a higher frequency range.

This design was intended for use for both the V2 brace system as a retrofitted solution and the V3 brace as the stock microphone solution; however, it was never actually deployed as the outbreak of COVID-19 halted development, and the later new IRL COVID-19 project yielded a new case design altogether which may replace this design before it has even been deployed (described in the following section 4.4 Accelerometer Form Factor Version III). However, this solution architecture (with perhaps a different material) remains a viable back-up option for double-sided adhesive mounted microphone studies.

4.4 Accelerometer Form Factor Version III

For several reasons, a new packaging and attachment form factor was desired. For instance, the hypothesis that the Rycotes could be damping the high-end microphone frequency response was indeed confirmed by Özmen et al. in a study that explored the impact of double-sided tapes on the performance of Dytran 3225F7 microphones [62]. Additionally, the Rycotes were reported by users to be cumbersome and irritating (both the process and during wear), and the strong adhesive was even occasionally to blame for damaging the microphones upon removal. As such, a solution that avoided in-between adhesive altogether was prioritized. Further, the new COVID implementation introduced a new water-proofing requirement considering the need for more stringent sanitization due to use with PUIs and COVID-positive subjects. Of course some old requirements were also maintained, like the basic need to reinforce the solder joints, as well as preserving frequency response linearity within the desired bandwidth (now narrower 50-2500 Hz for lung sounds [64], with the stretch goal of also conserving the wider knee joint sounds bandwidth of 50 Hz -10 kHz).

Inspiration was drawn from a preexisting Knowles prototype which Knowles offers to customers for demonstration purposes (**Figure 36**).

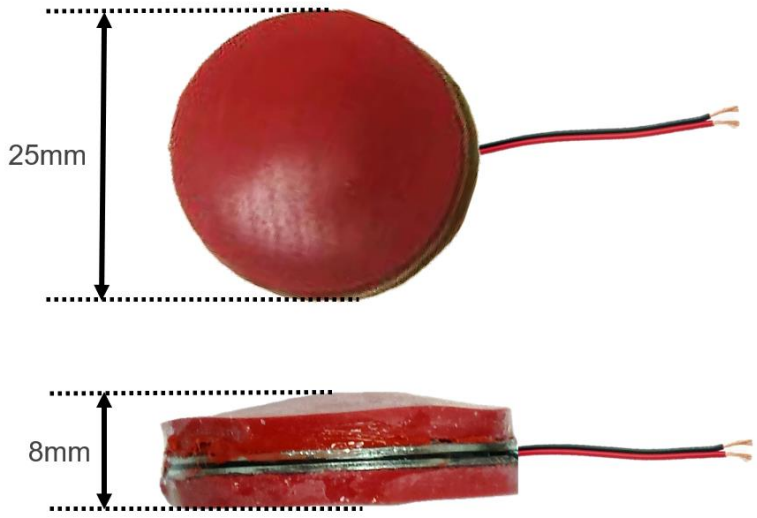

Figure 36. The demo packaging designed and provided by the manufacturers of the BU-23173 contact accelerometer (Knowles). The design consists of two sheets of latex attached to a stack of rigid metal washers, sandwiching the accelerometer in between. For attachment to a signal source, a force can be applied to the outer ring of washers, thereby deforming the latex sheets and applying a uniform backing force to the accelerometer. The latex effectively behaves like a trampoline or drum head, allowing the microphone is free to oscillate.

The design is considered a "suspension mount" where the accelerometer is sandwiched between two round sheets of flexible latex, all attached to an encircling stack of rigid washers. The design is specifically optimized for contact microphones, where the accelerometer is vertically centered within the stack that intentionally has a shorter profile than the mic; therefore, when the apparatus is placed on a subject and force is applied to the outside washer ring as intended, the microphone deflects under uniform force application. As such, the latex sheets perform as a trampoline or a drum head of sorts, allowing the microphone to more freely vibrate on the skin as compared to, for instance,

having a piece of backing tape running directly across the back of the microphone, potentially attenuating vibration.

With this suspension solution in mind, a new design was developed in collaboration with Mohsen Safaei. The idea of applying a backing force around the perimeter and thereby A) eliminating the need for adhesive between the sensor and the skin and B) enabling a method for repeatable application pressure by simply tuning the material properties of the flexible "sandwich" material, was highly desirable. However, the existing Knowles design was not deemed particularly "elegant" (relatively bulky, and several assembly steps). Instead, a design was devised that consolidated the entire assembly (latex sheets, washer stack, and accompanying adhesive) into a single flexible plastic overmold as shown in **Figure 37** (the process of choosing the exact plastic durometer is detailed in the following two sections).

This solution however did not yet address the method of application of the backing force; in other applications, the Knowles prototype could have been directly installed into a hole in a helmet or headset, the perimeter of which would have supplied the backing force to the washer stack. For this clinical COVID application though, considering the work is entirely exploratory, there is no preexisting wearable scaffolding into which the overmolded pieces could be integrated. On the contrary, the sensors have intentionally been left entirely independent from both a housing and each other to enable adaptable placement. Therefore, each individual mic required its own backing force solution as well. As such, the appropriately named "backing piece" was also designed as shown in **Figure 37**. The component is effectively a hollow cylinder, 3D-printed in a semi-flexible filament

(Cheetah 95A TPU, NinjaTek, USA) which is permanently attached to the overmolded microphone via silicone adhesive. The material was chosen specifically for its "stiff-enough" rigidity to maintain its structure under a backing force that is sufficient to ensure microphone contact, yet semi-flexibility to promote user comfort. The hollow portion allows just enough room for the microphone to deflect inside when pressed against the skin, in an attempt to remain low profile.

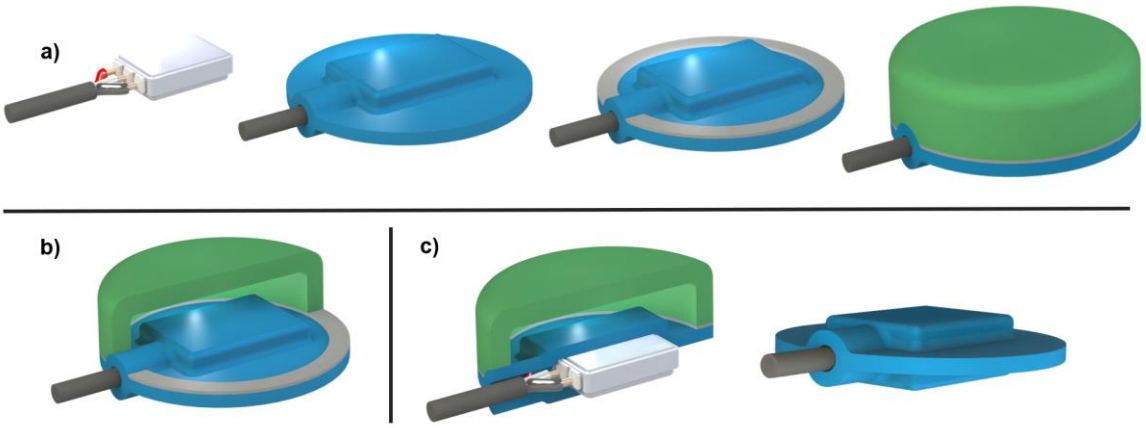

Figure 37. Renders of the proposed V3 mic packaging design, developed for the COVID clinical deployment. (a) The order of assembly, starting with a soldered microphone, then overmolding with a semi-flexible plastic or silicone material, applying a layer of adhesive, and then attaching the 3D-printed hollow backing piece which provides uniform force distribution akin to the Knowles prototype in **Figure 36**. (b) A section view of the hollow backing piece. (c) The microphone is suspended in the middle of the overmold.

4.4.1.1 FEA Modeling

To aid in picking the ideal overmold material, specifically in regards to maintaining the frequency response in the desired bandwidth, without having to manually build and test multiple prototypes across a wide range of overmold stiffnesses, an FEA model was constructed with the assistance of Mohsen Safaei in the Program ANSYS Workbench. In

sum, the simulation more or less virtually recreated the previous shaker tests used to characterize the version one and two packaging frequency responses.

To begin, the piezoceramic microphone was modeled as a hollow rectangular prism of the known outside dimensions (approximately 4mm x 8mm x 5.5mm) with an internal cantilever beam, initially of arbitrary dimensions. The entire component was approximated as structural steel, and then subjected to a harmonic acceleration (50-10050Hz) along one of the two sensing surfaces of the simulated microphone. The resulting frequency response was observed, and the beam parameters (namely, length and mass at the free end of the beam) were iteratively updated until the resonance approximated that of the Knowles datasheet, as shown in **Figure 38**.

With the base microphone frequency response established, the accompanying components were added into the simulation – the overmold, the backing piece, and the adhesive layer between the two. For the sake of minimizing computational expense, the geometries were all simplified before introduction into the model, largely by the removal of filets. Material properties were applied to each component respectively, as estimated from online datasheets for silicone epoxy, NinjaTek Cheetah filament, and most importantly the silicone overmold. More specifically, two silicone material properties (Young's modulus and density) were "parameterized" within ANSYS, enabling the simulation of multiple durometer types to be iteratively simulated in the mic model. A global mesh of 1e-3m was applied, with a finer mesh of 5e-4m applied to the microphone component as a whole.

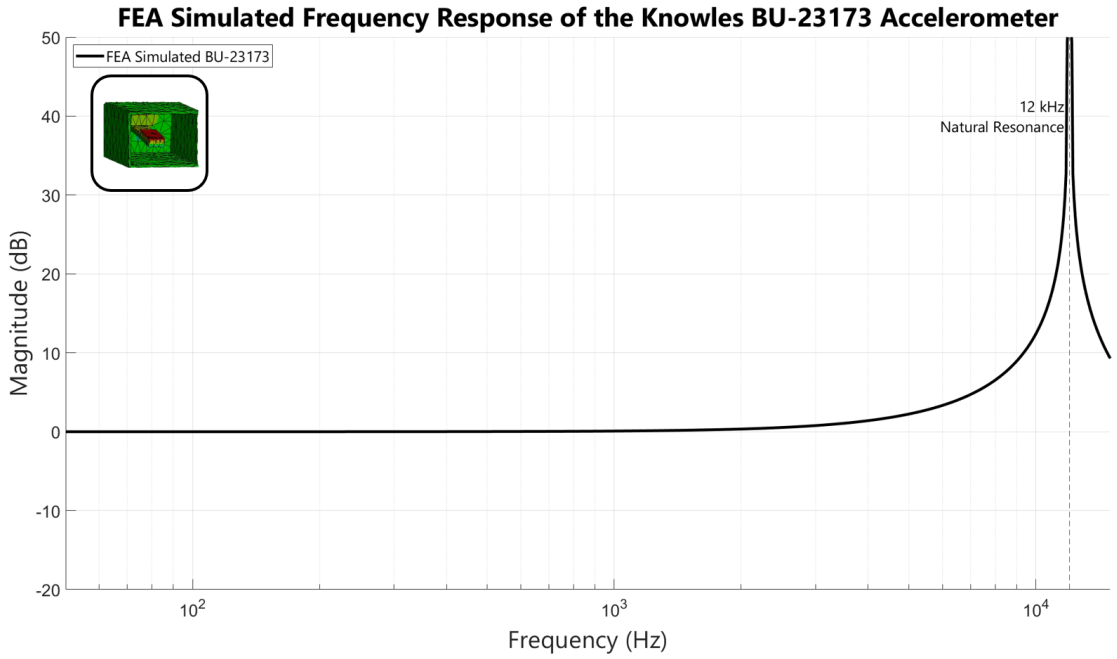

Figure 38. Resulting frequency response of the FEA simulated accelerometer. The parameters of the internal cantilever beam were iteratively updated until the response mirrored that of the Knowles BU-23173 datasheet.

With the geometry, materials, and mesh now decided, constraints and loads were then established. First, all touching surfaces were mated respectively (the outside of the mic to the inside of the overmold, and the adhesive to both the overmold and the backing piece). In a static analysis, the sensing surface of the assembly (the bottom face of the overmold) was defined by a fixed support constraint. Then, considering the intended application involves a steady backing force applied by tape across the backing piece, a constant 1N force (chosen based on the recommended 1-2N force range presented by Özmen et al. [62]) was applied to the top surface of the backing piece. The resulting deformation from this simulation is depicted in **Figure 39**.

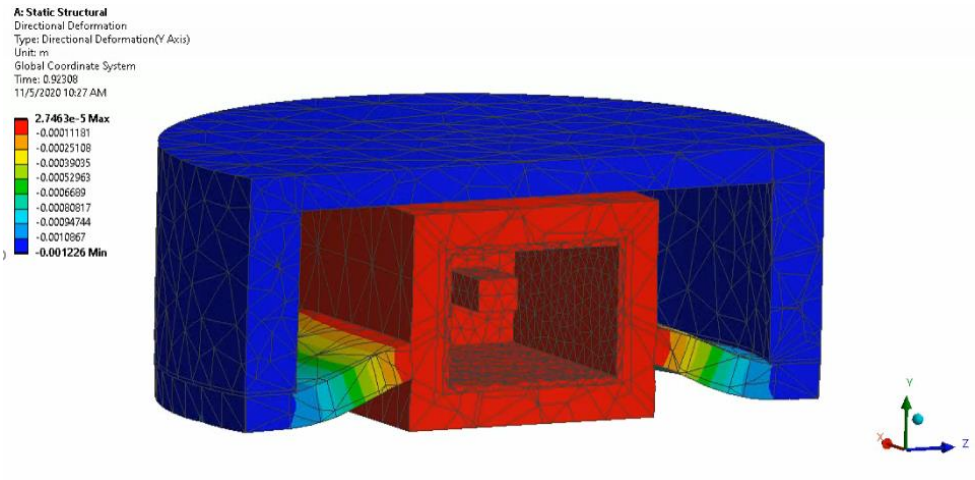

Figure 39. Resulting deformation of the overmold material caused by the 1N backing force on the backing piece within the FEA simulation. The component deformed as expected.

The above static results were then fed into a modal analysis, in which ANSYS predicts and stores the vibratory modes of the system in preparation for the final harmonic analysis; by storing the system behavior at the natural frequencies within the modal analysis, ANSYS can then more efficiently produce results for the subsequent harmonic analysis by simply recycling the modal results using the method of superposition, ultimately drastically reducing computational expense. Akin to the lone mic simulation, the entire assembly was harmonically accelerated from the bottom surface of the overmold from 50-10050 Hz, and finally the resulting frequency response was obtained. This process was repeated for overmold durometers from 20A shore hardness to 80A, as estimated by the density and YM values in **Table 6**.

Table 6. Density and Young's moduli of the FEA simulated flexible overmold materials.

Material	Shore Hardness (A scale)	Density (g/cm3)	Young's Mod (MPa)
Mold Max 20 Silicone Rubber	20	1.18	0.55
OOMOO 30 Silicone Rubber	30	1.34	0.689
Mold Max 40 Silicone Rubber	40	1.14	1.31
PR 110/50 Silicone Rubber	50	1.15	1.6
Mold Max 60 Silicone Rubber	60	1.45	2.282
PMC-770 Urethane Rubber	70	1.04	1.724
Econ 80 Urethane Rubber	80	1.06	4.619

The results of the simulation are presented in **Figure 40**. The simulations behaved as expected in that the stiffer the overmold material, the higher the resonance frequency. From this figure, it was concluded that for the COVID-19 lung sounds application, an overmold material durometer would need to be chosen from 60A hardness or stiffer, ideally a material closer to 80A which would theoretically respond with a maximum non-linearity still below 3dB within the lung sounds bandwidth, and is otherwise sufficiently linear.

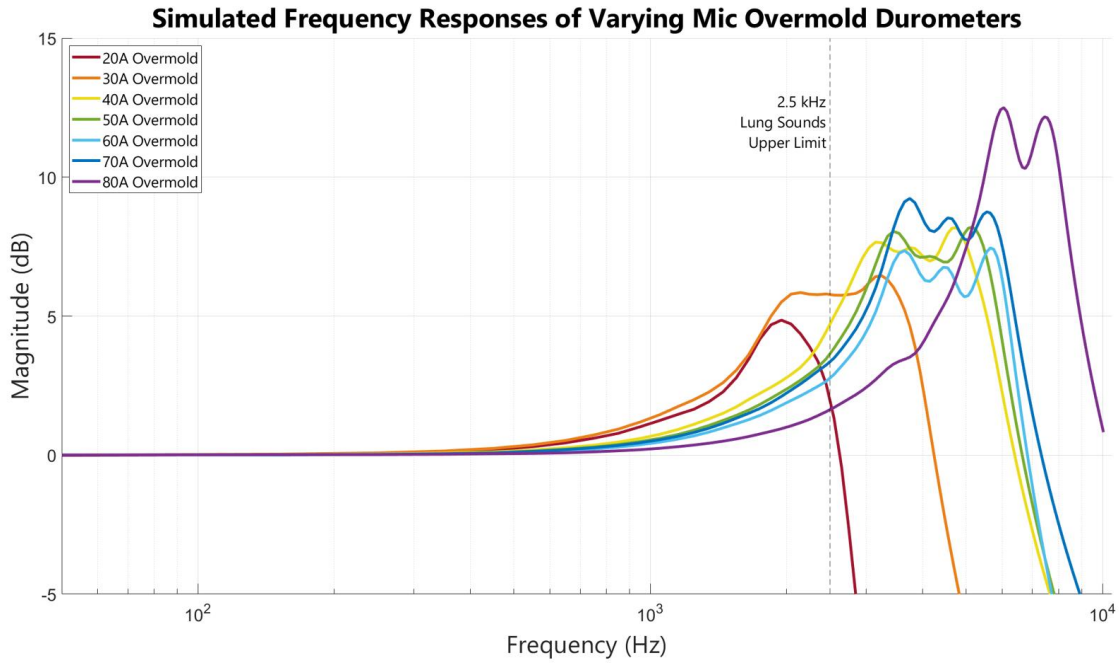

Figure 40. Resulting simulated frequency responses of the various overmold durometers. As durometer increases, so too does the natural resonance, as expected. This simulation suggests that the best overmold durometer in this situation would be nearest to 80A.

4.4.1.2 Physical Modeling

Considering the tight timeline of the project and the urgent need for approval of an overmold material in order to place the contract manufacturing order, physical modeling occurred concurrently with the development of the FEA model. As such, a prototypical overmold design was manually constructed within the lab. First, the leads were soldered to the microphone terminals which were then secured with a small bead of epoxy, per instruction from the contract manufacturer. Then using 3D printed negative molds matching the overmolded design formerly shown in **Figure 37**, the mics were carefully positioned and then various durometers of liquid silicone rubber or liquid polyurethane were manually injected (EcoFlex 20A, OOMOO 25A, Mold Max 40A, PMC 770 70A,

Smooth-On, USA). After curing, each overmold was then bound to its own 3D printed Cheetah filament backing piece using a silicone adhesive (Sil-Poxy, Smooth-On, USA). The baking pieces were all 3D printed of the same exact material and geometry. Note that lower durometer materials (20A, 25A) were employed while the FEA model was still in its infancy, otherwise they would have been avoided for sake of time had the impact on frequency response been known.

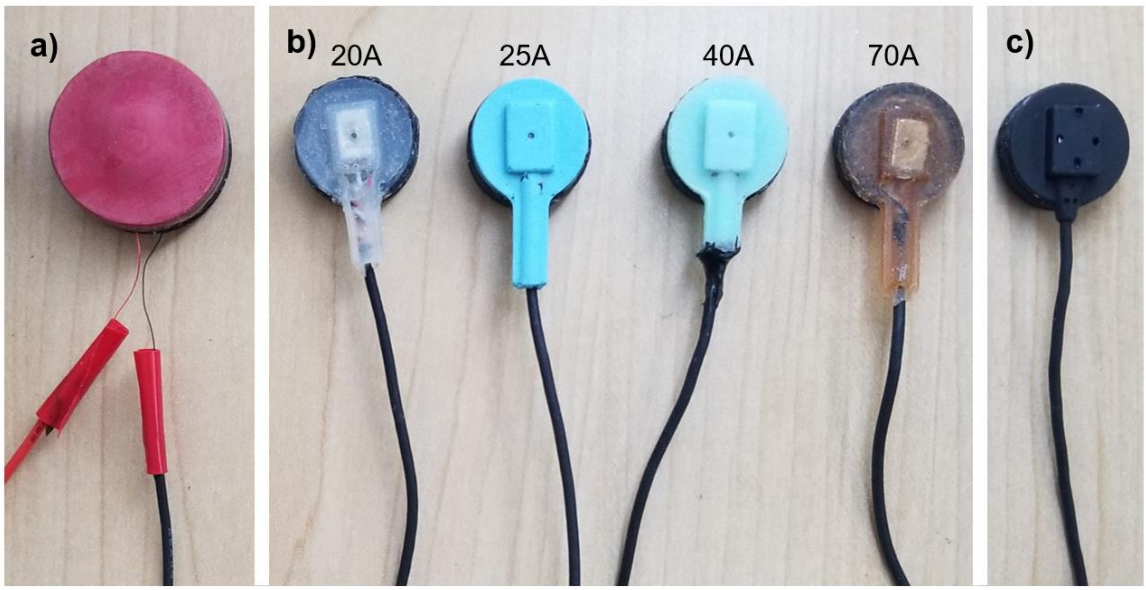

Figure 41. The three types of microphone housings in question. (a) Knowles demo housing. (b) Custom-built overmolded mics of varying durometers with backing pieces, per the proposed contract manufactured solution. (c) The Winchester accelerometer first article of 77A shore hardness.

Figure 41 depicts the three broad categories of prototypes that were tested – the Knowles demonstration prototypes, to simply be used as a reference point of an industry-accepted solution for the BU series microphone packaging; the above described custom built IRL assemblies; and later, the first articles of the contract-manufactured version of

the custom overmold made by Winchester Interconnect. Note - the Winchester overmolds were purchased after the FEA modeling suggested that a 70-80A durometer overmold would successfully avoid a resonance in the desired bandwidth, which was then further supported by the physical modeling of the custom overmolds. For added precaution though, first articles were tested in the same manner as the internal prototypes before officially approving the material durometer (77A) for the remainder of the units. The backing pieces for the Winchester models were likewise internally 3D printed and attached with Sil-Poxy after receipt of sensors.

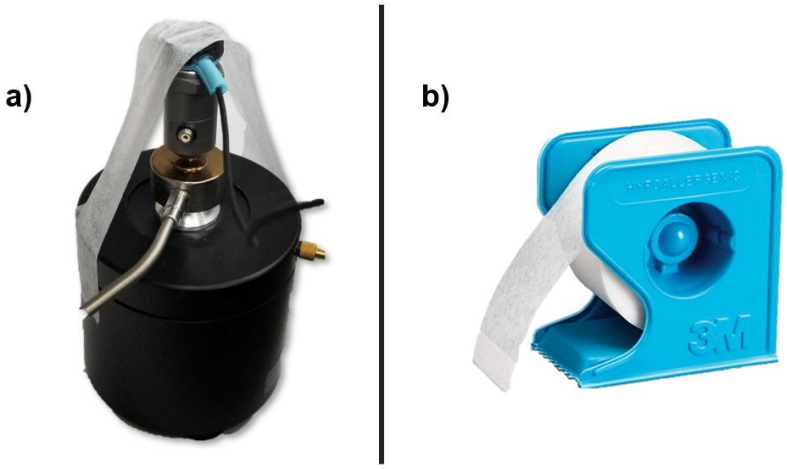

Figure 42. Demonstration of backing tape for overmolded mic packaging solutions. (a) An overmolded mic during shaker testing, held in place with backing force across the back of the backing piece. Using the load cell, the force was measured to be within 1-2N for every trial. (b) Example of the 3M MediPore tape recommended by clinical affiliates for its ubiquity in the clinic.

The mics were tested serially using the same shaker setup as before, only with a couple of changes. First, the Rycote double-sided stickies were exchanged for soft surgical backing tape (MediPore, 3M, USA) as suggested by a clinical affiliate for its ubiquity in

hospitals and reliable yet comfortable adhesion (**Figure 42**). Second, to ensure that the backing force remained consistently within the suggested 1-2 N within and across trials [62], the in-line load cell data was now monitored.

For the sake of clarity, the Knowles frequency response has been plotted separately from the custom overmold designs in **Figure 43**, along with the previous Kapton and 3D-printed housings of the following two sections for reference. The Knowles overmold performed comparably, but had the lowest resonance frequency of the three likely due to the low stiffness and large mass of the overmold, and as such would not be considered for our application.

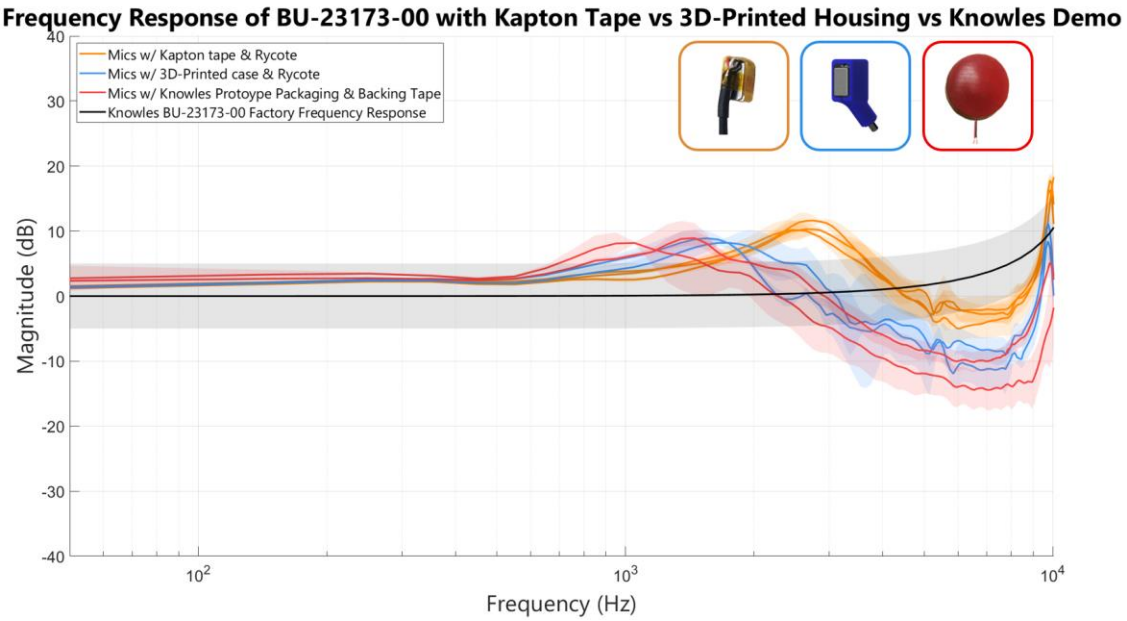

Figure 43. Frequency responses of the BU-23173 with the Knowles demo packaging as compared to the two previous mic versions. The Knowles demo case migrated the resonance even further down into the desired bandwidth.

As demonstrated in **Figure 44**, the trend previously suggested by the FEA modeling was confirmed – as overmold durometer increases, the resonance migrates to higher

frequencies, eventually beyond the lung sounds range. The 77A durometer Winchester microphone resonance had the least overlap with the lung sounds bandwidth of the group, however, presented some non-linearity below 200 Hz, which of course is not ideal for the 50-2500Hz lung sounds bandwidth. This aberration could potentially be described by the backing force which has been shown to attenuate low frequency oscillations [62], although this response is still somewhat unexpected as neither the FEA simulation nor the similar durometer in-house overmolds demonstrated this low frequency behavior. A final plot comparing the three ultimate microphone versions can be seen in **Figure 45**. Overall, while the Winchester solution holds promise, the low frequency behavior should be further characterized.

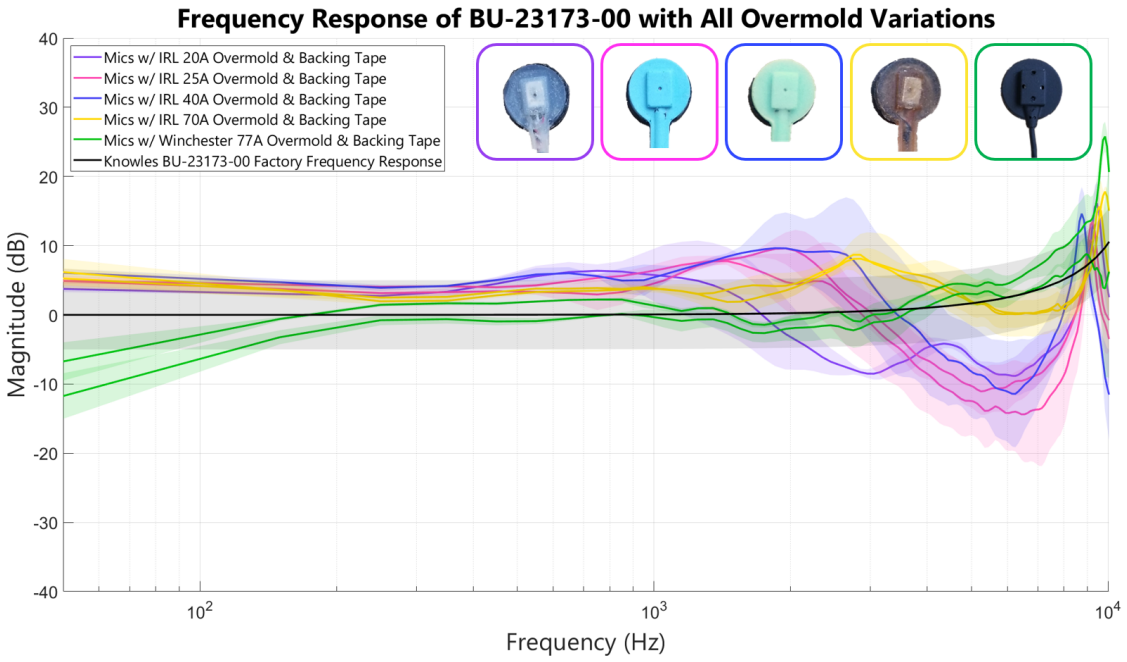

Figure 44. Frequency responses of all overmolded solutions, including the four custom-made overmolds of varying durometers (20A, 25A, 40A, 70A), and the first article from Winchester contract manufacturer of 77A. As predicted by the FEA modeling, the resonances increase in frequency as the stiffness increases. While the 77A overmold had

the latest resonance, it unfortunately demonstrated a non-linear response below 100Hz. This result could be due to backing force, but should ultimately be explored further.

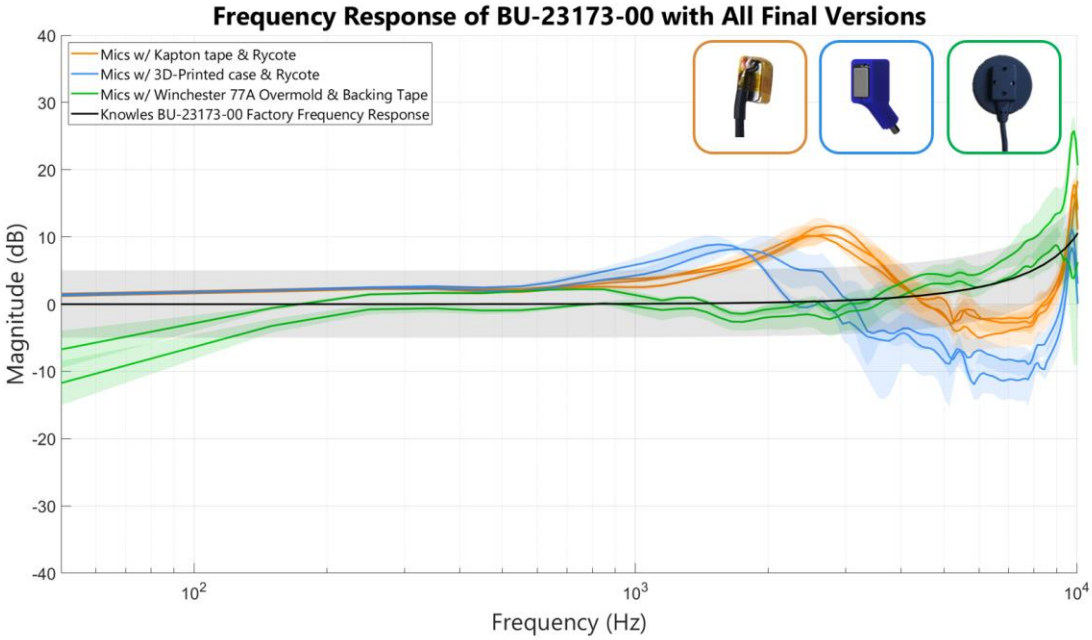

Figure 45. Summary of all three final mic solutions over the past 2 years. While the Winchester solution holds promise, the low frequency behavior should be further characterized.

4.5 Contact Accelerometer Discussion

This accelerometer packaging design process simultaneously answered many questions, while presenting a few new ones. For instance, the ~2.5kHz resonance of the V1 solution (Kapton tape and Rycote stickie) was surprising, considering this "packaging" iteration (or lack thereof) is the least obtrusive of all the methods, therefore it was expected that this modality would have the most similar frequency response to the baseline. This unexpected behavior could perhaps be caused by the Rycote itself, an idea that deserves exploration akin to that done for Dytran mics by Özmen et al. [62]. However, the Kapton

tape solution has still sufficiently supplied meaningful and repeatable data for countless trials thus far; if this solution is still implemented moving forward, the resonance should simply be taken into account during spectral analysis (should be careful not to inappropriately attribute this 2.5kHz information to the joint sounds, for instance).

Similarly, while the V2 3D-printed case and accompanying epoxy were estimated to alter the frequency response by reducing the natural frequency, the actual resonance location was surprisingly low (~1.5kHz). Again, this is perhaps caused by the Rycote means of attachment, but again, this hypothesis should be explored. The solution successfully protects the microphone as intended, but future users must decide if the resonance is a show stopper for their application.

The "trampoline" design of the V3 solution holds potential for future mic testing. Not only is this form factor a version of the industry-standard method of implementation, it also solves many of the tried and true complications of mic-skin interfacing - eliminates adhesive between the skin and the measuring surface, promotes consistent backing force, and provides mechanical and fluid-based protection for the mic/solder joints. However, an interesting catch-22 was stumbled upon in the process –to migrate the resonance far enough out of the desired lung sounds bandwidth, the overmold material must be made sufficiently rigid (for reference, 80A durometer is akin to the stiffness of a dense rubber shoe heel, i.e., not particularly flexible). This rigidity necessary for the resonance migration then hinders the desired "trampoline" effect, in that the overmold is no longer flexible enough to deform under the 1-2N backing force. This tradeoff between resonance and overmold rigidity simply begs the question whether or not the deformation is necessary to achieve the desired

result. In other words, it should be explored whether the backing piece still functions as intended (deforming the perimeter of the overmold despite not visibly doing so, and as such providing an indirect backing force to the microphone, and thereby lessening vibration attenuation as compared to a direct backing tape across the overmold itself), or if the overmold rigidity negates the presence of the backing piece altogether (by preventing the intended perimeter deformation from occurring), and perhaps the frequency response would be better served by removing the added mass of the backing piece.

Moving forward, many testing and prototyping avenues should be explored for mic housing and attachment. As mentioned above, the overmold catch-22 situation should be better characterized, as well as the impact of Rycote stickies on the Knowles microphone as compared to other means of attachment like thin double-sided tapes or backing tapes. Another important but challenging arena for investigation entails verifying that the sounds recorded by the microphones are indeed originating from the hypothesized source (the joint or lungs) and not from the means of attachment. Furthermore, while recording for the proof-of-concept lungs sounds data, a signal was played back audibly and background noises like soft speaking and the whirs of a 3D printer were emitted from the laptop speakers, revealing that these contact microphones were more sensitive to ambient noise than previously personally thought. This experience then begged the question, in the case of a subject coughing for instance, how can one be certain that the cough signature received by the microphone was gathered through contact vibrations though the skin and lungs as intended, as opposed to through ambient noise, and perhaps more importantly, does that matter? A similar question may be raised for the joint sounds application – how can one be

certain that the cyclical “clicks” are indeed from sounds originating from within the joint, and not cyclical deformation of say the adhesive pad? The fact that previous studies have reliably been able to differentiate between various knee conditions based on sounds alone holds promise that these questions are unfounded, but nonetheless, could still be worth exploring, and certainly worth consciously incorporating into design decisions (e.g., brainstorming attachment methods that do not create deformation or rubbing noises, designing the packaging to mitigate ambient noise, or even considering an alternative sensor with built in noise canceling properties).

Other future work includes adapting the V3 mic packaging (overmold) for use within the joint sounds bandwidth (i.e. moving the resonance), as well as considering the lower-profile but equal in function Knowles BU-23842-00 microphone, simply as a means to reduce sensor size. Further, the overmold presently entirely encases the microphone, including the contact surface, potentially impacting the frequency response in a manner similar to the former Rycote padding. A solution in which the contact surface is unobstructed could be a potential avenue for improving the frequency response. Lastly, for maximum repeatability and ease-of-use, a universal accelerometer housing should be explored, in which all mics can be placed at once, ideally without the use of adhesives.

CHAPTER 5. CONCLUSION

This dissertation has presented two areas of performed research. First, the evolution of a wearable, multimodal (acoustic, EBI, temperature, and motion), health sensing device was described, from its infancy as the first wearable joint health iteration that ultimately failed to thrive, followed by a highly successful clinically-deployed second iteration, then a promising third all-encompassing brace form factor to be tested in coming months, and finally concluding with a a fully adapted system for lung health monitoring of COVID-19 patients. Second, the packaging for one of the four sensing modalities was optimized for both performance and clinical-readiness.

Multiple significant conclusions were reached in this process. The V2 brace was the first fully untethered, wearable, multimodal sensing/diagnostic device capable of assessing both physiological (i.e., fluid presence and kinematics) and structural (i.e., acoustics) information about the underlying joint [57], also specifically designed for implementation by unfamiliar users. Likewise, to the best of the available knowledge, the subsequent COVID-19 lung adaptation is the first wearable device for longitudinal COVID-19 acoustic and bioimpedance monitoring, nonetheless lung monitoring in general. Generally speaking, a key contribution was simply facilitating the translation of lab-based hardware to clinical and potentially at-home use, through prioritization of design robustness (e.g., water-tightness, component strength), ergonomics (e.g., comfort, adaptable sizing), and usability (e.g., labeling, generally designing for device-naïve users). Again, to the best of the available knowledge, the custom overmolded accelerometer with backing piece for

unified force application is also the first of its kind. Likewise, the frequency response characterization of the various microphone packaging solutions via shaker tests had not been previously done for the Knowles BU-23173 microphone.

Future work should include assessing the final results of the V2 brace clinical studies, and later evaluating the V3 knee brace both internally and clinically, and possibly even with at-home users. Ideally, the aforementioned joint health score could be derived from the data and, eventually, the stretch goal of the DARPA-funded project which is building a closed-loop system (i.e., one that titrates treatment in the form of transcutaneous vagus nerve stimulation which is suspected to have positive/amplifying impacts on healing) could be realized. The lung sounds hardware should also be thoroughly tested internally, and then deployed clinically. Ideally someday, the electronics for either application could be updated to actively report the measured signals, enabling real-time decision making, for instance for use in critical scenarios like rapidly decompensating cardiopulmonary function. Naturally, all devices should be iteratively updated based on experience and user feedback. Concerning the microphone packaging in particular, the packaging and attachment methods should be further characterized by shaker tests and improved in regards to resonances within the desired bandwidths.

APPENDIX

Table 7. V1 brace bill of materials.

Line	Name	Quantity	Description
1	Audio Board	1	• Custom 1st Generation audio board • Responsible for audio recordings; has switches for device initiation/mode
2	Main Board	1	• Custom 1st Generation main board • Responsible for BIS, IMU, and temperature recordings • Time synched with and controlled by the audio board
3	Audio Board to Main Board Cable	1	• COTS 4-lead IDC cable (JST Sales, A04XSR04XSR36R152A)
4	Battery	2	• COTS 3.7V 500mAh Lithium battery (Adafruit, LP-523334 3.7 V 500mAh with PCM) • COTS connector for board interfacing, manually spliced to battery terminals (JST Sales, A02SUR02SUR32W152B)
5	SD Card	2	• COTS 32GB microSD memory card (Samsung, 32GB EVO UHS-I microSDHC)
6	Temperature Sensor Board	2	• Custom PCB with temperature sensor (Texas Instruments, TMP116)
7	Temperature Sensor Cable	2	• COTS 6-lead IDC cable (JST Sales, A06XSR06XSR36R152A)
8	IMU Sensor Board	2	• Custom PCB with IMU (Bosch Sensortec, BMX055)
9	IMU Sensor Cable	2	• COTS 10-lead IDC cable (JST Sales, A10XSR10XSR36R152A)
10	BIS Electrode Snap + Cable Assembly	4*	• COTS electrode snaps manually soldered to cable with coaxial connector (UMCC, 2015357-4) • *1 additional snap which is not electrically connected that simply aids in proximal sensor housing attachment
11	Cloth Electrodes	5	• COTS Cloth electrodes for BIS collection (3M, 3M-2670-5) • *1 additional electrode which is not electrically connected that simply aids in sensor housing attachment
12	Microphone + Cable Assembly	4	• COTS Piezo-ceramic contact accelerometer (Knowles, BU-23173-000) • Custom 3 conductor cable (New England Wire, 9ZGAT001WIRE) • COTS 3.5mm audio plug (CUI Devices, SP-35401) • Solder joint secured with COTS Kapton tape • Attaches to skin via double-sided adhesive foam pads (Rycote, 65567)
13	Circuit Housing	1	• Custom 1st Generation 3D printed PLA rigid case • 4 Individual components assembled with COTS hardware
14	Distal Sensor Housing ("Brace")	1	• Custom 3D printed NinjaFlex (85A TPU) flexible sensor housing • Placed distally to the patella • Houses 2x electrodes (I, V), 1x IMU board, and 1x temperature board
15	Proximal Sensor Housing	1	• Custom 3D printed NinjaFlex (85A TPU) flexible sensor housing • Placed proximally to the patella • Houses 2x electrodes (I, V), 1x IMU board, and 1x temperature board
16	Placement Stencil	1	• Custom 3D printed NinjaFlex (85A TPU) flexible stencil • Uses anatomical features for repeatable microphone and housing placement

Table 8. V2 brace bill of materials. Green text signifies new or updated components since the previous iteration.

Line	Name	Quantity	Description
1	Audio Board	1	• Custom **2nd Generation** audio board • Responsible for audio recordings; has switches for device initiation/mode • **New, smaller audio jacks (2.5mm)**
2	Main Board	1	• Custom **2nd Generation** main board • Responsible for BIS, IMU, and temperature recordings • Time synched with and controlled by the audio board • **New COTS Omnetics brand connectors for IMU, BIS, and temperature sensing (Omnetics, A22017-001 and A22014-001)**
3	**Battery Hard-Reset Switches**	**2**	• **Hard-wired switches for resetting either battery (audio board or main board), useful for instance, in the event of device troubleshooting**
4	Audio Board-to-Main Board Cable	1	• COTS 4-lead IDC cable (JST Sales, A04XSR04XSR36R152A)
5	Battery	2	• COTS 3.7V 500mAh Lithium battery (Adafruit, LP-523334 3.7 V 500mAh with PCM) • COTS connector for board interfacing, manually spliced to battery terminals (JST Sales, A02SUR02SUR32W152B)
6	SD Card	2	• COTS 32GB microSD memory card (Samsung, 32GB EVO UHS-I microSDHC)
7	Temperature Sensor Board	2	• Custom PCB with temperature sensor (Texas Instruments, TMP116) • **Now with through holes to interface with the new corresponding COTS 5-pin Omnetics connector (Omnetics, A22026-001)**
8	Temperature Sensor Cable	2	• **Custom 4-lead cable** • **COTS 5-pin Omnetics connectors on either end (one latching Omnetics, A22027-001, one standard Omnetics, A22000-001)** • **Features heat shrink system for graduated bend relief**
9	IMU Sensor Board	2	• Custom PCB with IMU (Bosch Sensortec, BMX055) • **Now with through holes to interface with the new corresponding COTS 12-pin Omnetics connector (Omnetics, A22046-001)**
10	IMU Sensor Cable	2	• **Custom 10-lead cable** • **COTS 12-pin Omnetics connectors on either end (one latching A22028-001, one standard A22005-001)** • **Features heat shrink system for graduated bend relief**
11	BIS Electrode Snap + Cable Assembly	4*	• **Custom 4 lead cable with 4 COTS overmolded electrode snaps on one end (SparkFun, CAB-12970) and a 5-pin Omnetics connector on the other (A22000-001)** • *2 additional snaps which are not electrically connected that simply aid in proximal sensor housing attachment
12	Cloth Electrodes	6*	• COTS Cloth electrodes for BIS collection (3M, 3M-2670-5) • *2 additional electrodes which are not electrically connected that simply aid in sensor housing attachment
13	Microphone + Cable Assembly	4	• COTS Piezo-ceramic contact accelerometer (Knowles, BU-23173-000) • Custom 3 conductor cable (New England Wire, 9ZGAT001WIRE) • **COTS 2.5mm audio plug (CUI Devices, SP-25401)** • Solder joint secured with Kapton tape • Attaches to skin via double-sided adhesive foam pads (Rycote, 65567)
14	Circuit Housing	1	• Custom **2nd Generation** 3D printed PLA rigid case • **3 Individual components** assembled with COTS hardware
15	Distal Sensor Housing	1	• Custom **2nd Generation** 3D printed **Cheetah (95A TPU)** flexible sensor housing • Placed distally to the patella • Houses 2x electrodes (I, V), 1x IMU board, and 1x temperature board
16	Proximal Sensor Housing	1	• Custom **2nd Generation** 3D printed **Cheetah (95A TPU)** flexible sensor housing • Placed proximally to the patella • Houses 2x electrodes (I, V), 1x IMU board, and 1x temperature board
17	Placement Stencil	1	• Custom **2nd Generation** 3D printed **Cheetah (95A TPU)** flexible stencil • Uses anatomical features for repeatable microphone and housing placement
18	**Microphone Wire Standoff**	**1**	• **Custom 3D printed Cheetah (95A TPU) flexible tool for securing/rerouting loose mic wires off and away from the skin**

Table 9. V3 brace bill of materials. Green text signifies new or updated components since the previous iteration.

Line	Name	Quantity	Description
1	**Flex Brace**	**1**	• **COTS Orthopedic knee brace (Össur, Flex Brace)** • **Used as a scaffolding for all below components**
2	Audio Board	1	• Custom **3rd Generation** audio board • Responsible for audio recordings; has switches for device initiation/mode • **Switch for battery hard-reset now integrated into board**
3	Main Board	1	• Custom **3rd Generation** main board • Responsible for BIS, IMU, and temperature recordings • Time synched with and controlled by the audio board • **New COTS Samtec brand connectors for IMU, BIS, and temperature sensing (Samtec, LSHM-110-02.5-L-DV-A-S-TR)** • **New switch for static VS dynamic bioimpedance measurements** • **Switch for battery hard-reset now integrated into board**
4	Audio Board-to-Main Board Cable	1	• COTS 4-lead IDC cable (JST Sales, A04XSR04XSR36R152A)
5	Battery	2	• COTS 3.7V 500mAh Lithium battery (Adafruit, LP-523334 3.7 V 500mAh with PCM) • COTS connector for board interfacing, manually spliced to battery terminals (JST Sales, A02SUR02SUR32W152B)
6	SD Card	2	• COTS 32GB microSD memory card (Samsung, 32GB EVO UHS-I microSDHC)
7	**Intermediary Sensor Board**	**2**	• **Custom sensor board introduced as a means for improved cable management for the new brace form factor** • **IMU sensor (Bosch Sensortec, BMX055) now embedded into this board; additional connections for temperature and BIS sensors**
8	Temperature Sensor Board	2	• Custom PCB with temperature sensor (Texas Instruments, TMP116) • Uses same V2 brace Omnetics connector
9	**Samtec Sensor Cable**	**2**	• **COTS Samtec brand 20-pin cable (Samtec, HLCD-10-XX.00-TR-TR-1, where XX denotes a modifiable length)** • **Responsible for sensor-board-to-main-board communication (of IMU, temperature and BIS data)**
10	BIS Electrode Snap + Cable Assembly	4	• **COTS overmolded electrode snap, cable, and board-interfacing connector assembly (Myoware, only the cable of AT-04-001 assembly)** • **Interfaces with corresponding COTS female board-mounted connector on intermediary sensor board**
11	Cloth Electrodes	4	• COTS Cloth electrodes for BIS collection (3M, 3M-2670-5)
12	Microphone + Cable Assembly	4	• COTS Piezo-ceramic contact accelerometer (Knowles, BU-23173-000) • Custom 3 conductor cable (New England Wire, 9ZGAT001WIRE) • COTS 2.5mm audio plug (CUI Devices, SP-25401) • Solder joint secured with Kapton tape • Attaches to skin via double-sided adhesive foam pads (Rycote, 65567)
13	**Intermediary Audio Cable**	**4**	• **COTS 2.5mm female to right-angle male audio plug cables (YCS, B00FHBXL94)** • **Introduced as a means for improved cabled management and mic protection for the new brace form factor**
14	**Audio Jack Housing**	**2**	• **Custom 3D printed PLA rigid housing to secure the female ends of the intermediary audio cables to the brace hinges**
15	Main Circuit Housing	1	• Custom **3rd Generation** 3D printed PLA rigid case • 3 Individual components assembled with COTS hardware
16	**Sensor Board Housing**	**2**	• **Custom 3D printed PLA rigid cases for the new intermediary sensor boards**
17	**Electrode + Temp Housing**	**2**	• **Custom 3D printed Cheetah (95A TPU) flexible cases** • **Each houses 2x electrodes (I, V) and 1x temperature board**
18	**Custom Foam Insert**	**2**	• **Custom cut COTS foam (Lazy Dog Warehouse, B078T96YPY) to replace stock brace foam while accommodating new electrode + temp housings** • **One proximal section, one distal**
19	Placement Stencil	1	• Custom **3rd Generation** 3D printed Cheetah (95A TPU) flexible stencil • Uses anatomical features for repeatable microphone and housing placement • **Simplified for solely mic placement**
20	**Drill Stencil**	**1**	• **Custom 3D printed Cheetah (95A TPU) flexible stencil for drilling through the carbon fiber brace to make passthroughs for the BIS electrodes and temperature sensor Omnetics connector**

Table 10. COVID device bill of materials. Green text signifies new or updated components since the previous iteration.

Line	Name	Quantity	Description
1	Audio Board	1	• Custom **2.5 Generation** audio board • Responsible for audio recordings; has switches for device initiation/mode • Switch for battery hard-reset integrated into board
2	Main Board	1	• Custom **2.5 Generation** main board • Responsible for BIS, IMU, and temperature recordings • Time synched with and controlled by the audio board • Uses Omnetics brand **right-angle connectors**
3	Battery Hard-Reset Switch	1	• Hard-wired switch for resetting main board battery, useful for instance, in the event of device troubleshooting
4	Audio Board-to-Main Board Cable	1	• COTS 4-lead IDC cable (JST Sales, A04XSR04XSR36R152A)
5	Battery	2	• COTS 3.7V 500mAh Lithium battery (Adafruit, LP-523334 3.7 V 500mAh with PCM) • COTS connector for board interfacing, manually spliced to battery terminals (JST Sales, A02SUR02SUR32W152B)
6	SD Card	2	• COTS 32GB microSD memory card (Samsung, 32GB EVO UHS-I microSDHC)
7	Temperature Sensor Board	1	• Custom PCB with temperature sensor (Texas Instruments, TMP116) • Uses 5-pin right-angle COTS Omnetics connector (Omnetics, MCP-05-RA) • Attaches directly to the mating connector at the main board
8	**Temperature Sensor Board + Cable Assembly**	1	• Custom PCB with temperature sensor (Texas Instruments, TMP116) **• New custom contract-manufactured (Winchester Interconnect) overmold and cable assembly for axillary temperature measurements**
9	IMU Sensor Board	**1**	• Custom PCB with IMU (Bosch Sensortec, BMX055) • Uses COTS 12-pin **right-angle connector** (Omnetics, MCS-12-RA) **• Attaches directly to the mating connector at the main board**
10	**IMU Sensor Board + Cable Assembly**	1	• Custom PCB with IMU (Bosch Sensortec, BMX055) **• New custom contract-manufactured (Winchester Interconnect) overmold and cable assembly for postural data**
11	BIS Electrode Snap + Cable Assembly	4	• Custom 4 lead cable with 4 COTS overmolded electrode snaps on one end (SparkFun, CAB-12970) and a 5-pin Omnetics connector on the other (A22000-001) **• Contract manufactured by Winchester Interconnect**
12	Cloth Electrodes	4	**• COTS Cloth electrodes for BIS collection (3M, 3M-2670-5)**
13	Microphone + Cable Assembly	4	• COTS Piezo-ceramic contact accelerometer (Knowles, BU-23173-000) • Custom 3 conductor cable (New England Wire, 9ZGAT001WIRE) • COTS 2.5mm audio plug (CUI Devices, SP-25401) **• New custom contract-manufactured (Winchester Interconnect) overmold and cable assembly** **• Attached via backing tape**
14	Main Circuit Housing	1	• Custom **4th Generation** 3D printed PLA rigid case • **4** Individual components assembled with COTS hardware **• To be contract-manufactured by Protolabs**
15	**Local Temperature Sensor Housing**	**1**	**• Custom 3D-printed Cheetah (95A TPU) flexible cases for protecting the local temperature sensor** **• Filled with epoxy**
16	**Local IMU Sensor Housing**	**1**	**• Custom 3D-printed Cheetah (95A TPU) flexible cases for protecting the local IMU sensor** **• Filled with epoxy**

REFERENCES

[1] B. Semiz, S. Hersek, D. C. Whittingslow, L. A. Ponder, S. Prahalad, and O. T. Inan, "Using Knee Acoustical Emissions for Sensing Joint Health in Patients With Juvenile Idiopathic Arthritis: A Pilot Study," *IEEE Sensors Journal,* vol. 18, no. 22, pp. 9128-9136, 2018.

[2] D. Whittingslow, B. Semiz, L. Ponder, P. Vega-Fernandez, O. Inan, and S. Prahalad, "Knee Joint Sounds: A Non-Invasive Modality for Classifying Knee Joint Health in Juvenile Idiopathic Arthritis," *American College of Rheumatology,* 2017. [Online]. Available: https://acrabstracts.org/abstract/knee-joint-sounds-a-non-invasive-modality-for-classifying-knee-joint-health-in-juvenile-idiopathic-arthritis/.

[3] D. Whittingslow, B. Semiz, L. Ponder, A. Wiens, O. Inan, and S. Prahalad, *Analysis and Implications of Non-Invasive Knee Acoustical Emissions in Juvenile Idiopathic Arthritis*. 2017.

[4] N. B. Bolus, H. K. Jeong, D. C. Whittingslow, and O. T. Inan, "A Glove-Based Form Factor for Collecting Joint Acoustic Emissions: Design and Validation," (in eng), *Sensors (Basel),* vol. 19, no. 12, p. 2683, 2019, doi: 10.3390/s19122683.

[5] H. Töreyin, H. K. Jeong, S. Hersek, C. N. Teague, and O. T. Inan, "Real-time activity classification in a wearable system prototype for knee health assessment via joint sounds," in *2016 38th Annual International Conference of the IEEE Engineering in Medicine and Biology Society (EMBC)*, 16-20 Aug. 2016 2016, pp. 3113-3116, doi: 10.1109/EMBC.2016.7591388.

[6] S. Hersek *et al.*, "Acoustical Emission Analysis by Unsupervised Graph Mining: A Novel Biomarker of Knee Health Status," *IEEE Transactions on Biomedical Engineering,* vol. 65, no. 6, pp. 1291-1300, 2018, doi: 10.1109/TBME.2017.2743562.

[7] S. Hersek *et al.*, "Wearable Vector Electrical Bioimpedance System to Assess Knee Joint Health," (in eng), *IEEE Trans Biomed Eng,* vol. 64, no. 10, pp. 2353-2360, 2017, doi: 10.1109/TBME.2016.2641958.

[8] H. K. Jeong, M. B. Pouyan, D. C. Whittingslow, V. Ganti, and O. T. Inan, "Quantifying the Effects of Increasing Mechanical Stress on Knee Acoustical

Emissions Using Unsupervised Graph Mining," *IEEE Transactions on Neural Systems and Rehabilitation Engineering,* vol. 26, no. 3, pp. 594-601, 2018.

[9] C. Teague *et al.*, "Novel approaches to measure acoustic emissions as biomarkers for joint health assessment," in *2015 IEEE 12th International Conference on Wearable and Implantable Body Sensor Networks (BSN)*, 9-12 June 2015 2015, pp. 1-6, doi: 10.1109/BSN.2015.7299389.

[10] D. C. Whittingslow, H.-K. Jeong, V. G. Ganti, N. J. Kirkpatrick, G. F. Kogler, and O. T. Inan, "Acoustic Emissions as a Non-invasive Biomarker of the Structural Health of the Knee," *Annals of Biomedical Engineering,* vol. 48, no. 1, pp. 225-235, 2020/01/01 2020, doi: 10.1007/s10439-019-02333-x.

[11] *Treatment Guide: Knee Pain*. (2018). Cleveland Clinic. [Online]. Available: https://my.clevelandclinic.org/ccf/media/files/ortho/knee_pain_guide

[12] G. Peat, R. McCarney, and P. Croft, "Knee pain and osteoarthritis in older adults: a review of community burden and current use of primary health care," (in eng), *Ann Rheum Dis,* vol. 60, no. 2, pp. 91-97, 2001, doi: 10.1136/ard.60.2.91.

[13] M. V. Paterno, M. J. Rauh, L. C. Schmitt, K. R. Ford, and T. E. Hewett, "Incidence of Second ACL Injuries 2 Years After Primary ACL Reconstruction and Return to Sport," (in eng), *The American Journal of Sports Medicine,* no. 1552-3365 (Electronic), 2014.

[14] C. Jinks, P. Jordan K Fau - Croft, and P. Croft, "Measuring the population impact of knee pain and disability with the Western Ontario and McMaster Universities Osteoarthritis Index (WOMAC)," (in eng), no. 0304-3959 (Print), 2002.

[15] U.-S. D. T. Nguyen, Y. Zhang, Y. Zhu, J. Niu, B. Zhang, and D. T. Felson, "Increasing prevalence of knee pain and symptomatic knee osteoarthritis: survey and cohort data," (in eng), *Ann Intern Med,* vol. 155, no. 11, pp. 725-732, 2011, doi: 10.7326/0003-4819-155-11-201112060-00004.

[16] W. L. Calmbach and M. Hutchens, "Evaluation of patients presenting with knee pain: Part II. Differential diagnosis," (in eng), no. 0002-838X (Print), 2003.

[17] W. L. Calmbach and M. Hutchens, "Evaluation of patients presenting with knee pain: Part I. History, physical examination, radiographs, and laboratory tests," (in eng), no. 0002-838X (Print), 2003.

[18] S. L. Di Stasi, D. Logerstedt, E. S. Gardinier, and L. Snyder-Mackler, "Gait patterns differ between ACL-reconstructed athletes who pass return-to-sport criteria and those who fail," (in eng), *The American journal of sports medicine,* vol. 41, no. 6, pp. 1310-1318, 2013, doi: 10.1177/0363546513482718.

[19] "The Top 10 Causes of Death." World Health Organization. https://www.who.int/news-room/fact-sheets/detail/the-top-10-causes-of-death (accessed 2020).

[20] "Lung Diseases." National Institute of Environmental Health Sciences. https://www.niehs.nih.gov/health/topics/conditions/lung-disease/index.cfm#footnote1 (accessed.

[21] W. Wang, J. Tang, and F. Wei, "Updated understanding of the outbreak of 2019 novel coronavirus (2019-nCoV) in Wuhan, China," (in eng), *J Med Virol,* vol. 92, no. 4, pp. 441-447, 2020, doi: 10.1002/jmv.25689.

[22] C. Bao, X. Liu, H. Zhang, Y. Li, and J. Liu, "Coronavirus Disease 2019 (COVID-19) CT Findings: A Systematic Review and Meta-analysis," (in eng), no. 1558-349X (Electronic), 2020.

[23] X. Sun *et al.*, "Cytokine storm intervention in the early stages of COVID-19 pneumonia," (in eng), no. 1879-0305 (Electronic), 2020.

[24] P. G. Gibson, L. Qin, and S. H. Puah, "COVID-19 acute respiratory distress syndrome (ARDS): clinical features and differences from typical pre-COVID-19 ARDS," (in eng), *Med J Aust,* vol. 213, no. 2, pp. 54-56.e1, 2020, doi: 10.5694/mja2.50674.

[25] C. Wu *et al.*, "Risk Factors Associated With Acute Respiratory Distress Syndrome and Death in Patients With Coronavirus Disease 2019 Pneumonia in Wuhan, China," *JAMA Internal Medicine,* vol. 180, no. 7, pp. 934-943, 2020, doi: 10.1001/jamainternmed.2020.0994.

[26] M. Ali H Al-Khafaji, MPH. "What is the prognosis of multiple organ dysfunction syndrome (MODS) in sepsis?" MedScape. https://www.medscape.com/answers/169640-99186/what-is-the-prognosis-of-multiple-organ-dysfunction-syndrome-mods-in-sepsis (accessed.

[27] M. H. Schoenberg, P. Weiss M Fau - Radermacher, and P. Radermacher, "Outcome of patients with sepsis and septic shock after ICU treatment," (in eng), no. 1435-2443 (Print), 1998.

[28] "Lung Disease Tests and Diagnoses." Northwestern Medicine. https://www.nm.org/conditions-and-care-areas/pulmonary/division-of-thoracic-surgery/lung-disease-tests-and-diagnoses (accessed.

[29] K. Kaewkannate and S. Kim, "A comparison of wearable fitness devices," (in eng), no. 1471-2458 (Electronic), 2016.

[30] A. Shcherbina *et al.*, "Accuracy in Wrist-Worn, Sensor-Based Measurements of Heart Rate and Energy Expenditure in a Diverse Cohort. LID - 10.3390/jpm7020003 [doi] LID - 3," (in eng), no. 2075-4426 (Print), 2017.

[31] S. Gillinov *et al.*, "Variable Accuracy of Wearable Heart Rate Monitors during Aerobic Exercise," (in eng), no. 1530-0315 (Electronic), 2017.

[32] F. El-Amrawy and M. I. Nounou, "Are Currently Available Wearable Devices for Activity Tracking and Heart Rate Monitoring Accurate, Precise, and Medically Beneficial?," (in eng), *Healthc Inform Res,* vol. 21, no. 4, pp. 315-320, 2015, doi: 10.4258/hir.2015.21.4.315.

[33] Y. Zheng *et al.*, "Unobtrusive Sensing and Wearable Devices for Health Informatics," *IEEE Transactions on Biomedical Engineering,* vol. 61, no. 5, pp. 1538-1554, 2014, doi: 10.1109/TBME.2014.2309951.

[34] I. Poitras *et al.*, "Validity and Reliability of Wearable Sensors for Joint Angle Estimation: A Systematic Review," (in eng), *Sensors (Basel),* vol. 19, no. 7, p. 1555, 2019, doi: 10.3390/s19071555.

[35] C. P. Walmsley, S. A. Williams, T. Grisbrook, C. Elliott, C. Imms, and A. Campbell, "Measurement of Upper Limb Range of Motion Using Wearable Sensors: A Systematic Review," (in eng), *Sports Med Open,* vol. 4, no. 1, pp. 53-53, 2018, doi: 10.1186/s40798-018-0167-7.

[36] S. Critcher, "Design and Evaluation of a Wearable Bioimpedance System for Monitoring Multiple Localized Knee Tissue Sites," M.S., The University of Alabama, Ann Arbor, 27744094, 2020. [Online]. Available: https://go.openathens.net/redirector/gatech.edu?url=https://search.proquest.com/docview/2428395892?accountid=11107

[37] C. Teague *et al.*, "Novel Methods for Sensing Acoustical Emissions From the Knee for Wearable Joint Health Assessment," *IEEE Transactions on Biomedical Engineering,* vol. 63, pp. 1-1, 03/17 2016, doi: 10.1109/TBME.2016.2543226.

[38] S. J. Song, C. H. Park, H. Liang, and S. J. Kim, "Noise around the Knee," (in eng), *Clin Orthop Surg,* vol. 10, no. 1, pp. 1-8, 2018, doi: 10.4055/cios.2018.10.1.1.

[39] H. Töreyin, H. K. Jeong, S. Hersek, C. N. Teague, and O. T. Inan, "Quantifying the Consistency of Wearable Knee Acoustical Emission Measurements During Complex Motions," *IEEE Journal of Biomedical and Health Informatics,* vol. 20, no. 5, pp. 1265-1272, 2016, doi: 10.1109/JBHI.2016.2579610.

[40] C. B. Frank, R. M. Rangayyan, and G. D. Bell, "Analysis of knee joint sound signals for non-invasive diagnosis of cartilage pathology," *IEEE Engineering in*

Medicine and Biology Magazine, vol. 9, no. 1, pp. 65-68, 1990, doi: 10.1109/51.62910.

[41] K. S. Kim, J. H. Seo, and C. G. Song, "An Acoustical Evaluation of Knee Sound for Non-invasive Screening and Early Detection of Articular Pathology," *Journal of Medical Systems,* vol. 36, no. 2, pp. 715-722, 2012/04/01 2012, doi: 10.1007/s10916-010-9539-3.

[42] M. Chu *et al.*, "Respiration rate and volume measurements using wearable strain sensors," *npj Digital Medicine,* vol. 2, no. 1, p. 8, 2019/02/13 2019, doi: 10.1038/s41746-019-0083-3.

[43] C. R. Merritt, H. T. Nagle, and E. Grant, "Textile-Based Capacitive Sensors for Respiration Monitoring," *IEEE Sensors Journal,* vol. 9, no. 1, pp. 71-78, 2009, doi: 10.1109/JSEN.2008.2010356.

[44] I. Frerichs *et al.*, "Wearable electrical impedance tomography for chest monitoring," *European Respiratory Journal,* vol. 56, no. suppl 64, p. 1355, 2020, doi: 10.1183/13993003.congress-2020.1355.

[45] J. Hong S Fau - Lee, H.-J. Lee J Fau - Yoo, and H. J. Yoo, "Wearable lung-health monitoring system with electrical impedance tomography," (in eng), no. 2694-0604 (Electronic), 2015.

[46] L. J. RTH, Forbes, "A treatise on the diseases of the chest and on mediate auscultation," 1830.

[47] Y. Hu, E. G. Kim, G. Cao, S. Liu, and Y. Xu, "Physiological Acoustic Sensing Based on Accelerometers: A Survey for Mobile Healthcare," *Annals of Biomedical Engineering,* vol. 42, no. 11, pp. 2264-2277, 2014/11/01 2014, doi: 10.1007/s10439-014-1111-8.

[48] T. Rahman *et al.*, "BodyBeat: A mobile system for sensing non-speech body sounds," *MobiSys 2014 - Proceedings of the 12th Annual International Conference on Mobile Systems, Applications, and Services,* 06/02 2014, doi: 10.1145/2594368.2594386.

[49] M. M. Islam, S. Mahmud, L. J. Muhammad, M. R. Islam, S. Nooruddin, and S. I. Ayon, "Wearable Technology to Assist the Patients Infected with Novel Coronavirus (COVID-19)," (in eng), *SN Computer Science,* vol. 1, no. 6, p. 320, 2020, doi: 10.1007/s42979-020-00335-4.

[50] D. R. Seshadri *et al.*, "Wearable Sensors for COVID-19: A Call to Action to Harness Our Digital Infrastructure for Remote Patient Monitoring and Virtual Assessments," *Frontiers in Digital Health,* 10.3389/fdgth.2020.00008 vol. 2, p. 8,

2020. [Online]. Available: https://www.frontiersin.org/article/10.3389/fdgth.2020.00008.

[51] S. Hersek, H. Töreyin, and O. T. Inan, "A Robust System for Longitudinal Knee Joint Edema and Blood Flow Assessment Based on Vector Bioimpedance Measurements," *IEEE Transactions on Biomedical Circuits and Systems*, vol. 10, no. 3, pp. 545-555, 2016, doi: 10.1109/TBCAS.2015.2487300.

[52] S. Mabrouk *et al.*, "Robust Longitudinal Ankle Edema Assessment Using Wearable Bioimpedance Spectroscopy," *IEEE Transactions on Biomedical Engineering*, vol. 67, no. 4, pp. 1019-1029, 2020, doi: 10.1109/TBME.2019.2927807.

[53] H. Töreyin, S. Hersek, C. N. Teague, and O. T. Inan, "A Proof-of-Concept System to Analyze Joint Sounds in Real Time for Knee Health Assessment in Uncontrolled Settings," *IEEE Sensors Journal*, vol. 16, no. 9, pp. 2892-2893, 2016, doi: 10.1109/JSEN.2016.2522964.

[54] J. Conant, "Non-Invasive Systems for Out-of-Clinic Monitoring of Biomechanical Measures," Master's in Electrical Engineering, Electrical and Computer Engineering, The Georgia Institute of Technology, 2016. [Online]. Available: https://smartech.gatech.edu/bitstream/handle/1853/56368/CONANT-THESIS-2016.pdf

[55] C. Teague, "A Robust System for Sensing Acoustic Emissions for Wearable Knee Health Assessement," Master's of Electrical Engineering, Electrical and Computer Engineering, Georgia Institute of Technology, 2016.

[56] O. Inan *et al.*, "Wearable Knee Health System Employing Novel Physiological Biomarkers," *Journal of Applied Physiology*, vol. 124, p. jap.00366.2017, 07/27 2017, doi: 10.1152/japplphysiol.00366.2017.

[57] C. Teague *et al.*, "A Wearable, Multimodal Sensing System to Monitor Knee Joint Health," *IEEE Sensors Journal*, vol. PP, pp. 1-1, 05/14 2020, doi: 10.1109/JSEN.2020.2994552.

[58] T. McGrath, R. Fineman, and L. Stirling, "An Auto-Calibrating Knee Flexion-Extension Axis Estimator Using Principal Component Analysis with Inertial Sensors," (in eng), *Sensors (Basel)*, vol. 18, no. 6, p. 1882, 2018, doi: 10.3390/s18061882.

[59] J. R. Basford and S. J. Johnson, "Form may be as important as function in orthotic acceptance: A case report," *Archives of Physical Medicine and Rehabilitation*, vol. 83, no. 3, pp. 433-435, 2002, doi: 10.1053/apmr.2002.29629.

[60] R. K. Chakraborty and B. Burns, "Systemic Inflammatory Response Syndrome," in *StatPearls*. Treasure Island (FL), 2020.

[61] P. Comstedt, M. Storgaard, and A. T. Lassen, "The Systemic Inflammatory Response Syndrome (SIRS) in acutely hospitalised medical patients: a cohort study," (in eng), *Scand J Trauma Resusc Emerg Med,* vol. 17, pp. 67-67, 2009, doi: 10.1186/1757-7241-17-67.

[62] G. C. Özmen, M. Safaei, L. Lan, and O. T. Inan, "A Novel Accelerometer Mounting Method for Sensing Performance Improvement in Acoustic Measurements from the Knee," *Journal of Vibration and Acoustics,* pp. 1-27, 2020, doi: 10.1115/1.4048554.

[63] L. Morrissette. "Cold Gold Frequently Asked Questions." https://contactmicrophones.com/FAQ.html (accessed 2020).

[64] S. Reichert, R. Gass, C. Brandt, and E. Andrès, "Analysis of respiratory sounds: state of the art," (in eng), *Clin Med Circ Respirat Pulm Med,* vol. 2, pp. 45-58, 2008, doi: 10.4137/ccrpm.s530.